
**SOLUTIONS FOR IMPROVED SEISMIC
PERFORMANCE OF NEW AND
EXISTING STRUCTURES**

Habilitation thesis

Aurel Stratan

2015

ACKNOWLEDGEMENTS

Writing this habilitation thesis gave me the opportunity to look back over the last 12 years of my professional experience, since defending the PhD thesis in 2003 at the Politehnica University of Timisoara. I saw a steady enlargement of the spectrum of activities, increase of the complexity of the work, and more liabilities. It also compelled me looking into the future and planning it in a structured way.

The scientific, professional and academic accomplishments described in this thesis would not have been possible without the contribution of a long list of people, of which only a few will be mentioned here. Therefore this work is not only mine, but also of all of them.

First of all I would like to deeply thank Professor Dan Dubina, who constantly supported me in the scientific and professional career, opening new opportunities, providing useful advices and motivating me to go on in difficult situations. This thesis would not have been written without his incentives.

I would like to thank my fellows from the department of Steel Structures and Structural Mechanics, Adrian Ciutina, Daniel Grecea, Florin Dinu, Raul Zaharia, Viorel Ungureanu, Mircea Georgescu, Adrian Dogariu, Edward Petzek and Ramona Szabo for providing a motivating and supportive working environment.

Thanks to all younger colleagues, former or present PhD students, Cristian Vulcu, Ionel Mărginean, Adriana Ioan, Norin Filip-Văcărescu, Călin Neagu, Nicu Muntean, Sorin Bordea, Andrei Crișan, Ioan Both and Cosmin Mariș for their dedicated work in different research projects.

Thanks to all partners in international and national research projects for their collaboration and motivation.

Last but not least, thanks to my family for sharing me with my job and patiently tolerating my work schedule.

SUMMARY

This habilitation thesis presents the main scientific, professional and academic achievements of Aurel Stratan following the defence of the PhD thesis in 2003 at the Politehnica University of Timisoara, as well as the future development plan.

The main research area of the author fits into the broad and multi-disciplinary area of earthquake engineering, with particular emphasis on seismic performance of steel structures and rehabilitation of existing buildings using metal-based solutions. The most important and relevant research directions pursued by the author are: "Re-centring eccentrically braced frames", "Cold-formed steel pitched-roof portal frames with bolted joints", "High strength steel in seismic resistant structures", "Seismic rehabilitation of existing reinforced concrete and masonry buildings with steel-based solutions", "Validation of the technical solution for braces with true pin connections", "Seismic performance of multi-storey steel structures with friction dampers" and "Prequalification of bolted beam to column joints with haunches". Experimental investigation methods represent the main tool of the research, supported at the same time by advanced numerical simulations and analytical tools. The habilitation thesis summarises the evolution of the research performed by the author following the defence of the PhD thesis, as well as the main outcomes, outlining also the context in which the research was performed, i.e. funding scheme, dissemination of results, and associated PhD theses. There were 12 grants supporting the research: 4 national grants, 7 international grants and 1 research contract with industry. The results were disseminated in 92 publications (journal and conference papers, and book chapters). Six PhD students were involved in the research (5 PhD theses were successfully defended and 1 is currently under development). Aurel Stratan had an active role in guiding the PhD candidates.

Professional development of Aurel Stratan followed a wide pallet of activities, including participation to training courses, structural design, industry-oriented research, involvement in professional organisations and technical committees, code drafting, development of the research infrastructure, organisation of scientific events, short-term scientific missions, involvement in administrative duties and peer-review of scientific publications. Though the author had a relatively limited involvement in structural design activity, it lead to important achievements, such as participation in the structural design of the Bucharest Tower Center, an office building with total height of 106.3 m, currently the third tallest structure in Bucharest. Aurel Stratan is member in several national professional organisations: AICPS, APCMR, AGIR-SBIS. He is also an active member in several national and international technical committees: Technical Committee TC13 "Seismic Design" of the European Convention for Constructional Steelwork (ECCS), CEN/TC 250/SC 8 "Eurocode 8: Earthquake resistance design of structures", CEN/TC 340/WG 5 "Revision of EN 15129 - Anti-seismic devices", ASRO CT 343 "Basis of design and structural eurocodes", CTS4 "Actions on structures", Ministry of Regional Development and Public Administration (MDRAP). The main work undertaken within these structures concerns improvement of national and European design guidelines in the field of earthquake-resistant design. Aurel Stratan is actively involved in maintaining and upgrading of the existing testing facilities in the laboratory of Steel Structures from the department of Steel Structures and Structural Mechanics. He was member of the scientific committee of three conferences, member in the organising committee of two conferences and chaired two sessions within international conferences.

In what concerns the academic area, Aurel Stratan teaches the courses of "Structural dynamics and earthquake engineering" and "Basis of structural design", as well as the project of "Steel structures" at bachelor level, and "Performance based design" and "Redesign of existing

structures" at the master levels. All of them are supported by teaching aids developed by the author, which includes a book and electronic course notes posted on faculty website. Several diploma works and master dissertations are coordinated each year, the latter being correlated with the on-going research projects. The author was recently involved in teaching activities of the European Erasmus Mundus Master Course "Sustainable Constructions under Natural Hazards and Catastrophic Events". He coordinated the module 2C09 "Design for seismic and climate changes" that were delivered in at the Politehnica University of Timisoara in the spring of 2014. Part of the lectures was delivered by Aurel Stratan at the University of Naples Federico II in March 2015, as part of the 2014-2016 edition of the European Erasmus Mundus Master Course.

In what concerns the future development plan, several new research directions are identified: extension of the concept of re-centring structures to dual Buckling-Restrained Frames (BRBFs) and Steel Plate Shear Walls (SPSWs), pseudo-dynamic and shaking table testing techniques, Buckling Restrained Braced Frames (BRBFs), seismic protection of buildings using passive and semi-active control, improved seismic design criteria for steel structures in case of ground motions with high frequency content in the long-period range, design criteria for connections in concentrically braced frames and prequalification of typical European connections, seismic vulnerability and risk assessment. Moreover, development of the international, national and industry-oriented cooperation is envisaged, as well as a more active role in grant applications and improvement of the research infrastructure. Last but not least, the teaching methods will be improved by involving the students through interactive learning techniques. Further development of the international cooperation at the academic level and continuing education are also targeted.

REZUMAT

Această teză de abilitare prezintă principalele realizări științifice, profesionale și academice ale lui Aurel Stratan după susținerea tezei de doctorat în 2003 la Universitatea Politehnica Timișoara, precum și direcțiile viitoare de dezvoltare ale acestora.

Principalul domeniu de cercetare a autorului se încadrează în domeniul vast și multi-disciplinar al ingineriei seismice, cu un accent special pe performanță seismică a structurilor din oțel și reabilitarea clădirilor existente folosind soluții bazate pe metale. Cele mai importante și relevante direcțiile de cercetare urmărite de autor sunt: "cadre contravântuite excentric cu capabilitate de re-centrare", "cadre portal din profile formate la rece cu îmbinări cu șuruburi", "utilizarea oțelului de înaltă rezistență la structurile anti-seismice", "reabilitarea seismică a clădirilor existente din beton armat și zidărie folosind soluții bazate pe metale", "validarea soluției tehnice pentru contravântuiri cu îmbinare cu bolț", "performanță seismică a structurilor metalice multietajate cu amortizori cu frecare" și "precalificarea îmbinărilor grindă-stâlp vutate cu șuruburi". Metoda de investigare experimentală reprezintă principalul instrument de cercetare, susținut în același timp de simulări numerice avansate și metode analitice. Teza de abilitare prezintă evoluția cercetărilor efectuate de autor după susținerea tezei de doctorat, precum și principalele rezultate obținute, subliniind, de asemenea, contextul în care a fost efectuată cercetarea, adică schema de finanțare, modul de diseminare a rezultatelor și tezele de doctorat asociate. Activitatea de cercetare descrisă a fost susținută de 12 de granturi: 4 granturi naționale, 7 granturi internaționale și 1 contract de cercetare cu industria. Rezultatele au fost diseminate în 92 publicații (articole în reviste și la conferințe științifice, precum și capitole de carte). În activitatea de cercetare au fost implicați șase doctoranzi (5 teze de doctorat au fost susținut cu succes, iar 1 se află în curs de elaborare). Aurel Stratan a avut un rol activ în îndrumarea doctoranzilor.

Dezvoltarea profesională a lui Aurel Stratan a inclus o paletă largă de activități, precum participarea la cursuri de formare, proiectare, cercetare aplicativă, implicarea în organizații profesionale și comitetele tehnice, elaborarea de coduri de proiectare, dezvoltarea infrastructurii de cercetare, organizarea de evenimente științifice, stagiile de cercetare, implicarea în activități administrative și recenzia a publicațiilor științifice. Deși autorul a avut o implicare relativ limitată în activitatea de proiectare, aceasta a condus la realizări importante, cum ar fi participarea la proiectarea structurală a Bucharest Tower Center, o clădire de birouri cu înălțimea totală de 106,3 m, în prezent pe locul trei în top-ul structurilor cele mai înalte din București. Aurel Stratan este membru în mai multe organizații profesionale naționale: AICPS, APCMR, AGIR-SBIS. El este de asemenea un membru activ în mai multe comitete tehnice naționale și internaționale: Comitetul Tehnic TC13 "Proiectarea seismică" a Convenției Europene de Construcții Metalice (ECCS), CEN / TC 250 / SC 8 "Eurocod 8: Proiectarea structurilor pentru rezistență la cutremur", CEN / TC 340 / WG 5 "Revizuirea EN 15129 - dispozitive anti-seismice", ASRO CT 343 "Bazele proiectării și eurocoduri pentru structuri", CTS4 "Acțiuni asupra construcțiilor", Ministerul Dezvoltării Regionale și Administrației Publice (MDRAP). Principala activitate întreprinsă în cadrul acestor grupuri se referă la îmbunătățirea codurilor de proiectare naționale și europene în domeniul proiectării antiseismice. Aurel Stratan este implicat activ în întreținerea și modernizarea echipamentelor experimentale existente în laboratorul de Structuri al departamentului de Construcții Metalice și Mecanica Construcțiilor. El a fost membru în comitetului științific a trei conferințe, membru în comitetul de organizare a două conferințe și a prezidat două sesiuni în cadrul unor conferințelor internaționale.

În ceea ce privește domeniul academic, Aurel Stratan este titular de curs la disciplinele "Dinamica structurilor și inginerie seismică" și "Bazele proiectării structurilor", precum și

proiectul de "Structuri metalice", la nivel de studii de licență, și "Proiectarea anti-seismică pe criterii de performanță" și "Procedee pentru reproiectarea construcțiilor" la nivelul studiilor de masterat. Toate acestea sunt susținute de materiale didactice elaborate de autor, care includ o carte și note de curs electronice postate pe site-ul facultății. Autorul coordonează anual elaborarea câtorva lucrări de diplomă și de disertație, subiectul celor din urmă fiind corelat cu proiectele de cercetare în curs de desfășurare. Autorul a fost implicat recent în activitățile de predare la cursul de master European Erasmus Mundus "Sustainable Constructions under Natural Hazards and Catastrophic Events". El a coordonat modulul 2C09 "Design for seismic and climate changes" predat la Universitatea Politehnica din Timișoara în primăvara anului 2014. O parte din prelegeri au fost susținute de către Aurel Stratan la Universitatea "Federico II" din Napoli în martie 2015, în cadrul ediției 2014-2016 a cursului de master European Erasmus Mundus.

În ceea ce privește planul de dezvoltare a carierei științifice, sunt identificate mai multe direcții de cercetare noi: extinderea conceptului de re-centrare la structuri duale cu contravântuiri cu flambaj împiedicat (BRBFs) și pereți de forfecare din oțel (SPSWs), tehnici experimentale pseudo-dinamice și dinamice, cadre cu contravântuiri cu flambaj împiedicat (BRBFs), protecția seismică a clădirilor folosind controlul pasiv și semi-activ, îmbunătățirea criteriile de proiectare seismică a structurilor metalice în cazul mișcărilor seismice cu un conținut ridicat de frecvențe în domeniul perioadelor lungi, criteriile de proiectare pentru îmbinări la cadrele contravântuite centric și precalificarea unor îmbinări europene tipice, evaluarea vulnerabilității și a riscului seismic. În plus, se are în vedere dezvoltarea cooperării internaționale, naționale și cu industria, precum și asumarea unui rol mai activ în aplicațiile de finanțare a cercetării și a infrastructurii de cercetare. Nu în ultimul rând, metodele de predare vor fi îmbunătățite prin implicarea studenților folosind tehnici interactive de predare. Sunt vizate, de asemenea, dezvoltarea în continuare a cooperării internaționale la nivel academic și a educației continue.

CONTENTS

ACKNOWLEDGEMENTS	I
SUMMARY	II
REZUMAT	IV
CONTENTS	VI
1 SCIENTIFIC, PROFESSIONAL AND ACADEMIC ACHIEVEMENTS	1
1.1 SCIENTIFIC ACHIEVEMENTS	1
1.2 LIST OF RELEVANT PUBLICATIONS	10
1.3 PROFESSIONAL ACHIEVEMENTS	11
1.4 ACADEMIC ACHIEVEMENTS	14
2 RESEARCH OUTCOMES	16
2.1 RE-CENTRING ECCENTRICALLY BRACED FRAMES	16
2.1.1 <i>The concept of re-centring structure</i>	16
2.1.2 <i>Design criteria for dual frames with re-centring capability</i>	17
2.1.3 <i>Experimental tests on one-storey eccentrically braced frame</i>	23
2.1.4 <i>Large-scale tests on re-centring dual eccentrically braced frame</i>	30
2.1.5 <i>link replacement order in higher-rise frames</i>	37
2.1.6 <i>Outcomes</i>	41
2.1.7 <i>Publications</i>	42
2.2 COLD-FORMED STEEL PITCHED-ROOF PORTAL FRAMES WITH BOLTED JOINTS.....	45
2.2.1 <i>Tests on joint specimens</i>	45
2.2.2 <i>Tests on full-scale pitched-roof portal frames</i>	56
2.2.3 <i>Outcomes</i>	61
2.2.4 <i>Publications</i>	62
2.3 HIGH STRENGTH STEEL IN SEISMIC RESISTANT STRUCTURES.....	64
2.3.1 <i>Steel-concrete connection in concrete-filled rectangular hollow section columns</i>	64
2.3.2 <i>Experimental tests on welded beam to concrete-filled RHS column joints</i>	69
2.3.3 <i>Numerical Investigation of welded beam to concrete-filled RHS column joints</i>	78
2.3.4 <i>Outcomes</i>	85
2.3.5 <i>Publications</i>	86
2.4 SEISMIC REHABILITATION OF EXISTING REINFORCED CONCRETE AND MASONRY BUILDINGS WITH METAL-BASED SOLUTIONS	89

2.4.1	<i>Strengthening of r.c. frames with buckling restrained braces</i>	89
2.4.2	<i>Strengthening of masonry walls with metal-based techniques</i>	96
2.4.3	<i>Publications</i>	103
2.5	VALIDATION OF THE TECHNICAL SOLUTION FOR BRACES WITH TRUE PIN CONNECTIONS.....	105
2.5.1	<i>Pre-test finite element analyses</i>	106
2.5.2	<i>Experimental investigation</i>	110
2.5.3	<i>Publications</i>	113
2.6	SEISMIC PERFORMANCE OF MULTI-STOREY STEEL STRUCTURES WITH FRICTION DAMPERS.....	114
2.6.1	<i>Experimental program</i>	116
2.6.2	<i>Seismic performance of multistorey frames with SERB dampers</i>	119
2.6.3	<i>Publications</i>	126
2.7	PREQUALIFICATION OF BOLTED BEAM TO COLUMN JOINTS WITH HAUNCHES	127
2.7.1	<i>Experimental program</i>	127
2.7.2	<i>Pre-test numerical simulations</i>	128
2.7.3	<i>Publications</i>	133
3	PROFESSIONAL DEVELOPMENT PLAN	134
3.1	SCIENTIFIC DEVELOPMENT PLAN	134
3.2	PROFESSIONAL DEVELOPMENT PLAN	136
3.3	ACADEMIC DEVELOPMENT PLAN	137
4	REFERENCES	138

1 SCIENTIFIC, PROFESSIONAL AND ACADEMIC ACHIEVEMENTS

This habilitation thesis presents the main scientific, professional and academic achievements of the author following the defence of the PhD thesis in 2003 at the Politehnica University of Timisoara.

1.1 SCIENTIFIC ACHIEVEMENTS

The main research area of the author fits into the broad and multi-disciplinary area of earthquake engineering, with particular emphasis of seismic performance of steel structures and rehabilitation of existing buildings using metal-based solutions. The most important and relevant research directions pursued by the author are:

- Re-centring eccentrically braced frames.
- Cold-formed steel pitched-roof portal frames with bolted joints.
- High strength steel in seismic resistant structures.
- Seismic rehabilitation of existing reinforced concrete and masonry buildings with steel-based solutions.
- Validation of the technical solution for braces with true pin connections.
- Seismic performance of multi-storey steel structures with friction dampers.
- Prequalification of bolted beam to column joints with haunches.

"Re-centring eccentrically braced frames" represents the backbone of the research interests of the author. Most structures designed according to modern seismic design codes follow the concept of dissipative behaviour, which relies on plastic deformations in order to absorb the seismic energy. Important structural and non-structural damage is therefore occurring in buildings under large and even moderate earthquakes. The most radical solutions to avoid such damage are base isolation and various implementations of active and semi-active structural control. Other strategies rely on supplemental damping conferred to the structure through various devices based on viscous, friction, or yielding dampers. Self-centring systems, a relatively new concept that addresses the drawbacks of the conventional yielding systems, have received much attention recently.

An alternative solution is to provide re-centring capability (as opposed to self-centring), by removable dissipative members and dual (rigid-flexible) structural configuration. Application of this approach to dual eccentrically braced frames with replaceable links was first suggested by the author in his PhD thesis (Stratan, 2003). Though experimental investigations on isolated replaceable links and numerical assessment of seismic performance of dual eccentrically braced frames with replaceable links were performed as part of the PhD thesis, the solution was still in its conceptual stage.

In the following years this idea was steadily developed. First a series of experimental tests were performed on one storey, one-bay eccentrically braced frame with replaceable links (Figure 1a), in order to investigate the connection design parameters and feasibility of link replacement at the system level. Additionally, numerical simulations on bolted links and dual structural systems were performed. These research activities were conducted at the Politehnica University of Timisoara, and were supported by a national research grant coordinated by the author: *grant no. 1434/27.04.2006 type CEEEX-ET module 2 (2006-2008). "Structuri metalice duale cu elemente disipative demontabile pentru construcții amplasate în zone seismice (Dual metal structures with removable dissipative elements for constructions in seismic areas)"*, financed by the Ministry of Education and Research.

Starting with 2010, the research reached a new level, after the team from the Politehnica University of Timisoara, CEMSIG research center, was awarded a *FP7 SERIES project: JRC N° 31817 / 2010 (2010-2014). "Full-scale experimental validation of dual eccentrically braced frame with removable*

links (DUAREM)", *Transnational Access within the framework of Grant Agreement No. 227887* financed by the European Commission. Project objectives were to (1) validate the re-centering capability of dual structures with removable dissipative members; (2) assess overall seismic performance of dual eccentrically braced frames; (3) obtain information on the interaction between the steel frame and the reinforced concrete slab in the link region. The research consortium was constituted by Politehnica University of Timisoara (the Lead User), University of Naples "Federico II", University of Liege, University of Ljubljana, and University of Coimbra. Within this funding scheme, a series of full-scale pseudo-dynamic tests were performed at the European Laboratory for Structural Assessment (ELSA) at Joint Research Centre (JRC) in Ispra, on a three-storey dual eccentrically braced structure with replaceable links (Figure 1b). A comprehensive set of numerical simulations were also performed in order to assess the seismic performance and optimal link replacement order of dual eccentrically braced frames with replaceable links. The outcomes of this research validated the concept of re-centring structure, proving the technical feasibility of link removal and replacement, as well as of the design approach. It cleared the route toward implementation into practice of this innovative structural design concept. An in-depth coverage of this research subject can be followed in section 2.1.



Figure 1. Experimental test on almost full-scale frame with bolted links in the Structural Laboratory of the Politehnica University of Timisoara, CEMSIG research centre (a) and the experimental mock-up in front of the reaction wall of the European Laboratory for Structural Assessment (ELSA) at JRC in Ispra (b).

Obtained results were disseminated in 25 publications (journal papers, conference proceedings and a report); for a complete list see section 2.1.7. A PhD thesis entitled "Seismic performance of re-centring dual eccentrically braced frames with removable links" was elaborated and defended as part of the research by Adriana Ioan under the supervision of Prof.dr.ing. Dan Dubina. The author of this habilitation thesis had an active role in guidance of the PhD candidate.

Within the second research direction, "**Cold-formed steel pitched-roof portal frames with bolted joints**", an experimental program was carried out in order to evaluate the performance of pitched roof cold-formed steel portal frames of back-to-back channel sections and bolted joints. Three different configurations of ridge and eaves joints were tested (Figure 2a). The behaviour and failure mechanisms of joints were observed in order to evaluate their stiffness, strength and ductility. Joints between cold-formed members with bolts in the web only result in a reduction of joint moment capacity and premature web buckling. The component method was applied in order to characterize the joint stiffness and moment capacity for the purpose of frame analysis and design. The influence of joints characteristics on the global frame response under lateral (seismic) loads was analysed by considering three connection models. Full-scale tests were performed on cold-formed pitched-roof portal frames (Figure 2b).

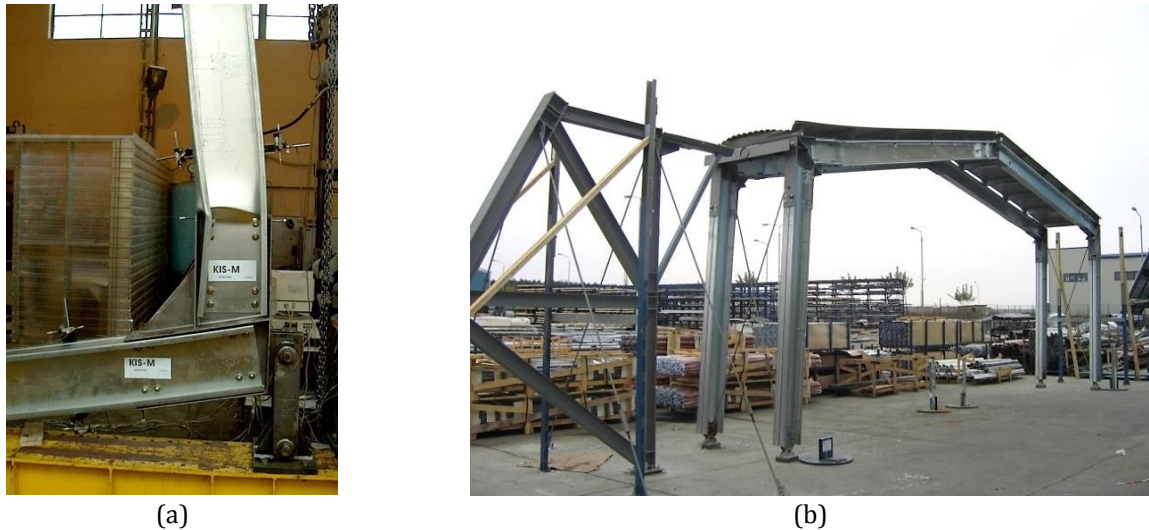


Figure 2. Component tests (a) and system-level tests (b) on cold-formed steel portal frames of back-to-back channel sections and bolted joints.

The research was funded through the national grant no. 32940/2004 (2004-2006) type A, CNCSIS code 164 "Incercari experimentale pe cadre portal din profile din otel formate la rece pentru cladiri civile si industriale in zone seismice - EXPOFORS (Experimental tests on portal frames from cold-formed steel profiles for civil and industrial buildings located in seismic areas)", financed by the ministry of research and education. The author of the habilitation thesis part of the research team.

The study suggested that the classical calculation model for connections, assuming the centre of rotation to be located at the centroid of the bolt group and a linear distribution of the forces on each bolt, is inappropriate for frames featuring cold-formed members. The force distribution is unequal due to the flexibility of the connected members. In fact, the force is an order of magnitude bigger in the outer bolt rows compared to most inner ones. A connection with bolts only on the web causes concentrated forces in the web of the connected member and leads to premature web buckling, reducing the joint moment capacity. This type of connections is always partial strength. If the load bearing capacity of the connected beam is to be matched by the connection strength, bolts on the flanges become necessary. The ductility of the connection is reduced both under monotonic and cyclic loads and the design, including the design for earthquake loads, should take into account only the conventional elastic capacity. Because there is no significant post-elastic strength, there are no significant differences in ductility and capacity of cyclically tested specimens compared with the monotonic ones. A more detailed coverage of this research subject can be followed in section 0.

Obtained results were disseminated in 12 publications (journal and conference papers); for a complete list see section 2.2.4. It has to be mentioned that the paper "Monotonic and cyclic performance of joints of cold formed steel portal frames" authored by D. Dubina, A. Stratan, A. Ciutina, L. Fulop & Zs. Nagy received the "Best Paper Award" at the Fourth International Conference on Thin-Walled Structures, Loughborough, UK, 22-24 June 2004. A PhD thesis entitled "Study of constructional solutions and structural performance of light-gauge halls from cold-formed steel profiles (Studiul soluțiilor constructive și performanțelor structurale ale halelor ușoare cu structura realizată din profile de oțel formate la rece)" was elaborated and defended as part of the research by Zsolt NAGY under the supervision of Prof.dr.ing. Dan Dubina. The author of this habilitation thesis was also actively involved in guidance of the PhD candidate.

The third research direction concerns "**High strength steel in seismic resistant structures**". Seismic resistant building frames designed as dissipative structures must allow for plastic deformations in specific members, whose behavior has to be predicted by proper design. In Dual

Frames (e.g. MRF + CBF or EBF) members designed to remain predominantly elastic during earthquakes, such as columns for instance, are characterized by high strength demands. Dual-steel structural systems, optimized according to a Performance Based Design Philosophy, in which High Strength Steel is used in "elastic" members and connection components, while Mild Carbon Steel in dissipative members, can be very reliable and cost effective. Based on this idea, a research program was carried out in order to evaluate the performance of moment resisting joints of HSS and MCS components, under monotonic and cyclic loading.

The research was funded through the national *grant no. 29/2005 (2005-2008) CEEX MATNANTECH "Sisteme constructive si tehnologii avansate pentru structuri din oteluri cu performante ridicate destinate cladirilor amplasate in zone cu risc seismic - STOPRISC (Structural systems and advanced technologies for structures from high-performance steels for buildings located in high-seismicity areas)"* financed by the ministry of education and research. The project was coordinated by Dan Dubina, while Aurel Stratan was the scientific responsible.

Tests on welded details indicated that welds between components of different steel grades performed adequately under both monotonic and cyclic loading, for all types of welds (fillet, single bevel and double bevel). The most important factor affecting the ductility of T-stub components under monotonic loading was the failure mode. Most ductile response was observed for components failing by end-plate bending (mode 1), while failure modes involving bolts (mode 2 and 3) were less ductile. The degree to which cyclic loading affected the ductility of T-stubs was, very much dependent on the failure mode. Specimens failing by end-plate bending (mode 1) were characterized by an important decrease of ductility with respect to monotonic loading, due to low-cycle fatigue. On the other hand, ductility of specimens involving bolt failure (modes 2 and 3) was not much affected by cyclic loading. Stiffening of Y-stubs increased their strength, but reduced slightly the ductility. T-stubs with end-plates realized from high strength steel showed comparable strength with those realized from mild carbon steel. However, one remarks that thinner end plates realized from high strength steel, at the same strength, are provide equal or even larger ductility (due to failure in mode 1 or 2) than thicker mild carbon steel, even if elongation at rupture of high strength steel was lower than the one of mild carbon steel.

The research was continued at the European level, through a research project coordinated by Politehnica University of Timisoara: *RFSR-CT-2009-00024 HSS-SERF 2009-2013 "High Strength Steel in Seismic Resistant Building Frames - HSS-SERF"*, financed by the European Commission - Research Fund for Coal and Steel. Other partners involved in the project were: Univ. of Stuttgart (Germany), Univ. of Liege (Belgium), Univ. of Ljubljana (Slovenia), Univ. "Federico II" of Naples (Italy), VTT Technical Research Centre (Finland), GIPAC Ltd. Design Office (Portugal), RIVA Acciaio S.p.A with Univ. of Pisa as subcontractor (Italy), and Ruukki Construction Oy (Finland).

A large numerical and experimental program was undertaken, addressing the following objectives: (1) to find reliable structural typologies and joint/connection detailing for dual-steel building frames, and to validate them by tests and advanced numerical simulations; (2) to develop design criteria and PBD methodology for dual-steel structures using HSS; (3) to recommend relevant design parameters (i.e. behaviour factor q , overstrength factor Ω) to be implemented in further versions of the seismic design code, such as EN 1998-1, in order to apply capacity design approach for dual-steel framing typologies; (4) to evaluate technical and economic benefit of dual-steel approach involving HSS.

The main outcomes and contributions of the project were the following: (1) principles and design recommendations for dual-steel frames (guidelines); (2) the investigated frame typologies based on the dual-steel approach with composite columns, are solutions with a high innovative character in the European context; (3) characterisation in terms of global ductility and over-strength demands of dual-steel frames; (4) proposal of a series of innovative beam-to-column joint typologies with composite columns (partially encased – PE, fully encased – FE, and concrete filled tubes – CFT), for

which the structural performance was confirmed by experimental and numerical investigations; (5) recommendations for weld details and appropriate component method design approaches.

The research activities specifically conducted at the Politehnica University of Timisoara included an experimental program (Figure 3) on two types of moment resisting joints in dual-steel frames of concrete filled high strength steel rectangular hollow section (CF-RHS) columns and mild carbon steel beams. The parameters considered in the configuration of the joints are given by two joint typologies (reduced beam section RBS, cover plates CP), two steel grades for the RHS tubes (S460, S700), and two failure modes (beam, joint components). Besides, two loading conditions (monotonic, cyclic) were considered, leading to a total number of 16 joint assemblies.

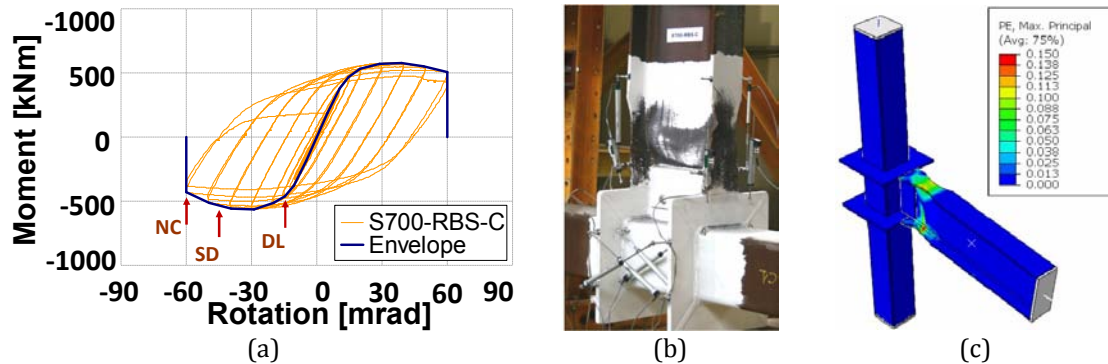


Figure 3. Moment-rotation characteristic (a), failure mode (b) and FEM simulations (c) of the S700-RBS-C joint.

As a general conclusion, the experimental investigations evidenced a good conception and design of the joints (RBS and CP), justified by: elastic response of the connection zone, formation of the plastic hinge in the beam, satisfactory response of connection components. In addition, the study proved the feasibility of using higher steel grades in non-dissipative members (columns) and joint components. Furthermore, the seismic performance of the welded beam-to-CFT column joints was evaluated. Corresponding to the Significant Damage performance level, the RBS and CP joint configurations evidenced rotation capacities larger than the 40 mrad, and therefore the seismic performance of the joints was considered as acceptable. A more detailed coverage of this research subject can be followed in section 0.

Obtained results were disseminated in 28 publications (journal and conference papers, as well as a research report); for a complete list see section 2.3.5. A PhD thesis entitled "Seismic performance of dual steel frames of CFRHS and welded beam-to-column joints" was elaborated and defended as part of the research by Cristian VULCU under the supervision of Prof.dr.ing. Dan Dubina. The author of this habilitation thesis was actively involved in guidance of the PhD candidate. Moreover, an international workshop on "Application of High Strength Steels in Seismic Resistant Structures" was organised by the University of Naples "Federico II" and Politehnica University of Timisoara, in cooperation with European Convention for Constructional Steelwork - Committee TC13 "Seismic Design" on June 28-29 2013, in Naples, Italy. Workshop proceedings were edited by Dan Dubina, Raffaele Landolfo, Aurel Stratan, and Cristian Vulcu at the Orizonturi Universitare publishing house (ISBN: 978-973-638-552-0).

The fourth research direction is "**Seismic rehabilitation of existing reinforced concrete and masonry buildings with steel-based solutions**". Two innovative strengthening solutions for masonry walls were investigated. First one consists in sheeting some steel or aluminium plates either on both sides or on one side of the masonry wall. Metallic plates are fixed either with prestressed steel ties, or using chemical anchors. The second one is derived from the FRP technique, but applies a steel wire mesh bonded with epoxy resin to the masonry wall. The

proposed strengthening solutions are an alternative to FRP technology enabling to obtain a ductile increase of strength, but without increasing the stiffness of the wall. It was concluded that steel plates increases mainly the ductility, while wire mesh increases the resistance. Both techniques were more efficient when applied on both sides. The prestressed tie connections were more appropriate and the specimens sheeted with aluminium plates have shown a better behaviour than ones sheeted with steel.



Figure 4. Testing of a masonry wall (a) and a buckling restrained brace (b).

A related subject concerned gravity-only designed reinforced concrete (RC) buildings located in seismic zones that need seismic upgrade in order to comply with modern seismic design requirements. The effectiveness of the Buckling Restrained Braces (BRB) in strengthening and increasing ductility in non-seismic reinforced concrete frame was examined. The BRB members have been designed to respond to the strengthening demand resulted from non-linear analysis and tested in order to observe their functionality. Numerical analysis showed that the use of BRB system has to be associated with local FRP confinement of columns at least (confinement of beams would be beneficial, too). BRB specimens have been designed according to the demands resulted from the analysis and according to FEMA 356 criteria. Using the same steel core, three types of BRB have been prepared, using three different unbonding materials i.e. polyethylene film, asphaltic bitumen and rubber. Both monotonic and cyclic tests have been performed. Cyclic tests have been carried out according to both AISC 2005 and ECCS Recommendations. All the three BRB solutions satisfied the demand, however the one using polyethylene film proved a better behaviour. It was concluded that the BRB systems can be designed and applied as an effective strengthening solution for poor seismic resistant RC Frames. A more detailed coverage of this research subject can be followed in section 0.

The research was supported by four projects, one of which was coordinated by the author:

- *RFC5-CT-2007-00050 STEELRETRO (2007-2010) "Steel solutions for seismic retrofit and upgrade of existing constructions"*, financed by the European Commission - Research Fund for Coal and Steel.
- *FP6 INCO-CT-2004-509119/ 2003 (2003-2008) "Earthquake Protection of Historical Buildings by reversible Mixed Technologies - PROHITECH"*, financed by the European Commission.
- *C18873/28.12.2005 (2006-2008) bilateral Romanian-Greek research program "Strengthening and rehabilitation of historical buildings by reversible technologies"*, financed by the ministry of education and research (program coordinator).
- *RFS2-CT-2014-00022 (2014-2015) "Steel based applications in earthquake-prone areas (STEELEARTH)"*, financed by the European Commission - Research Fund for Coal and Steel.

Obtained results were disseminated in 11 publications (journal and conference papers, as well as two books); for a complete list see section 2.4.3. A PhD thesis entitled "Dual frame systems of

buckling restrained braces" was elaborated and defended as part of the research by Sorin BORDEA under the supervision of Prof.dr.ing. Dan Dubina. The author of this habilitation thesis was also actively involved in guidance of the PhD candidate.

The fifth subject described herein concerns "**Validation of the technical solution for braces with true pin connections**". The research was triggered by a practical problem that came up during the design of a multi-storey building with two underground and 29 levels above ground in Bucharest, Romania by SC Popp & Asociatii SRL. The building is characterised by in-plan dimensions of a typical floor of 52.0x25.6 m, and a total height of 117.6 m. The structure uses steel framing for resisting gravity forces. In the transversal direction the main lateral force resisting system is composed of two reinforced concrete cores, while in the longitudinal one the cores are supplemented by steel braces located in the facade of the building. The braces are placed in X configuration developed over two storeys. This reduces the number of brace connections and helps in complying with code limitations on slenderness. Braces are realised from hot-finished Circular Hollow Sections (CHS) and have connections with pins. "True pin" connections with gusset plates and pin were adopted for brace connections. One of the brace connections has an eccentric pin, allowing for variation of the pin-to-pin length, which facilitates erection on one hand, and allows compensation for axial forces in braces due to gravity loads on the other hand. High strength steel was used for gussets and pin, in order to keep connection dimensions to a minimum.

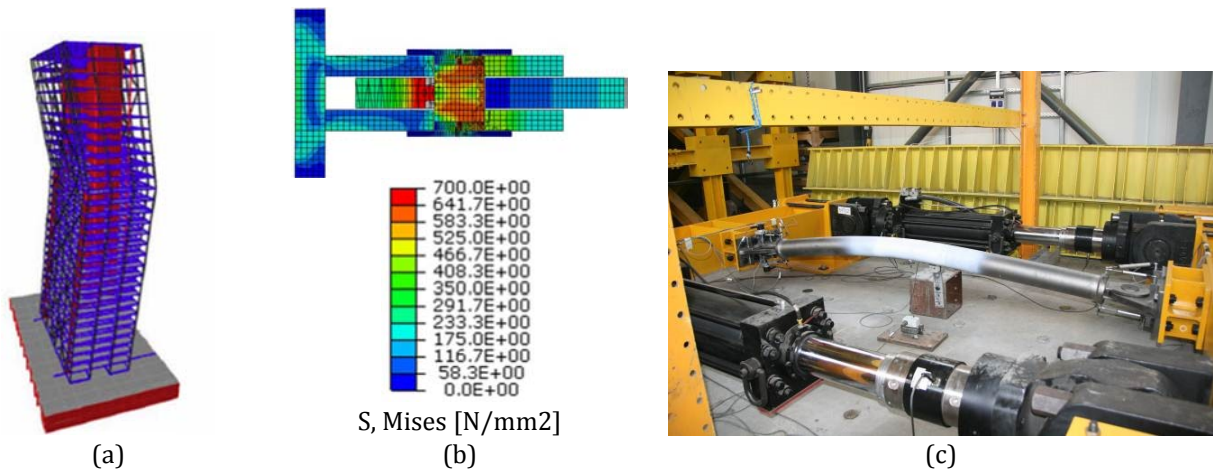


Figure 5. Building under design (a); FEM analyses on the true-pin connection (b) and experimental testing of the brace (c).

Numerical simulations and experimental testing were performed in order to validate the design of pinned brace for a seismic resistant multi-storey building (Figure 5). Based on finite element numerical simulations, a more compact solution was proposed and adopted, using high-strength steel components. Due to connection detailing and tubular shape of the cross-section, the brace assembly was shown to be sensitive to out of plane buckling, leading to failure of the connection in a brittle way. Firmly fixing the washers to the pin helps preventing brittle failure of the connection, even when buckling takes place out of the plane of the connection. The main causes of out of plane buckling are (1) the free out of plane rotations of the connection at small deformations due to the tolerance between the pin and the hole in gussets, (2) friction that restrains to some extent in-plane rotations of the connection and (3) initial member and connection imperfections. In-plane buckling of the brace assembly is favoured by the following: (1) design in-plane connection eccentricity, (2) reduction of out of plane rotation of the connection through smaller tolerances at the pin or larger spacing between gussets, (3) lower friction at the pin – gussets interface, (4) slender braces, and (5) brace cross section with different moments of inertia about the two principal axes (elliptical, RHS, wide flange). A more detailed coverage of this research subject can be followed in section 2.5.

Obtained results were disseminated in 3 publications (journal and conference papers); for a complete list see section 2.5.3. Research was supported by the *contract no. BC79/04.07.2011 (2011-2012) "Testarea și validarea contravânturilor din țevă rotundă și a îmbinărilor acestora pentru proiectul Smart Park din București, Clădire de birouri clasa A (clădire Turn, alte clădiri și parcaj) Șoseaua Străulești nr. 37, sector 1, București"*, financed by SC Popp & Asociații SRL.

The sixth subject investigated "**Seismic performance of multi-storey steel structures with friction dampers**". The general aim of the research program was to establish the seismic performance of multistorey steel concentrically braced structures equipped with strain hardening friction dampers. For this purpose experimental and numerical analyses have been conducted. Based on the experimental data numerical models were calibrated and applied to evaluate the performance of concentrically braced frames equipped with such devices in the braces. The aim of the experimental program was to evaluate and characterise the damper, in a first step, and the behaviour of the brace-damper assembly, in the second step (Figure 6).

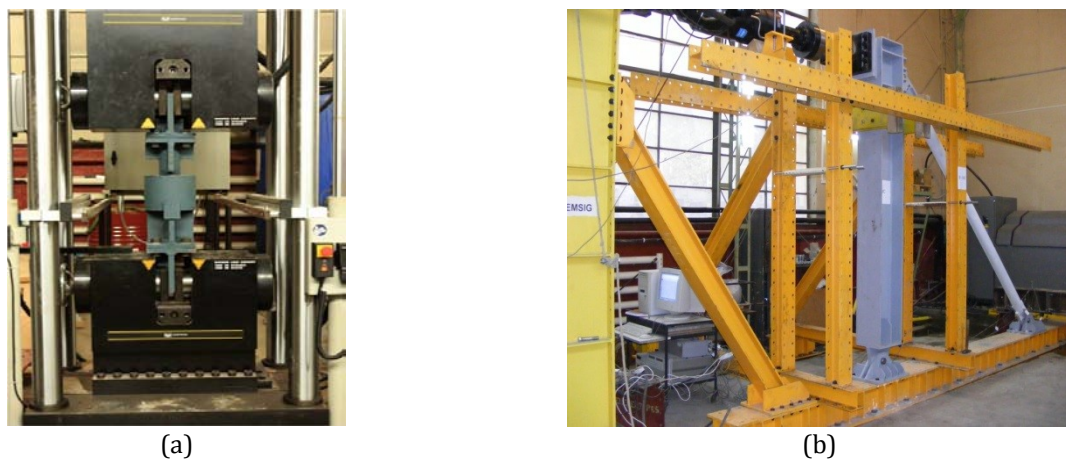


Figure 6. Experimental test setup for damper tests (a) and brace with damper tests (b).

The particular damper typology investigated within this research program showed to be efficient in reducing the seismic response of a building for earthquakes characterized by short corner period $T_c=0.5s$ (stiff soil) by preventing the formation of plastic hinges at SLS and reducing the permanent displacement of the structure. For earthquakes characterized by long corner period $T_c=1.6s$ (soft soil) this type of damper is not effective in improving the behaviour of the structure. Under this type of seismic motions the structures with dampers form plastic hinges in non-dissipative elements with values that exceed the acceptance criteria for the corresponding performance levels. A more detailed coverage of this research subject can be followed in section 0.

The research was funded through the national *grant no. 31042/2007 (2007-2011) type PN II Partnerships "Sisteme structurale și soluții tehnologice inovative pentru protecția clădirilor la acțiuni extreme în contextul cerințelor pentru dezvoltare durabilă – PROACTEX (Structural systems and innovative technologies for protection of buildings under extreme actions taking into account sustainable design criteria)"*, financed by the ministry of education and research.

Obtained results were disseminated in 10 publications (journal and conference papers); for a complete list see section 2.6.3. A PhD thesis entitled "Seismic performance of multistorey steel concentrically braced frames equipped with friction dampers" was elaborated and defended as part of the research by Norin FILIP-VĂCĂRESCU under the supervision of Prof.dr.ing. Dan Dubina. The author of this habilitation thesis was also actively involved in guidance of the PhD candidate.

The last research direction covered herein deals with "**Prequalification of bolted beam to column joints with haunches**" and represents an ongoing research. Modern seismic design codes require that the seismic performance of beam-to-column connections in steel moment resisting

frames to be demonstrated through experimental investigations, which often prove to be expensive and time-consuming. A solution to this problem is the pre-qualification of typical connections for the design practice. The research project EQUALJOINTS is currently underway and aims at seismic pre-qualification of several beam-to-column connection typologies common in the European practice. As a result, the current investigation outlines the experimental program on bolted extended end-plate connections with haunches that will be carried out at the Politehnica University of Timisoara in the framework of the mentioned project. The design objective was to get full-strength and rigid joints. A numerical model was calibrated based on the past experimental results carried out on T-stub elements and was used in order to validate the design procedure (Figure 7).

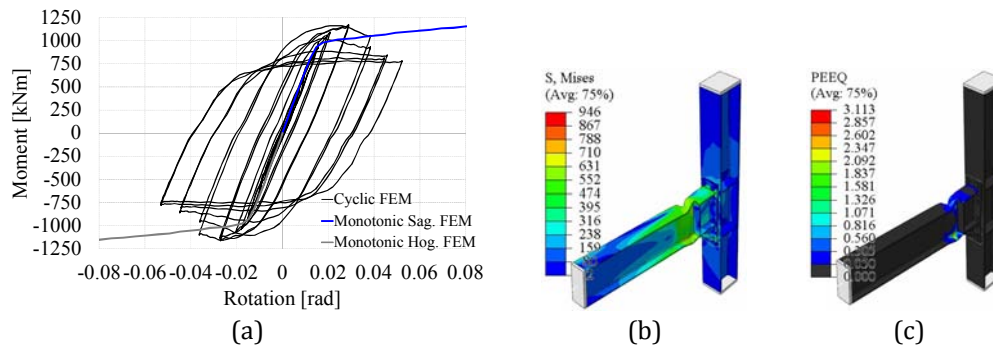


Figure 7. Cyclic response for EH2-TS-35: (a) moment-rotation curve (monotonic and cyclic loading conditions), (b) von Mises stress distribution, (c) equivalent plastic strain.

The pre-test numerical simulations carried out for the joint assemblies designed based on EN 1993-1-8 confirmed the intended failure mode, i.e. formation of the plastic hinge in the beam close to the haunch ending. However, other assumptions considered in design were not confirmed, in particular: force distribution in the bolt rows, and position of the compression centre (middle of the compressed haunch flange). In contrast, the active bolt rows were those situated near the flange in tension, and the compression centre was located at a distance equal to 60% of the haunch depth measured from the bottom flange of the beam. As a result, the design procedure was adjusted and the beam-to-column joint configurations were re-designed and analysed. The parametric study allowed investigating the influence of: member size, haunch geometry, web panel strength, and cyclic loading. Consequently, the study evidenced higher strain in members (beams) of larger cross-section, for the same joint rotation. In addition, the capacity and the initial stiffness of the connection increased for higher values of haunch angle and depth, but for economic and architectural reasons, haunches with minimum depth and a smooth slope are recommended. A more detailed coverage of this research subject can be followed in section 0.

This research is supported by the European grant no. RFSR-CT-2013 - 00021 (2013-2016). "European pre-QUALified steel JOINTS (EQUALJOINTS)", financed by the European Commission - Research Fund for Coal and Steel. The project is implemented by the following partnership: University of Naples Federico II (coordinator), Arcelormittal Belval & Differdange SA, Universite de Liege, Universitatea Politehnica Timisoara, Imperial College of Science, Technology and Medicine, Universidade de Coimbra, European Convention for Constructional Steelwork Vereniging, Cordioli & C. SPA.

Obtained results were disseminated in 3 publications (journal and conference papers); for a complete list see section 2.7.3. A PhD thesis entitled "Experimental study of haunched beam-to-column connections of bolted extended end plate under cyclic loading (Studiul experimental al îmbinărilor riglă-stâlp, cu placă de capăt extinsă, vută și șuruburi, solicitate în regim ciclic)" is under development by Cosmin MARIS under the supervision of Prof.dr.ing. Dan Dubina. The author of this habilitation thesis is actively involved in guidance of the PhD candidate.

1.2 LIST OF RELEVANT PUBLICATIONS

The following 10 papers were selected as the most representative for the research activities of the author described in this habilitation thesis.

- [1] Dubina, D., Stratan, A., Dinu, F. (2008). "Dual high-strength steel eccentrically braced frames with removable links". *Earthquake Engineering & Structural Dynamics*, Vol. 37, issue 15, pp. 1703-1720, (Online ISSN: 1096-9845, Print ISSN: 0098-8847).
- [2] Stratan, A., Ioan, A., Dubina, D., Poljanšek, M., Molina, J., Pegon, P., Taucer, F. (2014). "Dual eccentrically braced frames with removable links: Experimental validation of technical solution through large-scale pseudo-dynamic testing". *Proceedings of the Fifth National Conference on Earthquake Engineering and First National Conference on Earthquake Engineering and Seismology – 5CNIS & 1CNIS*, Bucharest, Romania, June 19-20, 2014. Radu Văcăreanu, Constantin Ionescu (Eds.), Bucharest: Conspress, 2014, ISBN (print) 978-973-100-342-9, ISBN (CD) 978-973-100-341-2, pp. 323-330, Paper No. 31 (on CD-ROM)
- [3] Dubina, D., Stratan, A., Nagy, Zs. (2009). "Full – scale tests on cold-formed steel pitched-roof portal frames with bolted joints". *Advanced Steel Construction* Vol. 5, No. 2, pp. 175-194. ISSN 1816-112X.
- [4] Vulcu, C., Stratan, A., Dubina, D. (2012). "Numerical simulation of the cyclic loading for welded beam-to-CFT column joints of dual-steel frames", *Pollack Periodica*, vol. 7, no. 2, pp. 35–46. DOI: 10.1556/Pollack.7.2012.2.3. Paper ISSN: 1788-1994, Online ISSN: 1788-3911.
- [5] Vulcu C., Stratan A., Ciutina A., Dubina D. (2011). "Beam-to-column joints for seismic resistant dual-steel structures", *Pollack Periodica* 6 (2), pp. 49-60. Paper ISSN: 1788-1994, Online ISSN: 1788-3911.
- [6] Dubina, D., Bordea, S., Stratan, A. (2009). "Performance Based Evaluation of a RC Frame strengthened with BRB Steel Braces". *Proc. of the International Conference on Protection of Historical Buildings PROHITECH 09*, Rome, Italy, 21-24 June 2009. Ed. F.M. Mazzolani. CRC Press, ISBN 978-0-415-55803-7, p. 1741-1746.
- [7] Dubina, D., Dogariu, A., Stratan, A., Stoian, V., Nagy-Gyorgy, T., Dan, D. and Daescu, C. (2007). "Masonry walls strengthening with innovative metal based techniques". *Proc. of the 3rd Intl. Conf. on Steel and Composite Structures (ICSCS07)*, Manchester, UK, 30 July - 1 August 2007, Eds. Wang and Choi. Taylor&Francis, ISBN: 978-0-415-45141-3, pp. 1071-1077.
- [8] Stratan, D., Dubina, R., Gabor, C., Vulcu, I., Marginean (2012). "Experimental validation of a brace with true pin connections", *Proceedings of the 7th International Workshop on Connections in Steel Structures*, May 30 - June 2, 2012, Timisoara, Romania, ECCS, Dan Dubina and Daniel Grecea (Eds), ISBN 978-92-9147-114-0, pp. 535-546.
- [9] Filip-Vacarescu, N., Stratan, A., and Dubina, D. (2014). "Experimental validation of a strain hardening friction damper". *Proceedings of the Romanian Academy Series a - Mathematics Physics Technical Sciences Information Science*, 15(1), 60-67.
- [10] Maris, C., Vulcu, C., Stratan, A., and Dubina, D. (2014). "Numerical Simulations of Bolted Beam to Column Connections with Haunches in Steel Moment Frames." *Proceedings of the Second International Conference for PhD Students in Civil Engineering and Architecture*, UTPRESS, Cluj-Napoca, Romania, 109–116.

1.3 PROFESSIONAL ACHIEVEMENTS

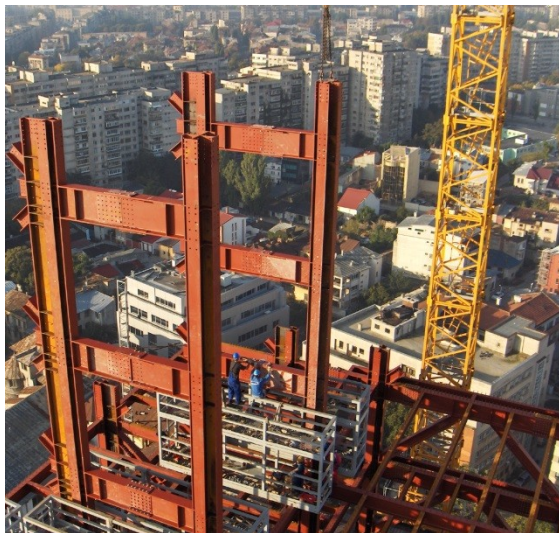
Professional development of Aurel Stratan followed a wide pallet of activities, including participation to training courses, structural design, industry-oriented research, involvement in professional organisations and technical committees, code drafting, development of the research infrastructure, organisation of scientific events, short-term scientific missions, involvement in administrative duties and peer-review of scientific publications.

Recognizing the fact that an academic and scientific career is in need of continuous learning and improvement of personal skills, Aurel Stratan followed two training courses related to experimental techniques, one of his major fields of interest:

- "New Approaches to Analysis and Testing of Mechanical and Structural Systems". International Centre for Mechanical Sciences, Udine, Italy, 2007.
- "Preparatory Course on Pseudodynamic Experimental Testing", European Laboratory for Structural Assessment (ELSA), JRC Ispra, Italia, 2010.

He also fulfilled a short-term scientific mission as invited researcher at VTT – the Technical Research Centre of Finland in Espoo (September 1-8, 2006). New research connections were sought, including through the participation to the COST C26 action "Urban Habitat Constructions under Catastrophic Events" (2006-2010).

Taking into account the highly applicative character of the domain of civil engineering, Aurel Stratan tried to keep close contact with structural design and industry-oriented research. Thus, he had a limited involvement in design activity, the most important of which is the participation in the structural design of the Bucharest Tower Center (Figure 8). The building has three basement levels, 26 floors and a total height of 106.3 m. As of 2015, it is the third tallest structure in Bucharest, after the Floreasca City Center and Basarab Tower (List of tallest buildings in Bucharest, 2015). Design of the Bucharest Tower Center received two awards: "ECCS European Award for Steel Structures 2007" and 1st prize of the Romanian Association of Structural Engineering (AICPS) in 2007 (structural design team: D. Dubina, F. Dinu, A. Stratan, A. Ciutina).



(a)



(b)

Figure 8. Bucharest Tower Center in Bucharest: erection phase (a) and completed building (b).

At the same time, close cooperation with industry was sought in the area of research and consultancy. Participation in the development of "Requirements for multi-storey buildings in seismic areas" for the Rautaruukki Corporation from Finland within the RUUKKI/2009 contract (coordinator D. Dubina) can be mentioned. Moreover, Aurel Stratan was the coordinator in the

contract BC79/04.07.2011 (2011-2012) that investigated an optimal solution for a true-pin brace connection used in the design of a high-rise building in Bucharest by Popp & Asociatii, described in detail in section 2.5.

Aurel Stratan is member in several national professional organisations: APCMR - Asociația Producătorilor de Construcții Metalice din România (Romanian Association of Steelwork Producers); AGIR-SBIS - Asociația Generală a Inginerilor din România (General Association of Engineers from Romania), Societatea Bănățeană de Inginerie Seismică SBIS (Romanian Association of Engineers, Banat Seismic Society); AICPS - Asociația Inginerilor Constructori Proiectanți de Structuri (Romanian Association of Structural Engineers). He is also an active member in several national and international technical committees:

- Technical secretary of Technical Committee TC13 "Seismic Design" of the European Convention for Constructional Steelwork (ECCS)
- Member of CEN/TC 250/SC 8 "Eurocode 8: Earthquake resistance design of structures", European Committee for Standardization (CEN)
- Member of CEN/TC 340/WG 5 "Revision of EN 15129 – Anti-seismic devices", European Committee for Standardization (CEN)
- Member of ASRO CT 343 "Bazele proiectării și eurocoduri pentru structure (Basis of design and structural eurocodes)", Romanian Standards Association - Asociația de standardizare din România (ASRO).
- Member of CTS4 "Acțiuni asupra construcțiilor (Actions on structures)", Ministerul Dezvoltării Regionale și Administrației Publice (MDRAP) – Ministry of Regional Development and Public Administration.

The main work undertaken within these structures concerns improvement of national and European design guidelines in the field of earthquake-resistant design. As an example, the outcomes of the activities performed within the Technical Committee TC13 "Seismic Design" of the European Convention for Constructional Steelwork (ECCS) were recently published in the following book:

- Jean-Marie Aribert, Darko Beg, José Miguel Castro, Herve Degee, Florea Dinu, Dan Dubina, Ahmed Elghazouli, Amr Elnashai, Vigh L. Gergely, Victor Gioncu, Mohammed Hjiiaj, Benno Hoffmeister, Raffaele Landolfo, Pierre-Olivier Martin, Federico M. Mazzolani, Paolo Negro, Vincenzo Piluso, Andre Plumier, Carlos Rebelo, Gerhard Sedlacek, Aurel Stratan (2013). "Assessment of EC8 provisions for seismic design of steel structures", Raffaele Landolfo (Ed.), European Convention for Constructional Steelwork.

Aurel Stratan had an important activity in code-drafting. It concerned elaboration of national codes, especially the ones related to seismic design of steel structures, and also development of Romanian versions and National Annexes of structural Eurocodes. The following is a list of national codes in which Aurel Stratan was a member in the drafting team:

- 2013 revision of the Romanian seismic design code P100-1/2013. "Cod de proiectare seismică - Partea I - Prevederi de proiectare pentru clădiri". Volumul I și II. Monitorul oficial al României, nr. 558 bis/2013.
- 2006 revision of the Romanian seismic design code P100-1/2006. "Cod de proiectare seismică - Partea I - Prevederi de proiectare pentru clădiri". Buletinul Construcțiilor, Vol. 12-13, 2006.
- GP 078-03 "Ghid privind proiectarea halelor usoare cu structura metalica (Design guide for light-gauge industrial steel halls)", Bul. Construcțiilor Vol 16, 2004, p 59-273.
- GP 082-03. "Ghid de proiectare a imbinarilor ductile la structuri metalice in zone seismice (Design guide for ductile connections of steel structures in seismic areas)". Bul. Constr. Vol. 16, 2004, p. 3-58.

Below is a list of standards for which the author elaborated the Romanian versions and/or the National Annexes:

- SR EN 1998-1:2004/NA:2008 "Eurocode 8: Design of structures for earthquake resistance – Part 1: General rules, seismic actions and rules for building. National Annex". Romanian Standards Association - Asociația de standardizare din România (ASRO).
- EN 15129:2010 "Anti-seismic devices". Romanian Standards Association - Asociația de standardizare din România (ASRO).
- SR EN 1993-1-12:2007 "Eurocode 3 - Design of steel structures - Part 1-12: Additional rules for the extension of EN 1993 up to steel grades S 700". Romanian Standards Association - Asociația de standardizare din România (ASRO).
- SR EN 1993-1-7:2007 "Eurocode 3 - Design of steel structures - Part 1-7: Plated structures subject to out of plane loading". Romanian Standards Association - Asociația de standardizare din România (ASRO).

Most of the research performed at the CEMSIG research centre has a strong experimental and numerical component, which requires a solid infrastructure. Aurel Stratan is actively involved in maintaining and upgrading of the existing testing facilities. He participated in the following contracts that specifically addressed the development of the research infrastructure of the research centre:

- Contract nr. 662/2014 (2014-2015) POS CCE ID1827/SMIS48741 "Platforma integrată de cercetare-dezvoltare pentru comportarea construcțiilor la acțiuni extreme (ACTEX)" – member in the management team.
- 90 CP/ I/ 2007 (2007-2010) Grant tip PN II Modul I, Capacități: "Dezvoltare laborator pentru încercări pe structuri la scară mare - INSTRUCT" – scientific responsible.
- 42/2006 (2006-2008). Grant tip Platforme/Laboratoare de formare si cercetare interdisciplinara: "Centru de Studii Avansate si Cercetare în Ingineria Materialelor si Structurilor – CESCIMS" - colaborator.
- 32940/2004 (2004-2005). Grant E, Tema 3, cod CNC SIS 31 "Stand experimental pentru încercări ciclice" – colaborator.



(a)



(b)



(c)

Figure 9. Instron universal testing machine for dynamic tests of 1000 kN capacity, with hydraulic grips(a); Reaction wall 5.0x6.2 m and strong concrete slab 5.0x9.5 m for static and pseudo-dynamic tests (b); Hydraulic actuators MTS 650/1015 kN and hydraulic power unit.

Among the infrastructure / equipment that has been developed or upgraded with the direct contribution of Aurel Stratan, the following ones could be mentioned: reaction structure (5.0x6.2 m) and strong concrete slab (5.0x9.5 m) for quasi-static and pseudo-dynamic tests; hydraulic actuators MTS 650/1015 kN, with hydraulic and control systems; Instron universal testing machine for dynamic tests of 1000 kN capacity, with hydraulic grips; UTS universal testing machine of 250 kN capacity, with hydraulic grips; Zwick universal testing machine of 10 kN capacity; Charpy impact testing machine (Figure 9). A major development of the existing research infrastructure is currently

underway within the POS CCE ID1827/SMIS48741 ACTEX project. As part of the management team and technical and scientific responsible of the project, Aurel Stratan is coordinating the purchasing of a uniaxial shaking table, two dynamic and two static actuators, optical metallographic microscope, high-resolution video data acquisition system, dynamic data acquisition system, high-performance computing (HPC) system, workstations and advanced structural analysis software. Aurel Stratan was/is member of the scientific committee of the following conferences:

- A 12-a Conferință Națională de Construcții Metalice, Timișoara, 26-27 noiembrie 2010.
- A 13-a Conferință Națională de Construcții Metalice, București, 21-22 noiembrie 2013.
- A 14-a Conferință Națională de Construcții Metalice, Cluj-Napoca, 22-24 noiembrie 2015.

He was also involved as member in the organising committee of the "International conference in metal structures", Poiana Brasov, Romania, September 20-22, 2006 and the XIII edition of the "Zilelor academice Timișene (Timisaora academic Days)", 24 may 2013. Aurel Stratan was among the editors of the international workshop on "Application of High Strength Steels in Seismic Resistant Structures" was organised by the University of Naples "Federico II" and Politehnica University of Timisoara, in cooperation with European Convention for Constructional Steelwork - Committee TC13 "Seismic Design" on June 28-29 2013, in Naples, Italy. Workshop proceedings were edited by Dan Dubina, Raffaele Landolfo, Aurel Stratan, and Cristian Vulcu at the Orizonturi Universitare publishing house (ISBN: 978-973-638-552-0).

Aurel Stratan chaired sessions within the following international conferences:

- Session 23 "Earthquake & Vibration", Second International Workshop on Performance, Protection & Strengthening of Structures under Extreme Loading, Shonan Village Center, Hayama, Japan, August 19-21, 2009
- Session on "Seismic-resistant structures 5" within the 7th European Conference on Steel and Composite Structures EUROSTEEL 2014, 10-12 September 2014, Napoli, Italy

Aurel Stratan seeks a more active role at the administrative level by acting as member of the Council of the Faculty of Civil Engineering (2013-present), member in the council and scientific secretary of the Department of Steel structures and Structural Mechanics (2004-present), and scientific coordinator of the Research Center for Mechanics of Materials and Structural Safety – CEMSIG (2011-present).

Aurel Stratan is a reviewer in the following ISI journals: "Earthquake Engineering and Structural Dynamics", John Wiley & Sons, ISSN: 1096-9845;"Steel and Composite Structures", Techno-Press, ISSN: 1598-6233; "Journal of Earthquake Engineering", Taylor & Francis, ISSN 1559-808X.

1.4 ACADEMIC ACHIEVEMENTS

Currently Aurel Stratan teaches the courses of "Structural dynamics and earthquake engineering" and "Basis of structural design", as well as the project of "Steel structures" at bachelor level, and "Performance based design" and "Redesign of existing structures" at the master levels. The first of these courses is supported by a book published by the author: Stratan, A. (2007). "Dinamica structurilor și inginerie seismică (Dynamics of Structures and Earthquake Engineering)", Ed. Orizonturi Universitare, Timișoara, ISBN 978-973-638-388-0, 223 p. It was received the 1st award at the "Cartea Tehnică 2008" contest by the "Asociația Generală a Inginerilor din România, Filiala Timiș (Romanian Association of Engineers)".

Electronic supporting material is provided for other courses, some of which are posted on the faculty website and constantly updated:

- Stratan, A. "Dinamica Structurilor și Inginerie Seismică".
<http://www.ct.upt.ro/users/AurelStratan/index.htm>, Suport de curs pentru anul 3 CCIA și 3 CFDP, 155 p.

- Stratan, A. "Structural Dynamics and Earthquake Engineering". <http://www.ct.upt.ro/users/AurelStratan/index.htm>, Suport de curs pentru anul 3 PI, 153 p.
- Stratan, A. "Basis of Structural Design". <http://www.ct.upt.ro/users/AurelStratan/index.htm>, Suport de curs pentru anul 2 PI, 229 p.

Another work published by the author and that serves as support for master students is:

- Dan Dubina, Florea Dinu, Aurel Stratan, Norin Filip-Văcărescu (2014). "Calculul structural global al structurilor metalice. Recomandări, comentarii și exemple de aplicare în conformitate cu SR EN 1993-1-1 și SR EN 1998-1". Buletinul Construcțiilor, nr. 7/2014. ISSN 1222-1295, 201p.

Aurel Stratan coordinates several diploma works and master dissertations each year, the latter being correlated with the on-going research projects.

The author was recently involved in teaching activities of the European Erasmus Mundus Master Course "Sustainable Constructions under Natural Hazards and Catastrophic Events". He coordinated the module 2C09 "Design for seismic and climate changes" that were delivered in at the Politehnica University of Timisoara in the spring of 2014. Lecture notes are available at:

- Stratan, A., Grecea, D., D'Aniello, M., Dubina, D. (2014). "Design for seismic and climate changes: Lecture notes". <http://www.ct.upt.ro/suscos/2C09.htm>, European Erasmus Mundus Master Course - 520121-1-2011-1-CZ-ERA MUNDUS-EMMC, 2013-2015 edition, 859 p.

Part of the lectures was delivered by Aurel Stratan at the University of Naples Federico II in March 2015, as part of the 2014-2016 edition of the European Erasmus Mundus Master Course.

The author supported extra-curricular activities of the students from the faculty of civil engineering by delivering lectures within events organised by the International Association of Civil Engineering Students (IACES):

- Lecture "Earthquake engineering: an introduction" within the summer course IACES "TIMELESS", Timisoara, Romania, 18-25 July 2010.
- Lecture "Earthquake Action" within the summer course IACES "Exchange Building Challenges", Timisoara, Romania, 11 - 17 July 2005.

2 RESEARCH OUTCOMES

2.1 RE-CENTRING ECCENTRICALLY BRACED FRAMES

2.1.1 THE CONCEPT OF RE-CENTRING STRUCTURE

Most structures designed to modern codes would experience inelastic deformations even under moderate seismic action, and permanent (residual) displacements after a major earthquake. In such cases, the repair is difficult and there are different strategies to reduce structural damage. The most radical solutions to avoid such damage are base isolation and various implementations of active and semi-active structural control. Other strategies rely on supplemental damping conferred to the structure through various devices based on viscous, friction, or yielding dampers. While these solutions are efficient, they all require specialised knowledge at the design and erection stage, careful maintenance, and present a high initial cost.

However, the structural damage can be controlled by a more conventional design approach. Vargas and Bruneau (2006) investigated a design approach aiming at concentrating damage on removable and easy to repair "structural fuses", with the main structure designed to remain elastic or with minor inelastic deformations. With emphasis on buckling restrained braced frames, Kiggins and Uang (2006) showed that even if such structures exhibit a favourable energy-dissipating mechanism, the low post-yield stiffness of the braces leave the system vulnerable to unfavourable response such as large permanent drift. The potential benefit of using buckling-restrained braces in a dual system to minimize permanent deformations was shown to reduce significantly the residual story drifts.

Self-centring systems, a relatively new concept that addresses the drawbacks of the conventional yielding systems, have received much attention recently. Among many practical implementations, the following are most relevant to our study: self-centring moment-resisting frames with post-tensioned beam to column joints (Herning et al. 2011) and column bases (Chi and Liu 2012), self-centring concentrically braced frames (Roke and Jeffers 2011).

An alternative solution is to provide re-centring capability (as opposed to self-centring), by removable dissipative members and dual (rigid-flexible) structural configuration.

A dual eccentrically braced frame (EBF) with removable dissipative members (links) is shown in Figure 10 (Stratan and Dubina 2004). The link to the beam connection is done by a flush end-plate and high-strength friction grip bolts. The main advantage over other dissipative devices is that removable links can be designed using methods already available to structural engineers and can be fabricated and installed using standard procedures.

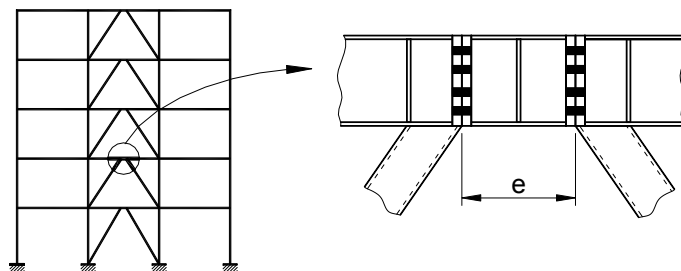


Figure 10. Bolted link concept (Stratan and Dubina 2004).

The re-centring of the system is attained by designing the structure as a combination of eccentrically braced frames (EBFs) and moment-resisting frames (MRFs). The elastic response of the flexible subsystem (MRF) provides the restoring forces, once the links damaged during an earthquake are removed. For this principle to be efficient the flexible subsystem should remain in the elastic range. Standard capacity design principles can be used to meet this objective. However, nonlinear structural analysis is advised. To ensure the elastic response of the flexible subsystem some members could be made in high-strength steel (Dubina et al. 2008). Additionally, the damaged links should be reasonably easy to remove. If the link deformations are small, links could be simply unbolted and then removed. In case of large residual link deformations, unbolting may prove difficult. In such a case the residual deformations should first be released by flame cutting the link.

2.1.2 DESIGN CRITERIA FOR DUAL FRAMES WITH RE-CENTRING CAPABILITY

Dual steel frames are obtained by combination of moment resisting frames (MRFs) and concentrically braced frames (CBFs) or eccentrically braced frames (EBFs). There are three requirements for design of dual frames in EN 1998-1 (2004): (1) a single behaviour factor is used for determining the design seismic action, (2) seismic forces should be distributed between the different frames according to their elastic stiffness and (3) each structural subsystem (MRFs, CBFs, EBFs) should be designed according to their specific provisions. An additional requirement can be found in other codes (e.g. NEHRP, 2003, P100-1, 2006): the MRFs should be able of resisting at least 25% of the total seismic force. This last requirement is based on judgement (NEHRP, 2003). According to code rules, the main benefit of dual configuration is the possibility to adopt larger values of behaviour factor (EN 1998-1, 2004; NEHRP 2003) in comparison with simple braced frames or structural walls, due to larger redundancy of the dual system.

Several researchers (Akiyama, 1999; Iyama and Kuwamura, 1999; Astaneh-Asl, 2001) investigated seismic performance of dual systems, consisting of rigid and flexible subsystems. Akiyama (1999) showed that "flexible-stiff" structural types belong to the most efficient earthquake resistant structures. It is believed that the flexible subsystem will prevent excessive development of drifts, while the rigid subsystem will dissipate seismic energy by plastic deformations. Iyama and Kuwamura (1999) studied the probabilistic aspect of dual systems. The dual system was obtained by combining a generic CBF and MRF, with different natural periods of vibration. The obtained dual structure was termed "fail-safe", because it provides an alternative load path to earthquake loading (MRF) in case of failure of the primary system (CBF). Analyses on single degree of freedom systems showed that a dual system has a higher safety factor than a homogeneous system, considering the unknown characteristics of future earthquakes. It was also showed that the benefits of the dual system is enhanced when the difference between the natural periods of the subsystems is large, and when the ductility of the subsystems is small. Astaneh-Asl (2001) studied steel shear wall structures, emphasizing the importance of multiple lines of resistance, naturally achieved by combining a steel shear wall and a MRF.

A different use of dual frames is the one in which removable dissipative members are employed in the rigid subsystem. Provided the flexible subsystem does not yield, and the inelastic deformations are constrained to the removable members alone, the flexible subsystem would provide the restoring force necessary to re-centre the structure once the damaged dissipative members are removed. It would be possible then to install new dissipative members, regaining the original strength of the structure.

Vargas and Bruneau (2006) investigated a design approach aiming to concentrate damage on removable and easy to repair structural elements ("structural fuses"), with the main structure designed to remain elastic or with minor inelastic deformations. A systematic procedure was proposed to design buildings with metallic structural fuses. Kiggins and Uang (2006) showed that

even if buckling restrained braced frames exhibit a favourable energy-dissipating mechanism, the low post-yield stiffness of the braces leave the system vulnerable to unfavourable behavioural characteristics such as large permanent drift. The potential benefit of using buckling-restrained braces in a dual system to minimize permanent deformations was investigated and shown to reduce significantly residual story drifts.

In order to analyse the factors controlling the two requirements for structures with removable dissipative elements (isolation of damage and re-centring capability), it is useful to consider a simple dual system consisting of two inelastic springs connected in parallel (see Figure 11a). Provided that the flexible subsystem is not very weak, plastic deformations appear first in the rigid subsystem. In order to maximize system performance, plastic deformations in the flexible subsystem should be avoided. At the limit, when the yield force F_{yf} and yield displacement δ_{yf} are attained in the flexible subsystem, the rigid subsystem experiences the yield force F_{yr} and the total displacement $\delta_{yr} + \delta_{plr}$ (see Figure 11b). Equating the two displacements:

$$\delta_{yf} = \delta_{yr} + \delta_{plr} \quad (1)$$

and considering the relationship between force and deformation ($F = k \cdot \delta$), it can be shown that:

$$\mu_D = \frac{\delta_{yr} + \delta_{plr}}{\delta_{yr}} = \frac{\delta_{yf}}{\delta_{yr}} = \frac{F_{yf}}{F_{yr}} \cdot \frac{K_r}{K_f} \quad (2)$$

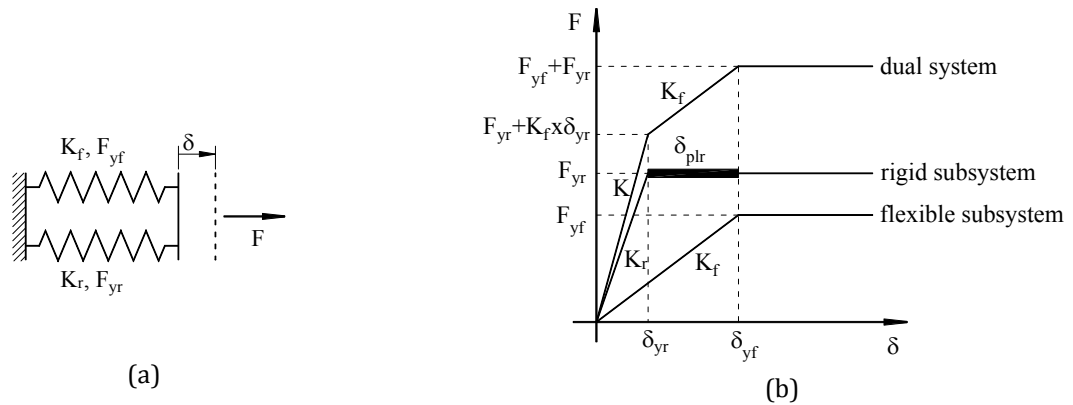


Figure 11. Simplified model of a generalized dual system.

The notation μ_D represents the "useful" ductility of the rigid subsystem, for which the flexible subsystem still responds in the elastic range. It can be observed that there are two factors that need to be considered in order to obtain a ductile dual system with plastic deformations isolated in the rigid subsystem alone. The first one is the ratio between the yield strength of the flexible and rigid subsystems (F_{yf}/F_{yr}), while the second one is the ratio between the stiffness of the rigid subsystem and the one of the flexible subsystem (K_{yf}/K_{yr}). The larger are these two ratios, the larger is the "useful" ductility μ_D of the dual system.

Re-centring capability of the dual system is not easily attainable. Though the dual configuration results in smaller permanent drifts δ_{pd} in comparison with permanent deformations of the rigid system alone δ_{pr} (see Figure 12a), they are not eliminated completely after unloading. After unloading of the dual structure, there is a residual force in the rigid subsystem (F_{pr}) equal to the opposing force in the flexible subsystem (F_{pf}), see Figure 12b. However, permanent deformations can be eliminated if the rigid subsystem is realised to be removable. Once removable elements are dismantled, stiffness and strength of the system is provided by the flexible subsystem alone. If the

flexible subsystem is still in the elastic range, it will return the system to the initial position, implying zero permanent deformations.

When designing a dual system, the size of structural members will be governed by the characteristics of the rigid subsystem, which provides most of the strength and stiffness to lateral forces. If removable dissipative members are used, then the characteristics of the flexible subsystem should be chosen such that it would remain in the elastic range up to displacements corresponding to attainment of ultimate deformations in the rigid subsystem. This requirement could be expressed as:

$$\delta_{yf} \geq \delta_{ur} = \delta_{yr} + \delta_{plr} \quad (3)$$

where δ_{ur} ultimate displacement of the rigid subsystem.

Thus, the ability of the flexible subsystem of a dual structure with removable dissipative members in the rigid subsystem to provide the re-centring capability (see equations (2) and (3)) depends on:

- the demand of inelastic deformations in the rigid subsystem $\delta_{ur} = \delta_{yr} + \delta_{plr}$, and
- the yield displacement $\delta_{yf} = F_{yf}/K_f$ in the flexible subsystem.

The yield displacement in the flexible subsystem is controlled by both strength and stiffness ($\delta_{yf} = F_{yf}/K_f$). Therefore, the code requirement for the flexible subsystem in dual frames in terms of strength only may not assure the desired behaviour for dual structures with removable dissipative members.

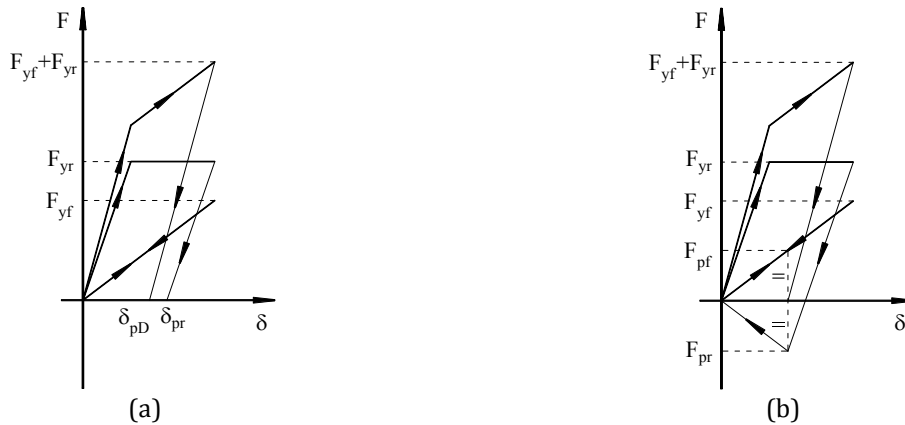


Figure 12. Permanent deformations in a conventional dual system (a) and in a dual system with removable dissipative members (b).

The basic design requirement for dual frames with removable dissipative members is to prevent yielding in MRFs up to the attainment of ultimate deformation capacity in the EBF with removable links, checking the equation (3). Simple procedures suitable for design are required in order to estimate the ultimate displacement in EBFs, as well as displacement at yield in the MRFs. Therefore, strength (F_y) and stiffness (K) need to be known for basic components of the system: an eccentrically braced frame (see Figure 13a) and a moment-resisting frame (Figure 14).

From the free-body diagram of the basic EBF (see Figure 13a), and considering the fact that plastic deformations should be constrained to the link, and sketching the free-body diagram of half the basic EBF (see Figure 13b), the yield strength of the EBF (F_{yEBF}) could be determined as:

$$F_y^{EBF} = \frac{L}{H} V_{pl,link} \quad (4)$$

where $V_{pl,link}$ is the shear strength of the link.

The most important components contributing to the stiffness of an EBF are the link shear deformation and brace axial deformation. It can be shown that the stiffness to lateral forces of these two components can be expressed as:

$$K_{link}^{EBF} = \frac{L}{H^2} (L - e) \frac{G \cdot A_s}{e} \quad (5)$$

$$K_{br}^{EBF} = 2 \frac{E \cdot A}{l_{br}} \cos^2 \alpha \quad (6)$$

where G is the shear modulus, A_s is the link shear area, E is the Young's modulus, A is brace cross-section area, l_{br} is the brace length, while the other notations are shown in Figure 13.

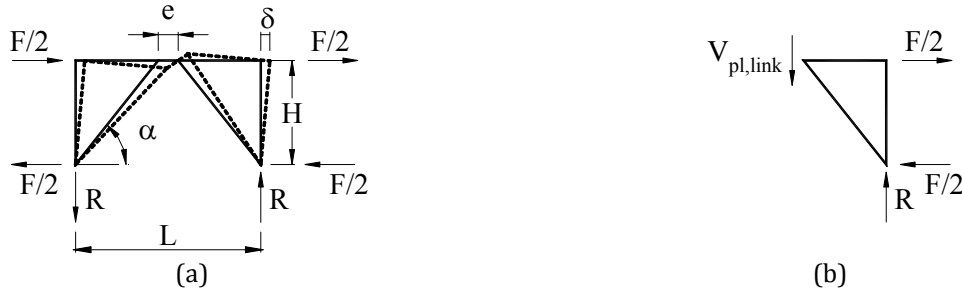


Figure 13. Basic one-storey EBF component.

The total stiffness of the EBF can be obtained by combining the contribution due to shear of the link with the one due to axial deformation of braces:

$$K^{EBF} = \frac{K_{link}^{EBF} \cdot K_{br}^{EBF}}{K_{link}^{EBF} + K_{br}^{EBF}} \quad (7)$$

Once the strength (eq. (4)) and stiffness (eq. (7)) of the one-storey components of a EBF are known, the ultimate displacement of the EBF can be determined as the sum of the yield displacement and the plastic displacement (see eq. (3)). The latter is controlled by the plastic deformation capacity of the link ($\gamma_{pl,u}$) and the geometry of the EBF. Thus, the ultimate displacement of the EBF can be determined as:

$$\delta_u^{EBF} = \delta_y^{EBF} + \delta_{pl}^{EBF} = \frac{F_y^{EBF}}{K^{EBF}} + \frac{e}{L - e} \cdot H \cdot \gamma_{pl,u} \quad (8)$$

The basic MRF component can be idealised as an assembly of a beam and two columns shown in Figure 14a, assuming inflexion points at half the storey height. From the free-body diagram of the MRF (see Figure 14a), and considering the fact that plastic deformations should develop at beam ends, and sketching the free-body diagrams of the beam and the column (see Figure 14b), the yield strength of the MRF could be determined as:

$$F_y^{MRF} = \frac{2M_{pl,b}}{H} \quad (9)$$

where $M_{pl,b}$ is the beam plastic moment.

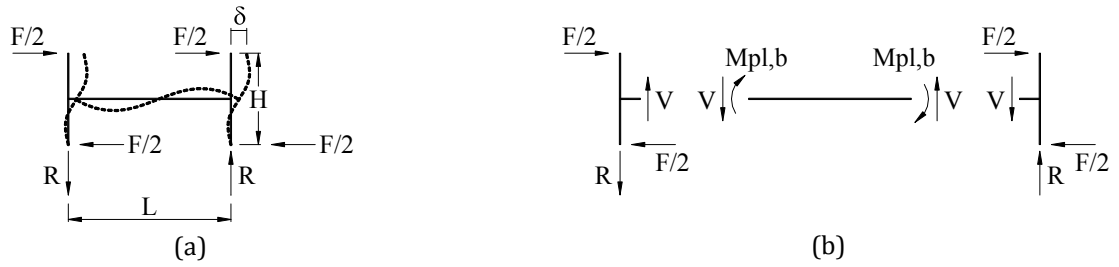


Figure 14. Basic one-storey MRF component.

Considering the flexural deformations only, the stiffness of the basic MRF component can be determined as:

$$K^{MRF} = \frac{2}{H^2 \left(\frac{L}{6 \cdot E \cdot I_b} + \frac{H}{12 \cdot E \cdot I_c} \right)} \quad (10)$$

where I_b is the moment of inertia of the beam and I_c is the moment of inertia of the column.

Once the strength (see eq. (9)) and stiffness (see eq. (10)) of the one-storey components of a MRF are known, the yield displacement of the MRF can be determined as:

$$\delta_y^{MRF} = \frac{F_y^{MRF}}{K^{MRF}} \quad (11)$$

In order to assure the re-centring capability to the dual eccentrically braced frames, it is necessary that yielding in the moment-resisting frames is prevented up to large enough plastic deformations in the dissipative components (links) of the eccentrically braced frames. The design verification that needs to be checked is thus:

$$\delta_u^{EBF} \leq \delta_y^{MRF} \quad (12)$$

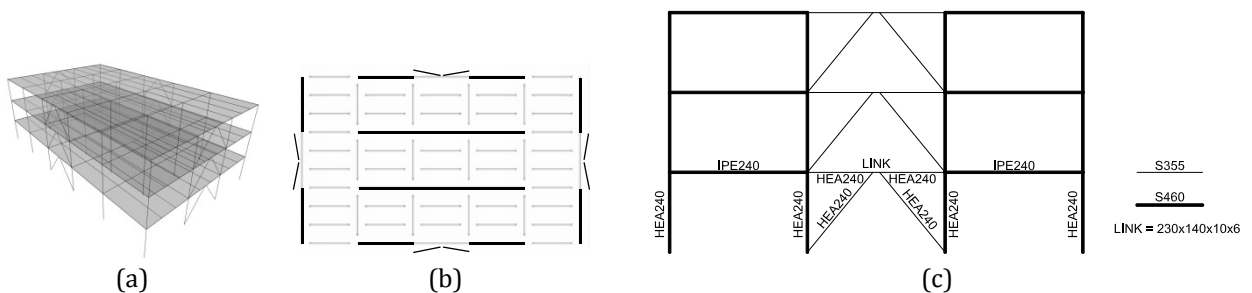


Figure 15. Structural configuration: a) 3D view; b) plan view; c) transversal end wall frame

A medium rise frame structure was considered to check numerically the analytical procedure. The building has 3 spans of 6 meters and 5 bays of 6 meters. Building has 3 storeys of 3.5 meters each. In each direction, the main lateral load resisting system is made by two braced frames, located on the perimeter (Figure 15a). Additionally, there are 4 moment resisting frames on transversal directions and 10 moment resisting frames on longitudinal direction (represented with thick lines), to assure the restoring forces after an earthquake (Figure 15b). All other beams have pinned ends. The columns are pinned at the base. The design was carried out according to EN1993, EN1998 and

Romanian seismic design code P100-1/2006. A 5.0 kN/m² dead load and 3.0 kN/m² live load were considered. The building is located in Bucharest, characterised by the following seismic parameters: 0.24g design peak ground acceleration, soft soil conditions with $T_c=1.6s$, a behaviour factor $q=6$ and interstorey drift limitation of 0.008 of the storey height. Columns are made of HEA240 profiles. Beams in the moment resisting frames are made of IPE240. Braces and beams in the braced frames are made of HEA240 profiles while links are made of welded H section 230x140x10x6 mm (Figure 15.c).

In order to concentrate the plastic deformations in links and keep the MRFs in the elastic range, different steel grades were used for members (Dubina et al., 2008). Thus, the beams in moment resisting frames and the columns are made from HSS steel (grade S460), while all other members, including braces and links are made from mild carbon steel (grade S355) (Figure 15.c). A removable bolted link was used.

The analysis was performed with SAP2000 computer program. Inelastic behaviour of beams, columns and braces were modelled with concentrated plastic hinges. The inelastic shear link element model was based on the Ricles and Popov (1994) proposal, but adapted to the bilinear envelope curve available in SAP2000. The stiffness of bolted links was reduced to an equivalent stiffness of 0.25 of the theoretical shear stiffness of continuous links (Dubina et al., 2008). The ultimate link deformations at ULS was considered $\gamma_{pl,u}=0.10$ rad. In order to assess the structural performance of the structure, nonlinear static analyses were performed. Analyses were done on a planar end wall transversal frame, extracted from the 3D structure, with seismic mass corresponding to half of the total floor masses, in order to take into account that, in the 3D structure, the end wall braced frames carry horizontal seismic forces from internal frames also. The lateral force pattern, used in the push-over analysis, has a "uniform" distribution and is proportional to mass, regardless of elevation (uniform response acceleration). One matter of interest in case of dual frames is the contribution of the moment resisting frames to the stiffness and strength of the entire structure. Therefore, in order to evaluate the participation of each part, the structure was analyzed in 3 different situations, which are (Figure 16):

- EBF: outer frames are pinned, no contribution to the lateral resisting system
- MRF: outer frames are rigid, braces are removed
- DUA (EBF + MRF): both braces and moment frame are active

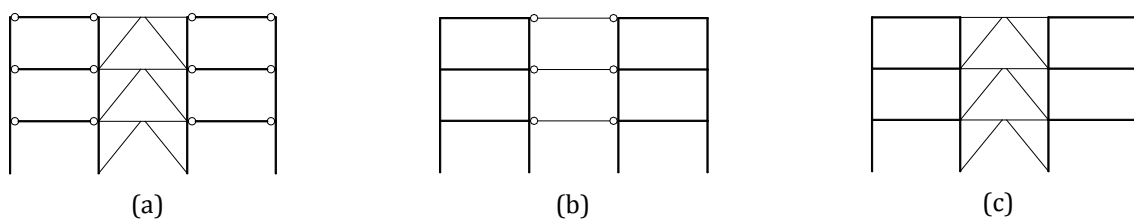


Figure 16. Contribution to the dual structure: a) EBF configuration; b) MRF configuration; c) DUA configuration.

Table 1. Comparison of analytical and numerical predictions of storey displacements.

	δ_{uEBF} , mm	δ_{yMRF} , mm	$\delta_{yMRF}/\delta_{uEBF}$
Analytical	20.6	82.8	4.0
Numerical	22.6	80.5	3.6

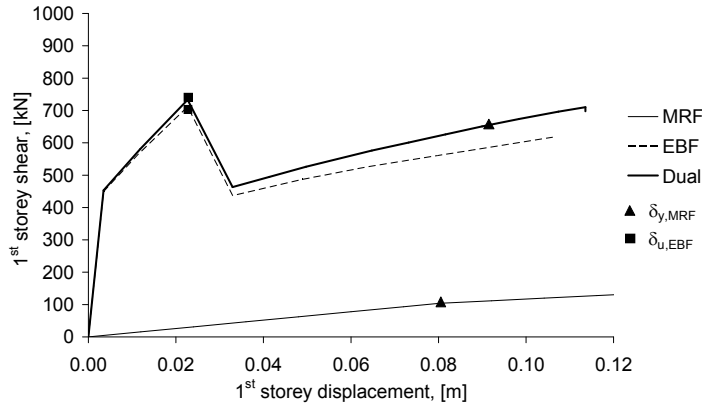


Figure 17. Storey pushover curves for EBF, MRF and DUA configurations

The analytical procedure involves checking that the displacement corresponding to ultimate deformation of the EBF is smaller than the displacement corresponding to first yield in the MRF. Storey pushover curves for the EBF, MRF and DUA structures are shown in Figure 17. First plastic hinge in beams is marked on the curves, together with the attainment of ultimate rotation in the links. Table 1 presents a comparison of yield displacements in the MRFs and ultimate displacements in the EBF for the first storey, where largest demands are present. Fair agreement can be observed between analytical and numerical results.

2.1.3 EXPERIMENTAL TESTS ON ONE-STOREY ECCENTRICALLY BRACED FRAME

Three series of experimental tests on removable link assemblies were carried out at the Politehnica University of Timisoara in order to determine cyclic performance of bolted links and to check the feasibility of the removable link solution (Stratan and Dubina 2004, Dubina et al. 2008, Danku, 2011). The first series of tests was realised on isolated links (see Figure 18a), while the other two on almost full-scale model of a single bay and single storey eccentrically braced frame with removable link (see Figure 18b).

The first series of tests on links showed an important influence of the connection on the total response of the bolted link, in terms of stiffness, strength and overall hysteretic response. Shorter links were found to be suitable for the bolted solution, as plastic deformations were constrained to the link, while the connection response was almost elastic, allowing for an easy replacement of the damaged link.

The second series of tests consisted in 8 almost full-scale frame specimens, representing a one-bay one-storey eccentrically braced frame sub-assembly (see Figure 18). The main parameter of the test was the thickness of the end-plates of link-beam connections. The links were designed and constructed with three thicknesses of the end plate: $t = 10$ mm, $t = 15$ mm and $T = 20$ mm. Two tests were performed for each type of link-beam connection: one monotonic and one cyclic. Cyclic tests were performed according to the ECCS procedure. Monotonic tests were performed at positive displacement (compression in the beam). Additionally, for specimens with 15mm and 20mm thick link end-plates, monotonic tests under negative displacement (tension in the beam) were performed as well. Table 2 summarizes synthetically the experimental program. For testing the eight specimens a single frame was used, changing after each test the damaged removable links.

To ensure a predominantly elastic response of the link-beam connection, the capacity design was used. Thus, connection action effects, shear force $V_{j,Ed}$ and flexural moment $M_{j,Ed}$ were determined according to the following relationships:

$$V_{j,Ed} = \gamma_{ov} \cdot \omega \cdot V_{pl,link} \quad (13)$$

$$M_{j,Ed} = \frac{V_j \cdot e}{2} \quad (14)$$

where

$V_{p,link}$ is the shear resistance of the link, according to EN 1998-1 (2004) and P100-1 (2006)

γ_{ov} is the ratio between the actual and the nominal values of the yield strength of dissipative elements (considered equal to 1.25, according to EN 1998-1 (2004) and P100-1 (2006))

ω is the ratio between the maximum and the yield shear force (amounting to 1.5, according to data from previous experimental tests and literature)

e is the link length.

Shear strength ($V_{j,Rd}$) and flexural strength ($M_{j,Rd}$) of the link connection were determined according to EN 1993-1-8.

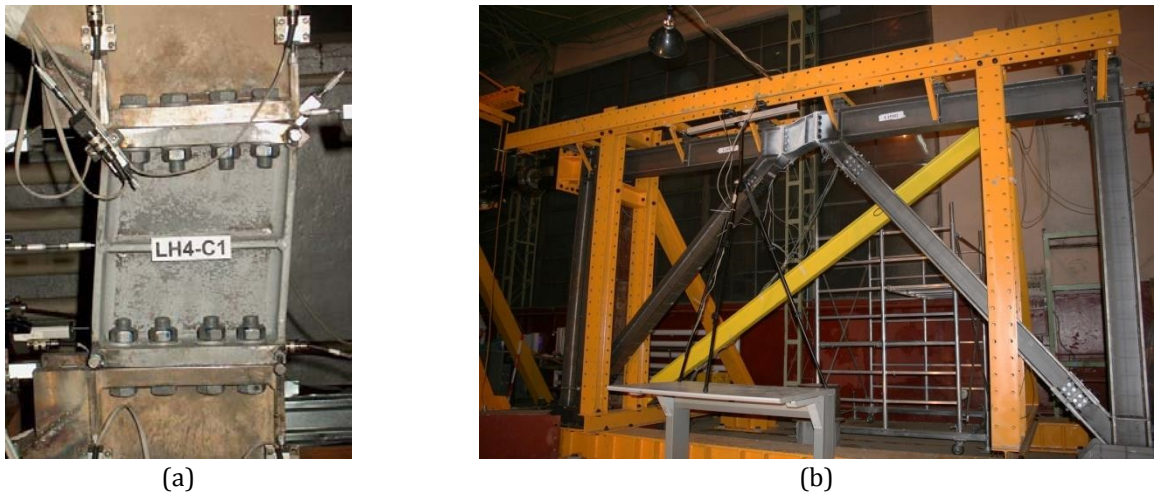


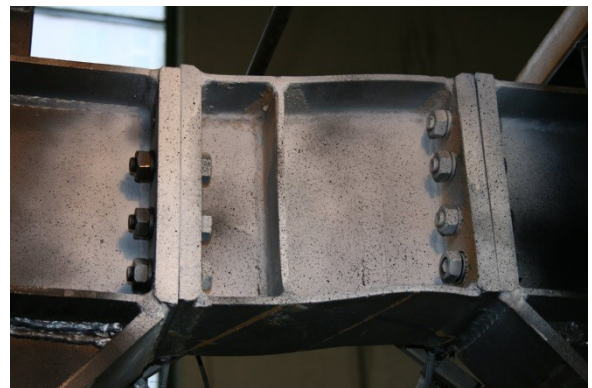
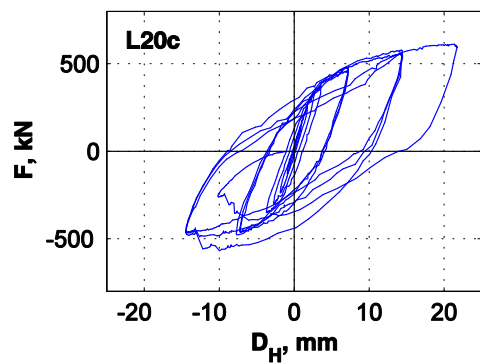
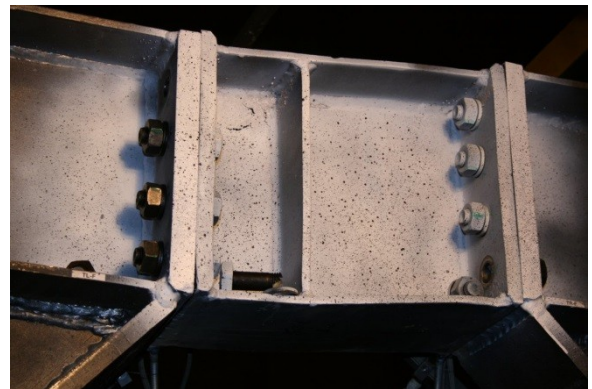
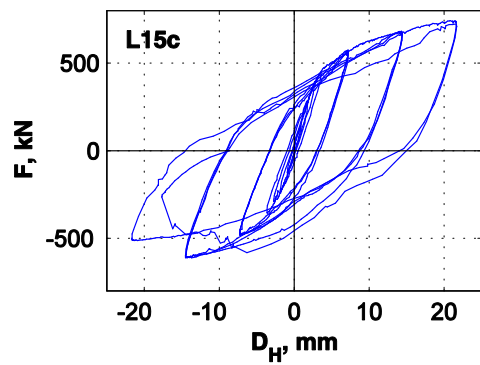
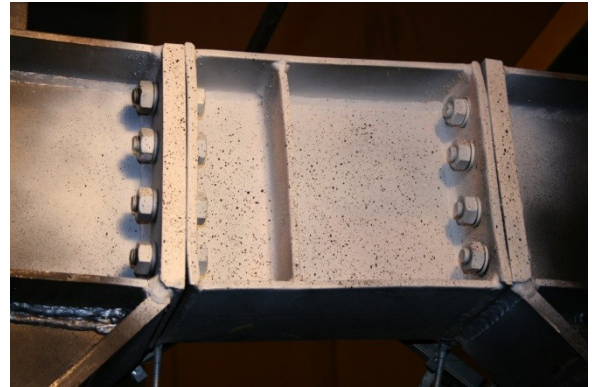
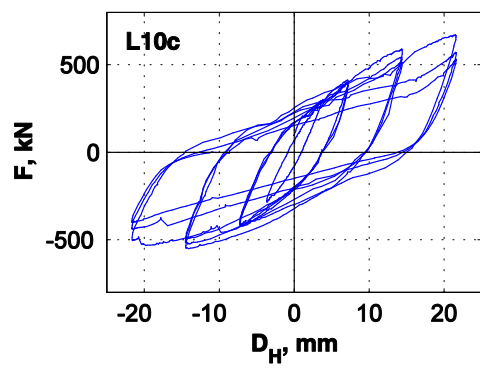
Figure 18. Experimental test on removable bolted link (a) and tests on almost full-scale frame with bolted links (b).

Table 2. Experimental program.

Specimen	L10m1	L15m1	L20m1	L10c	L15c	L20c	L15m2	L20m2
End-plate thickness t_{ep} , mm	10	15	20	10	15	20	15	20
Loading type	monotonic (positive)			cyclic			monotonic (neg.)	

Table 3. Properties of link connections.

t_{ep} , mm	Bolts	$V_{j,Ed}$, kN	$V_{j,Rd}$, kN	$M_{j,Ed}$, kNm	$M_{j,Rd}$, kNm	Failure mode
10	M16 gr 8.8	268.3	137.8	40.2	33.4	Mode 1-2
15			223.9		49.5	Mode 2
20			268.8		52.4	Mode 3



(a)

(b)

Figure 19. Lateral force vs. displacement (a) and failure mode (b) of the specimens L10c, L15c and L20c.

Table 3 presents the design values of shear force and bending moment in the link connection, the design resistance of shear force and bending moment, as well as failure mode of the endplate. Only one connection has the necessary strength in shear and bending – the one with a thickness of 20 mm. The governing failure mode of the end plate is mode 3, through bolt fracture. The other two connections (with end-plate thicknesses of 15 mm and 10 mm) were considered in order to investigate the possibility of relaxing the connection design criteria given by equations (13) and (14), as well as by the factor ω . The connection with end-plate thickness of 15 mm is not strong enough in shear, while the end plate fails in mode 2 – combined bolt and end-plate. The connection with end-plate thickness of 10 mm is not strong enough neither in shear nor in bending, and the end plate fails in mode 2, but close to mode 1 (end plate only). Friction grip mechanism was not accounted for when determining the shear strength of the connections, though bolts have been

pretensioned. It was considered that cyclic loading and inelastic response of the link would render friction grip ineffective.

Figure 19 presents the lateral force vs. displacement relationship (a) and failure mode (b) for specimens L10c, L15c and L20c, subjected to cyclic loading.

Monotonic tests under positive loading showed excellent ductility, the link-beam connection having a quasi-elastic response. These specimens failed by complete yielding of the link. Specimens tested monotonically under negative loading showed lower capacities and ultimate deformations than the one subjected to positive loading. This response occurred due to tensile forces present in the link connection under negative loading.

Response of specimens subjected to cyclic loading was influenced to a great extent by the different behaviour of the connection under positive and negative loading. Thus, the failure mode of these specimens was governed by negative semi-cycles.

Endplate thickness did not have a significant influence on the initial stiffness at the frame level, but affected the ductility of the structure under negative displacements. Endplate thickness had a minimal influence on the overall response of frames for monotonic tests under positive loading due to compression forces in the connection, which reduced tensile stresses in bolts and favoured the elastic response of the joint.

The monotonic negative loading generated tensile forces in the link connection. The compound effect of tensile axial force and bending generated high demands in the end plate and bolts. As a result, the maximum force and deformation capacity of the removable link and of the frame decreased (Figure 20). The weakest performance was observed for the specimen with the thicker end plate, due to the fact that deformation demands concentrated mostly in the bolts, with a relatively brittle behaviour.

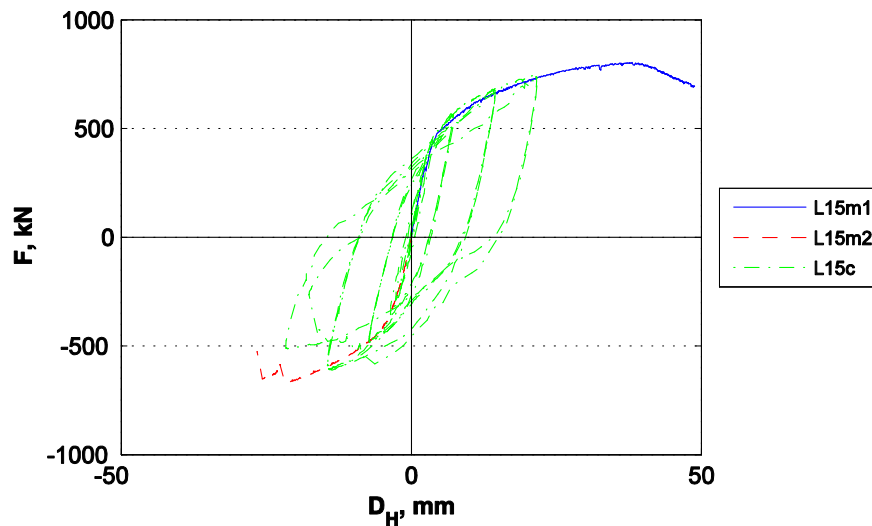


Figure 20. Lateral force vs. displacement for specimens L15m1, L15m2 and L15c.

Under cyclic loading, the effect of end-plate thickness is not so straightforward. Thus, under negative loading, tensile axial force leads to higher demands in the bolts, which produces a reduction in the maximum force and deformation capacity of the frame. The most important reduction of maximum force and deformation capacity was observed for connections with thicker end-plates (L15c and L20c), as most of the inelastic demands concentrate in the bolts. For the specimens with thin end plate (L10c), the inelastic deformation demands is shared by the end plate and bolts, which leads to an improved ductility of these specimens. However, the small thickness of the end plate leads to a gradual degradation of stiffness and strength due to low-cycle fatigue effect.

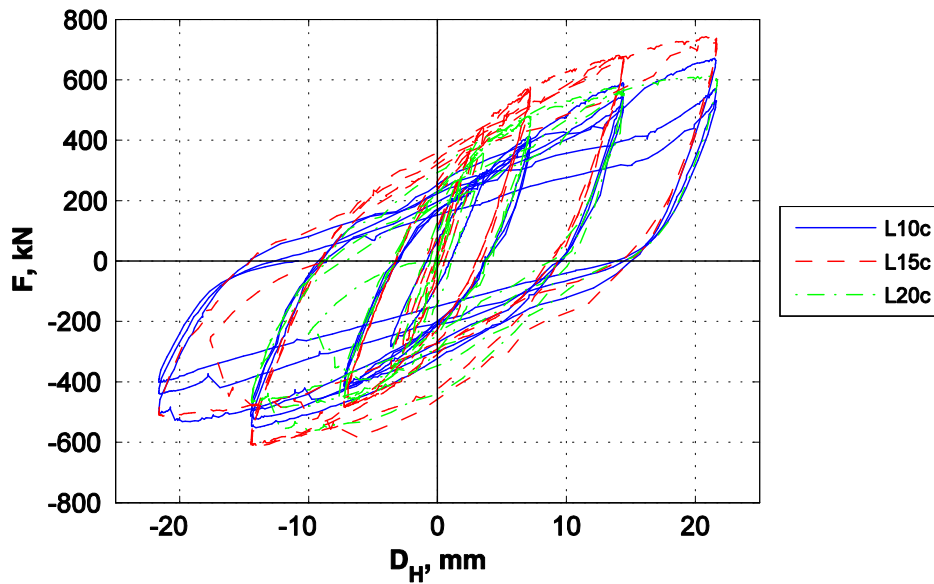


Figure 21. Lateral force vs. displacement for specimens L10c, L15c and L20c: influence of end plate thickness.

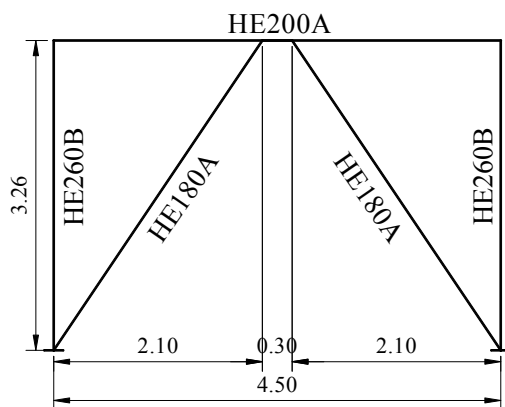


Figure 22. Dimensions and layout of the tested frame.



Figure 23. Experimental setup.

At the frame level, the experimental tests showed that the removable link solution is feasible. Inelastic deformations were constrained to the removable links alone, all other frame members and connections remaining in the elastic range. Additionally, it was possible to replace the damaged removable links with new elements.

The third series of tests concerned experimental validation of link removal process. The main objective of test was to check the procedure used to remove the link following plastic deformations likely to occur under a design earthquake. Oxy-fuel cutting was used in order to release the residual stresses in the link after unloading.

In order to provide the elastic restoring force necessary in order to pull back the eccentrically braced steel frame after link removal, the columns were realised with a fixed base. The main structural dimensions and layout are shown in Figure 22, while the experimental setup in Figure 23. The force was applied at the column top by a hydraulic servo-actuator. The load cell integrated in the actuator was used to record the applied force.

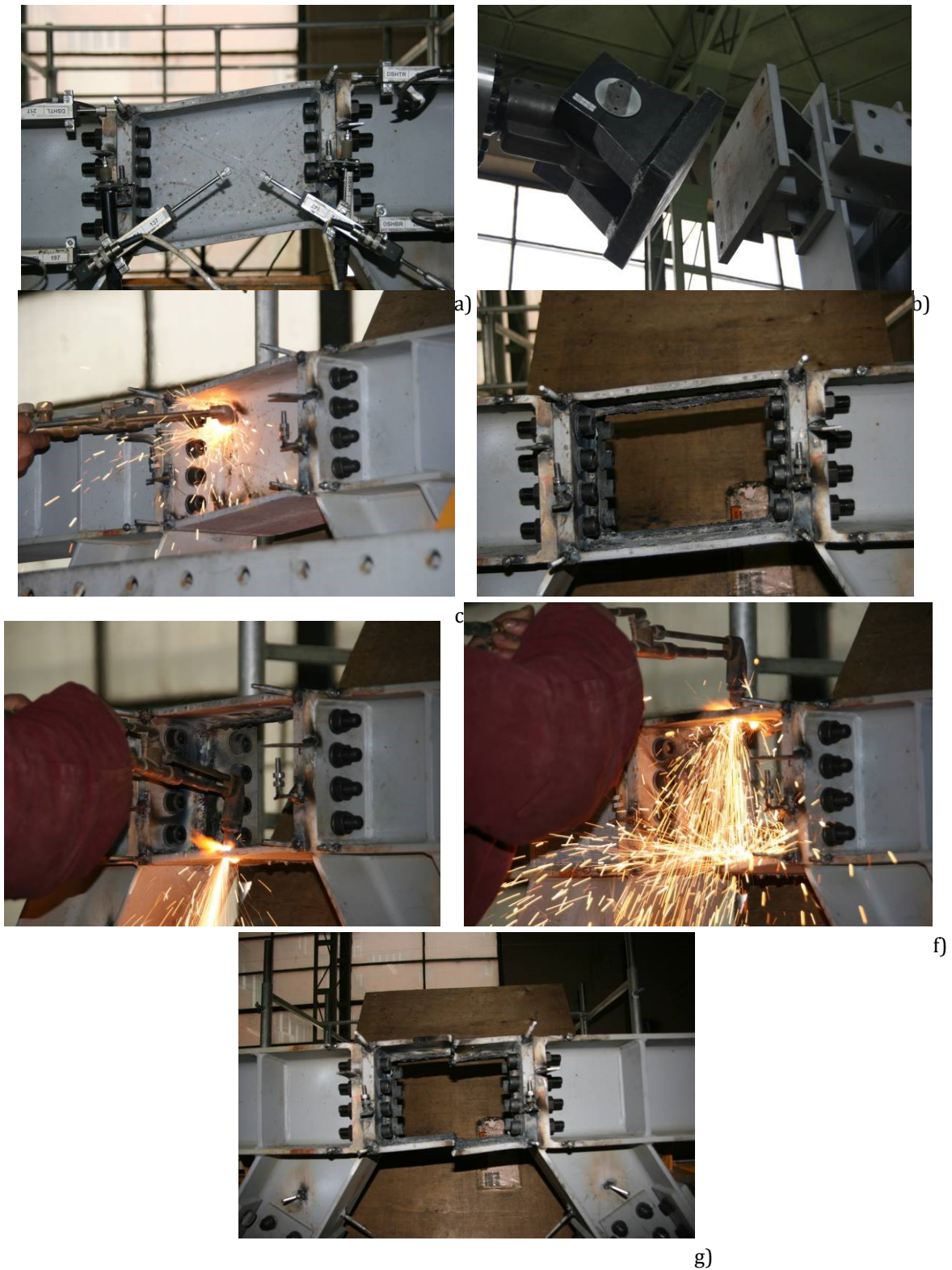


Figure 24. Link removal procedure for the second specimen.

Displacement transducers were used to monitor different absolute or relative deformations or displacements between different components. They were positioned in order to record deformations that can be divided into three main categories: (1) global deformations of the frame; (2) deformations of the dissipative element – bolted link; (3) slip and deformations of the non-dissipative elements.

The specimen was loaded monotonically up to a lateral top displacement of 37.4 mm (Figure 24a), corresponding roughly to a link shear deformation of 0.1 rad, but with an intermediate unloading at 0.05 radians. After unloading and removal of the actuator (see Figure 24b) the top displacement amounted to 23 mm. After oxy-fuel cutting of the link's web (see Figure 24c-d), the top displacement dropped to about 11 mm. It was concluded that removing the link web by oxy-fuel cutting is not enough for eliminating the residual stresses in the link, due to the fact that flanges have an important contribution to the ultimate shear strength of the link. Therefore, the bottom flange of the link was also cut (see Figure 24e), followed by the upper one (see Figure 24f). Following complete removal of the link by oxy-fuel cutting both the web and the flanges, the residual top displacement amounted to a value of 0.65 mm (see Figure 25 and Figure 26).

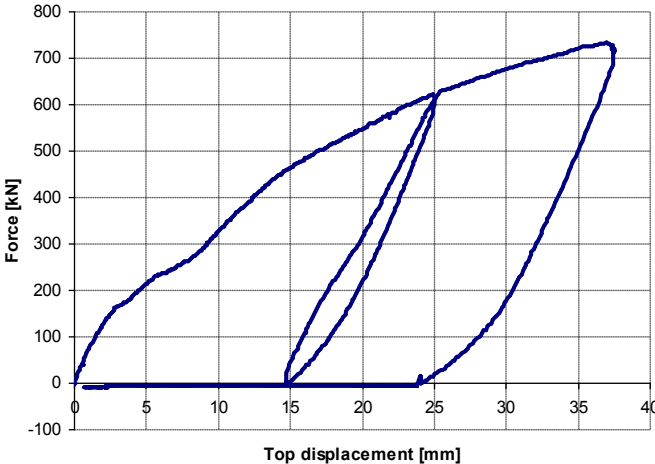


Figure 25. Load-displacement curve.

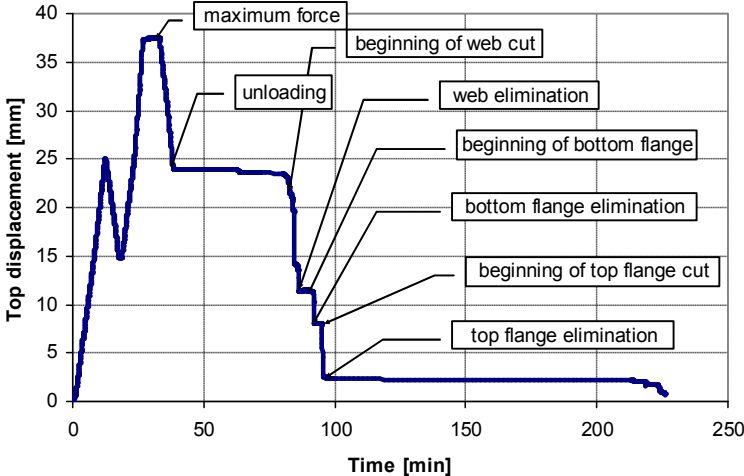


Figure 26. Top displacement vs. time response.

The non-dissipative elements such as the braces and the columns did not suffer any unwanted damage, nor did their connections (except from slips in the braces connections). These elements remained in the elastic domain. The fixed column base did not slip, and the beam-to-column connections behaved in a satisfactory manner.

From the performed tests it can be concluded that both the web and flanges have to be flame cut in order to allow easy replacement of the links. There were no particular technological problems or special safety measures necessary during link removal and replacement.

2.1.4 LARGE-SCALE TESTS ON RE-CENTRING DUAL ECCENTRICALLY BRACED FRAME

A full-scale experimental investigation on a dual eccentrically braced frame with replaceable links was performed at the European Laboratory for Structural Assessment (ELSA) of the Joint Research Centre (JRC) in Ispra, Italy. Its objectives were to: (1) validate the re-centring capability of dual structures with removable dissipative members (links), (2) assess overall seismic performance of dual eccentrically braced frames and (3) obtain information on the interaction between the steel frame and the reinforced concrete slab in the link region. The prototype structure had 3 spans of 6 meters and 5 bays of 6 meters, and 3 storeys with the height of 3.5 meters each. The main lateral load resisting system is composed of eccentrically braced frames. Additionally, there are 4 moment resisting frames in transversal directions and 10 moment resisting frames in longitudinal (test) direction, to assure the restoring forces after an earthquake. Considering that in the transversal direction the lateral force resisting system is located on the perimeter frames only, and in order to reduce the cost of the experimental campaign, the test structure is composed of the two end frames only (Figure 27a).

The test structure was devised in order to study two alternative solutions of the slab – link interaction. In the south frame the removable link was disconnected from the reinforced concrete slab, by an additional secondary beam placed in parallel with the beam containing the link (Figure 27b). A conventional solution was adopted in the north frame, where the slab was cast over links, but no shear studs were used in the link region.



Figure 27. The experimental mock-up in front of the reaction wall (a) and plan layout (b) of the test structure.

The prototype structure was designed according to EN1990, EN1991, EN1992, EN1993, EN1994 and EN1998. Gravity loads of 4.9 kN/m² (permanent load) and 3.0 kN/m² (live load) were considered. The structure was assumed to be located in an area characterised by 0.19g peak ground acceleration and stiff soil conditions (EC8 spectrum for soil type C). A behaviour factor $q = 4$ (ductility class M) and inter-storey drift limitation of 0.0075 of the storey height were assumed. The structural steel components were designed using S355 grade steel, with two exceptions. Grade S460 steel was used for the columns, in order to obtain a larger capacity without increasing the stiffness. This approach helps promote elastic response of non-dissipative components. Links were designed using S235 grade steel (which was replaced during fabrication with the equivalent DOMEX 240 YP B).

Pre-test numerical simulations

In order to assess the structural performance and to validate the feasibility of the link removal procedure, numerical analyses were made on a model of the test structure using SeismoStruct software (Seismosoft, 2011). In the pseudo dynamic (PsD) test campaign the equation of motion will be solved for the frame 1 (with links) disconnected from the slab, and the resulting displacements applied to both frames. Therefore, a 2D numerical model was used in which force-based plastic hinge elements for beams and columns were used. For braces, the physical theory model is used (two force based plastic hinge elements per brace; initial out-of-plane member imperfection).

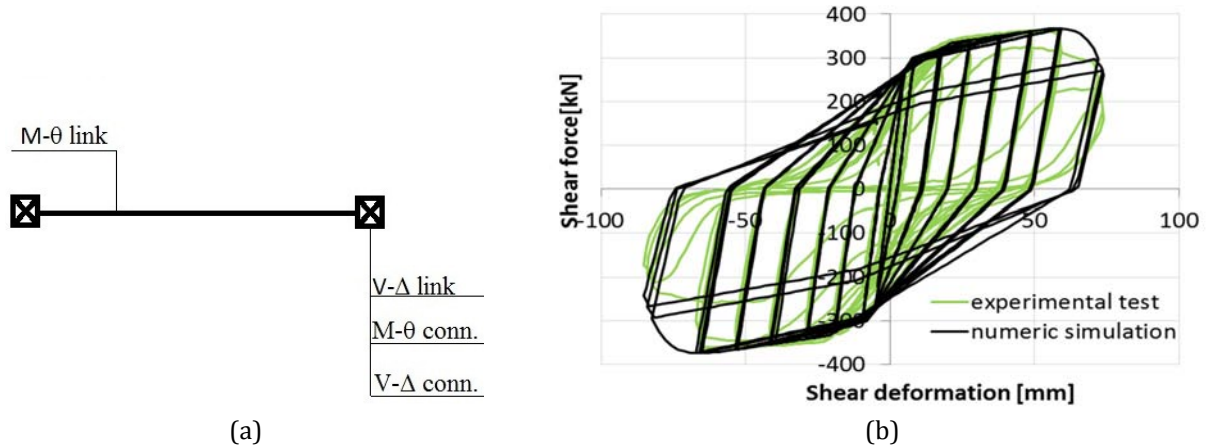


Figure 28. Link model (a); Shear force – displacement relationship for the LH5 link (b).

Bolted links were modelled using a force-based inelastic beam with a rotational spring at each end. The former was used in order to model the flexural stiffness of the link, while the latter were used in order to account for shear stiffness of the link, as well as rotational deformations and slip in the bolted connection (Figure 28a). The rotational springs were modelled using multi-linear link elements that can simulate the deteriorating behaviour of strength, stiffness and slip. Material characteristics obtained from quality certificates were used. The numerical model of the removable links was calibrated using the experimental results obtained from removable links tests at Politehnica University of Timisoara, for a link with the effective length of 400 mm, with properties similar to the links in the DUAREM structure. Figure 28b shows a comparison between the experimental and calibrated numerical response. The calibrated numerical model was adopted for the DUAREM links and introduced in the numerical model of the test structure. Shear deformation reported in Figure 28 refer to the total deformation of the link, with contributions due to shear of the element and rotation and slip in the two connections of the link.

Pushover analyses were performed on the model described above in order to estimate the capacity of actuators and check the plastic mechanism. Two lateral load patterns were considered: modal (inverted triangular) and uniform. The pushover curves are shown in Figure 29, together with some characteristic events: first yielding in links, attainment of ultimate deformation capacity in links, first yielding in elements other than links. It can be observed that all elements outside links yield after attainment of ultimate deformation capacities in links. This proves that moment-resisting frames can provide the restoring force up to complete failure of links.

Seven natural records were selected by matching EC8 elastic response spectrum used in the design. The records were selected from the RESORCE database (Akkar et al., 2014), the main selection criteria being the matching of the control period to the one of the target spectrum ($T_c = 0.6$ sec). The records were then scaled to the target spectrum using EN 1998-1 rules. Structural performance was evaluated for the limit states shown in Table 5. The key parameters of structural response at

the limit states considered are shown in Table 4. Acceptance criteria for shear links were based on FEMA 356 (0.005 rad at DL, 0.11 rad at SD and 0.14 rad at NC).

At the Damage Limitation (DL) limit state all structural components except links are in the elastic range. Shear deformations in links exceed the FEMA 356 limits, but this is expected, since the design carried out according to EN 1998-1 did not impose any limitation on yielding of structural members at DL limit state. Even so, permanent interstorey drifts remain very low (0.007 % or 0.2 mm in average, and a maximum value of 0.028 % or 0.98 mm). In these conditions, the advantage of the proposed system is obvious, since the damaged dissipative members (links) can be easily replaced due to negligible permanent drifts. Even if some structural damage is present, it can be repaired easily by replacing the bolted links.

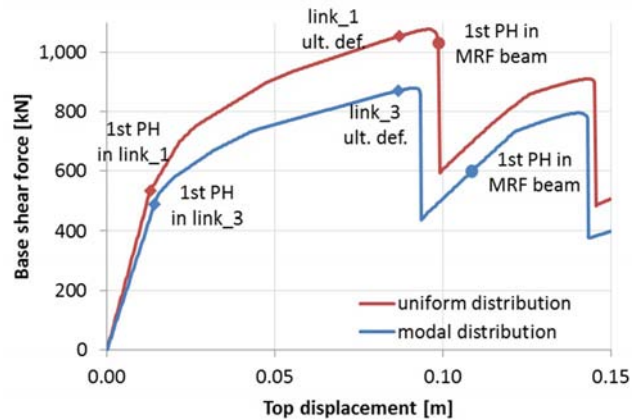


Figure 29. Pushover curves.

Table 4. Key parameters of response.

Record	Peak transient interstorey drift, %			Permanent interstorey drift, %			Shear deformation in links, rad		
	DL	SD	NC	DL	SD	NC	DL	SD	NC
00385_H1	0.45	0.86	2.82	0.001	0.001	0.155	0.054	0.108	0.432
14336_H1	0.46	0.76	1.68	0.003	0.005	0.016	0.056	0.093	0.256
15613_H2	0.43	0.76	2.87	0.003	0.003	0.154	0.051	0.101	0.441
15683_H2	0.40	0.91	3.06	0.028	0.011	0.128	0.046	0.123	0.169
16035_H2	0.51	0.86	2.14	0.004	0.002	0.125	0.058	0.108	0.327
16889_H1	0.39	0.72	3.69	0.006	0.025	0.238	0.044	0.094	0.570
17167_H1	0.56	1.17	2.82	0.006	0.033	0.199	0.069	0.155	0.429
mean	0.46	0.86	2.73	0.007	0.011	0.145	0.054	0.108	0.432

At the Significant Damage (SD) limit state damage is still constrained to links only, which exhibit plastic deformation demands very close to the acceptable 0.11 rad. Permanent drifts are only slightly larger than at the DL limit state, the average values being about 0.011 % or 0.4 mm, and the maximum ones of 0.033 % or 1.2 mm. Due to low permanent drifts, the structure is easily repairable at this limit state as well.

At the Near Collapse (NC) limit state the structural damage is widespread. Shear deformations in links are well over the acceptable values (0.432 rad compared to 0.14 rad). However, due to moment resisting frames, the overall performance of the structure can be considered acceptable for this limit state, average transient drifts being of the order of 2.73%. Plastic deformation demands are present in moment resisting frames (beams and columns) and braces. Even so, permanent interstorey drifts are not very large (average of 0.15% or 5.1 mm). However, repairing of the structure is considered not to be feasible at these large levels of seismic input.

Experimental program

The instrumentation of the experimental mock-up consisted of 38 local displacement transducers (to monitor the link deformations and the slip in the splice connection of every EBF brace and the EBF beams from the first storey, in the south frame), nine global displacement transducers (to monitor the global longitudinal and transversal displacements of the structure), 22 inclinometers (to monitor the rotations of the beam to column and column base-joint zones) and 32 strain gages (to monitor the yield at the middle of the EBF braces and at the end of the MRF beams of the first storey). Potential dissipative areas were white-washed to visually observe yielding.

Table 5. Limit states and corresponding scaling factors for seismic input

Limit state	Mean return period, years	Probability of exceedance	a_g/a_{gr}	a_g, g
Full operation (FO)	-	-	0.062	0.020
Damage Limitation (DL)	95	10% / 10 years	0.59	0.191
Significant Damage (SD)	475	10% / 50 years	1.00	0.324
Near Collapse (NC)	2475	2% / 50 years	1.72	0.557

Table 6. Sequence of PsD and link removal tests.

Links	Test	Scope
Set 1	Full operation (FO1)	Assess elastic response of the structure.
	Damage Limitation (DL)	Observe structural response to a moderate earthquake.
	Replacement of set 1 links (LR1)	Investigate removal of links by unbolting and their replacement.
Set 2	Full operation (FO2)	Assess elastic response of the structure.
	Significant Damage (SD)	Observe structural response to a design-level earthquake.
	Pushover (PO1)	Induce large permanent drifts.
	Replacement of set 2 links (LR2)	Investigate removal of links by flame cutting and their replacement.
Set 3	Full operation (FO3)	Assess elastic response of the structure.
	Near collapse (NC)	Observe structural response to a severe-level earthquake.
	Pushover (PO2 and PO3)	Investigate ultimate capacity of the structure.

Seven natural records were selected by matching EN 1998-1 elastic response spectrum used in the design and were used to perform pre-test numerical simulations (Stratan et al. 2014). The records were selected from the RESORCE database (Akkar et al. 2014), the main selection criteria being the matching of the control period to the one of the target spectrum ($T_c = 0.6$ sec). The records were then scaled to the target spectrum using EN 1998-1 rules. Structural performance was evaluated for the limit states shown in Table 5. Record selected for pseudo-dynamic (PsD) tests is 15613_H2 (recorded at Yarimca (Eri) station during the Izmit aftershock event in Turkey on 13.09.1999). Based on pre-test numerical simulations, it provided response closest to the mean response from all records in terms of top displacement, interstorey drifts and shear deformations in links. Testing sequence on the mock-up in the reaction wall facility of ELSA consisted in modal evaluation, snap-back and PsD tests. Table 6 summarises the sequence of PsD tests and link replacements performed on the test structure. Links were replaced two times: after DL test and after SD test.

F01, F02 and F03 tests

Each of the three series of PsD tests shown in Table 6 started with a Full Operation test (F01, F02 and F03). Seismic input was chosen small enough to allow assessment of the elastic response of the structure and check instrumentation. There was no visible or measured damage during the F01

test. The peak top displacement amounted to 5.7 mm, while permanent drifts were negligible. Similar response was observed during the FO2 and FO3 tests.

DL and LR1 tests

During the damage limitation (DL) test, the peak top displacement was 32 mm (0.3%), while the residual one of 5 mm (0.05%). A low residual inter-storey drift amounting to a maximum of 3 mm (less than 0.1%) was observed. Relatively small plastic deformations occurred in the links (Figure 30), the largest peak rotation was 0.032 rad and the largest residual deformation was 0.014 rad (link in the 3rd storey of the south frame). No slip occurred in the brace or beam splice connections. No damage was observed in the steel elements of the structure with the exception of links. Minor cracks were observed in the concrete slab.

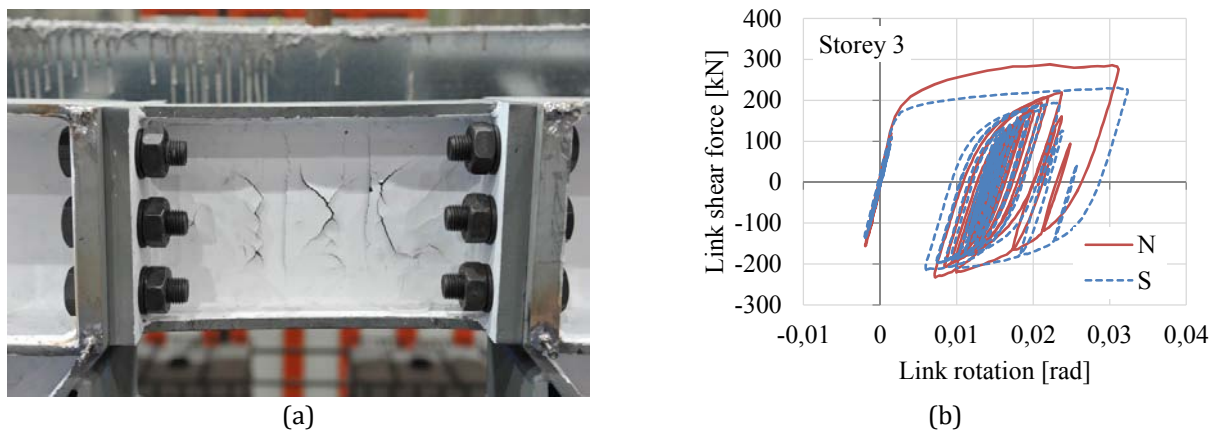


Figure 30. DL test: link from storey 3 of the south frame (a) and hysteretic response of the links from the 3rd storey (b).

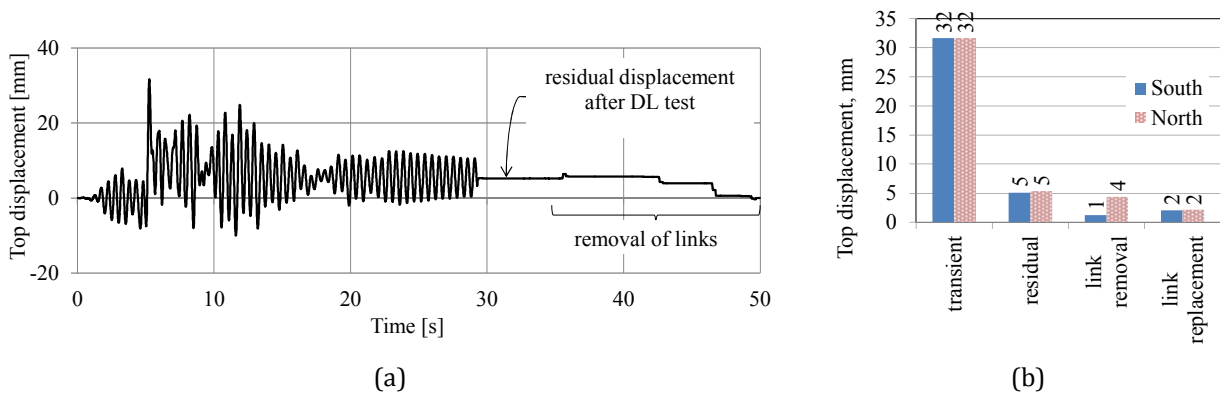


Figure 31. Top displacement time history for the south frame (a) and peak values of top displacement during DL and LR1 tests (b).

After the DL test, the first set of damaged links was removed and replaced with a new set of links. Considering that residual drifts after the DL tests were small (maximum values of about 5 mm for both frames), the links were removed after untightening the bolts, starting with the first floor of the north frame. After untightening the bolts, a hydraulic jack was used for pushing apart brace ends, in order to pull out the links. The forces that had to be applied by the hydraulic jack in order to pull out easily the links varied between 360 kN and 430 kN. To facilitate mounting of the new links, the replacement links were fabricated by 2 mm shorter than the original ones. The installation of the new links did not raise particular problems and the hydraulic jack was not needed. Installation of

the links in the south frame was straightforward because the slab didn't obstruct the access. It was more difficult in the north frame where the slab was cast across the links which had to be inserted from the side.

As can be seen in Figure 31, the residual top displacement at the end of the DL test (5 mm) decreased after the elimination of the damaged links to 1 mm for the south frame and 4 mm for the north frame. Better re-centring was observed in the south frame, where the link is not connected to the concrete slab. An additional re-centring was observed during the replacement of the links (2 mm final top displacement for both frames). After link replacement procedure, a negligible residual top displacement was observed ($H/5250$ for both frames), considerably smaller than the erection tolerance ($H/300$) according to EN 1090-2, the structure being essentially re-centred.

SD, P01 and LR2 tests

The peak top displacement recorded during the significant damage (SD) test was 50 mm (0.48%), and the residual one was 13 mm (0.12%). The peak transient interstorey drift amounted to 20 mm (0.57%), while the residual interstorey drift was approximately 5 mm (0.14%). Moderate deformations occurred in the links (Figure 32), the largest amounting to 0.061 rad transient and 0.022 rad residual (in the link from the 1st storey of the south frame). No slip occurred in the brace or beam splice connections. No damage was observed in the steel elements of the structure with the exception of links. Moderate cracks were observed in the concrete slab.

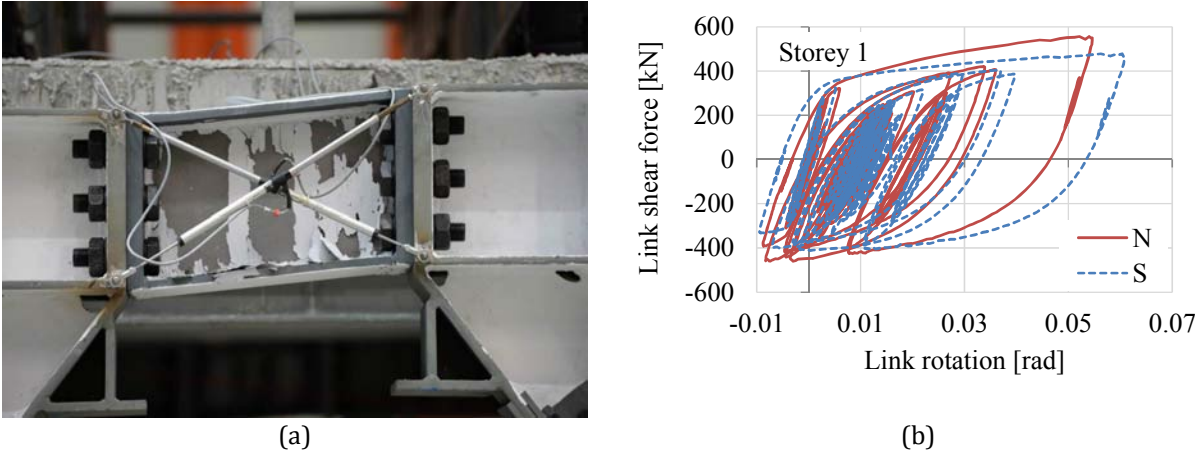


Figure 32. SD test: link from storey 1 of the south frame (a) and hysteretic response of the links from the 1st storey (b).

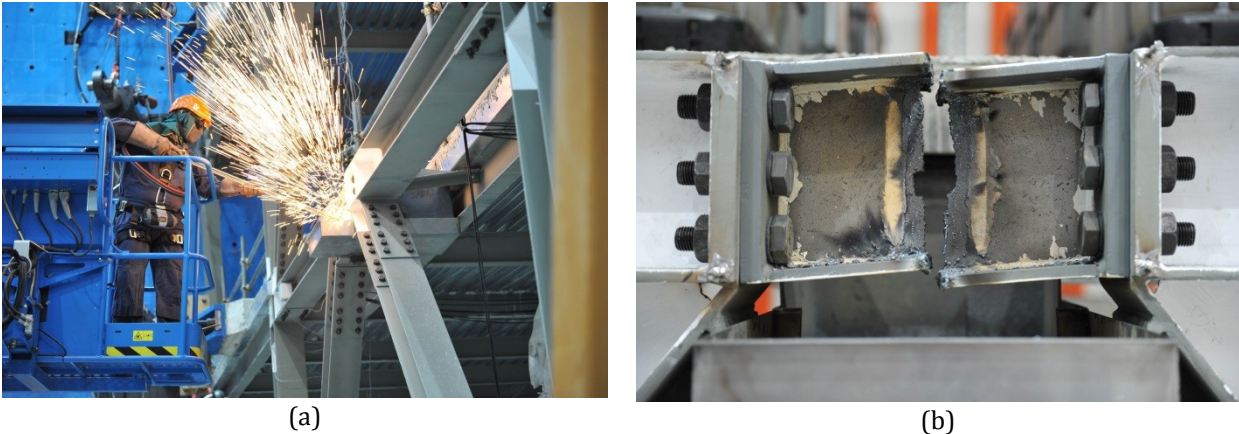


Figure 33. Flame cutting for releasing residual link forces (a) and a link after flame cutting (b).

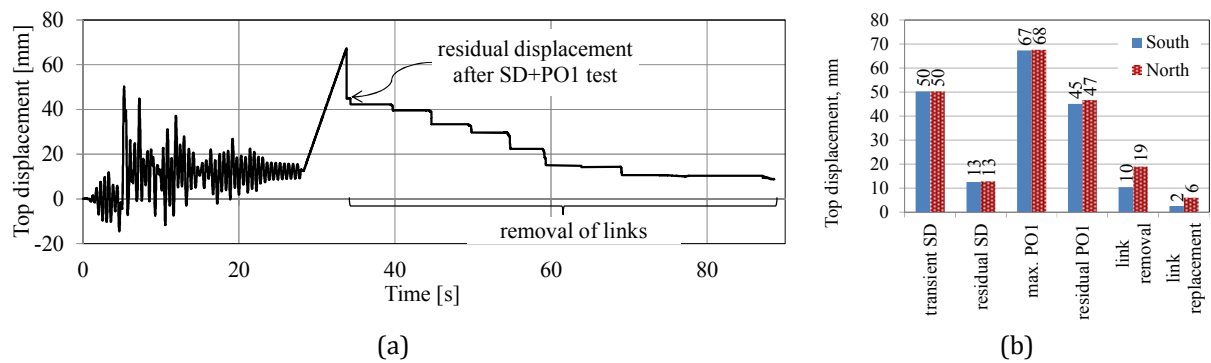


Figure 34. SD, PO1 and LR2 tests: top displacement for the south frame (a) and peak values of top displacement (b).

Since the residual deformations after the SD tests were relatively small, the pushover test PO1 was performed, to generate large enough residual displacements that would require flame cutting of the links. The test was controlled by the displacement of the south frame in the third floor with an inverted triangular distribution of forces. The displacements applied to the north frame were identical to those on the south frame.

The maximum top displacement recorded during the PO1 tests was of 67 mm and 68 mm for the south and north frames respectively. No yield was observed in the steel elements outside the links. Larger deformations occurred in the links (maximum of 0.075 rad peak rotation and 0.066 rad residual one). There was no slip detected in the brace or beam splice connections. More visible cracks were observed in the concrete slab. After the completion of the PO1 test, the structure exhibited a significant residual top displacement of 45 mm (0.43%), while the corresponding residual inter-storey drift amounted to a maximum of 18 mm (0.5%).

After the PO1 test, the second set of damaged links was removed (LR2) and replaced with a new (third) set of links. In this case, removal of the links required that they be flame cut (Figure 33), in order to release residual forces locked in the damaged links, prior to untightening the bolts. Links were flame cut and removed starting from the top storey downwards. The residual top displacement at the end of link removal (LR2 test) was 10 mm in the south frame and 19 mm in the north frame (Figure 34). Better re-centring was observed in the south frame, where the links were not connected to the concrete slab. Although it was not necessary to use a hydraulic jack for removing the links, it was needed to place the new set of links in the structure. The forces that had to be applied by the hydraulic jack in order to easily insert the links varied between 286 kN and 486 kN. An additional re-centring was also observed during the replacement of the links. Final residual top displacements after placement of new links amounted to 2 mm (H/5250) for the south frame and 6 mm (H/1750) for the north one. Both values are considerably smaller than the erection tolerance 11.7 mm (H/300) according to EN 1090-2, the structure being essentially re-centred.

NC, PO2 and PO3 tests

The near collapse (NC) test was stopped automatically at 5.3 seconds of the input accelerogram because the difference in displacement recorded by the actuator and the external transducer exceeded the limit of 10 mm. In order to continue with the PsD test, the structure was brought to a state corresponding to the distribution of displacements measured before the oil pressure was released. After the restart, the test was stopped again a few steps later as the actuators of the first floor reached their maximum capacity when the structure entered the second mode of vibration. This corresponded to a situation where the actuators from the first floor were acting in a direction

opposite to that of the actuators of the second and third floors. The maximum displacement recorded at the top of the structure was 118.1 mm. The seismic links reached high deformations, exceeding the maximum limit of the transducers (± 25 mm) placed across the links of the first two floors.

The test campaign continued with a push-over test PO2 with an inverted triangle distribution of forces. Equal displacements between the north and south frames were imposed at the third floor and the actuators of the first and second floors were in force control. Although equal displacements were imposed on the north and south frames of the third floor, the two lower floors rotated in the horizontal plane due to the different stiffness between the two frames. The test was stopped at 231.6 mm displacement at the top floor. An additional cyclic push-over test PO3 with a uniform force distribution in order to avoid force saturation at the actuators was carried out under displacement control considering a Maximum displacements at the third floor were 405 and 499.4 mm on the north and south frames respectively.

The last three tests produced extensive damage throughout the structure. Very large deformations occurred in the links, 0.15 – 0.38 rad for the first two levels and 0.09 – 0.13 rad for the third level. Links from the first two storeys fell down, with failure occurring in the welds connecting the links to the end plates. Significant damage was also observed in the column base zones and at the end of the MRF beams, just outside the haunch. The concrete slab was heavily damaged in the north frame.

2.1.5 LINK REPLACEMENT ORDER IN HIGHER-RISE FRAMES

In order to validate numerically the design methodology of current practice EBF structures with removable links and the link replacement procedure, two dual structural configurations were designed: the first, like in the case of the experimental specimen (Stratan et al., 2015), having a central EBF (the link being placed at mid-span) and two side MRFs, being further referred to as "configuration A" (see Figure 35a) and the second having a central MRF and two side EBFs. (the links being placed marginally, connected to columns on one side) being further referred to as "configuration B" (Figure 35b). The links from EBFs were conceived as removable (bolted) dissipative elements because they are intended to provide the energy dissipation capacity and to be easily replaceable. The more flexible moment resisting frames provide the necessary re-centring capability to the structure

Both structures have 3 spans of 7.5 meters and 5 bays of 7.5 meters, and 6 stories of 3.5 meters each (4.0 m at the ground level). The main lateral load resisting system is composed of eccentrically braced frames (2 on each horizontal direction for structure A and 4 on each horizontal direction for structure B). Additionally, there are 4 moment resisting frames on each horizontal direction in case of configuration A and 2 moment resisting frames on each horizontal direction in case of configuration B, to assure the restoring forces after an earthquake. All the other frames are gravitational loads resisting systems (with pinned composite steel-concrete beams).

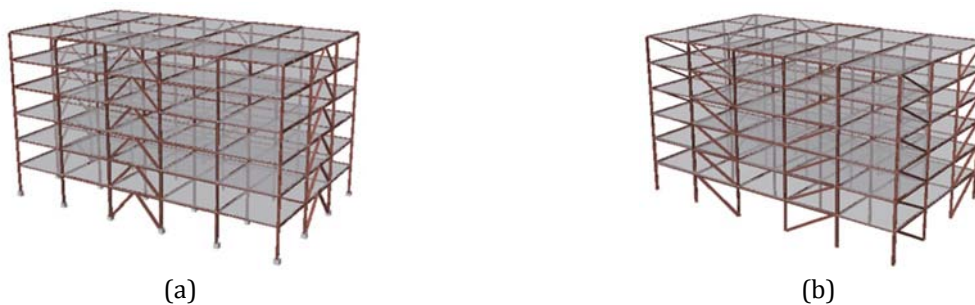


Figure 35. Configuration A (a) and configuration B (b) structures.

The capacity design of the structure was carried out according to EN1990, EN1991, EN1993, EN1994 and EN1998. A 4.9 kN/m² dead load and 3.0 kN/m² live load were considered. The building was analyzed for stiff soil conditions (EC8 type 1 spectrum for soil type C), characterized by 0.35g peak ground acceleration. A behaviour factor $q = 4$ (ductility class M) and inter-storey drift limitation of 0.0075 of the storey height are used.

The perimeter columns are fixed at the base and all the central ones (resisting to gravity loads only) are pinned at the base. Short links were used, with the length $e = 800$ mm and with equivalent stiffness reduced from the theoretical shear stiffness of continuous links (to account for the shear stiffness of the link and rotational deformations in the bolted connection), made from welded H sections. All the structural elements from EBFs are made from mild carbon steel S355, while the ones from MRFs are made from high-strength steel S460.

The element sections presented in Table 7 and Table 8 were obtained.

Table 7. Elements sections for configuration A.

Storey	Links	EBF beams	Braces	EBF columns	MRF beams	MRF columns
1	640x260x22x12	HEA650	HEM300	HEM340	IPE450	HEB340
2	590x260x22x10	HEA600	HEM280	HEM340	IPE400	HEB340
3	540x240x22x10	HEA550	HEM260	HEB340	IPE360	HEB300
4	490x230x22x9	HEA500	HEM240	HEB340	IPE360	HEB300
5	440x230x20x8	HEA450	HEM220	HEB300	IPE300	HEB300
6	390x210x16x6	HEA400	HEM180	HEB300	IPE300	HEB300

Table 8. Elements sections for configuration B.

Storey	Links	EBF beams	Braces	EBF columns	MRF beams	MRF columns
1	540x260x20x9	HEA550	HEM300	HEM340	IPE600	HEB340
2	490x230x20x8	HEA500	HEM280	HEM340	IPE550	HEB340
3	440x230x20x8	HEA450	HEM260	HEM340	IPE550	HEB300
4	390x230x20x8	HEA400	HEM240	HEM340	IPE500	HEB300
5	350x230x18x8	HEA360	HEM240	HEB340	IPE500	HEB300
6	330x190x15x5	HEA340	HEM200	HEB340	IPE400	HEB300

In order to obtain a global numerical model that can be used in further post-test numerical simulations on current practice dual eccentrically braced frames with removable links, a calibration was performed based on experimental results of pseudo-dynamic tests of the DUAREM testing programme.

A time-history analysis was performed using SeismoStruct program, applying at each of the three levels of the DUAREM specimen model, the displacements obtained from the experimental tests. The values used for material characteristics were the ones obtained from tensile tests on steel samples originating from experimental specimen material batch, performed at Politehnica University Timisoara.

Force-based plastic hinge elements for beams, columns and braces were used. Bolted links were modelled using a force-based inelastic beam with two rotational springs at the end (see Figure 28a). The former was used in order to model the flexural stiffness of the link, while the latter were used in order to account for shear stiffness of the link, as well as rotational deformations in the bolted connection. The rotational springs were modelled using the smooth hysteresis curve (as defined by SeismoStruct) for link elements, having the initial stiffness computed as described before, the ratio between ultimate shear force (V_u) and yield shear force (V_y) equal to 1.7 and the ultimate shear deformation $\gamma_u=0.15$ rad.

The results of numerical simulations and experimental testing were compared in terms of first storey link rotation versus shear force and drift versus base shear force (see Figure 36). A very good match was observed, the new calibrated numerical model being adopted for further numerical simulations on current practice structures.

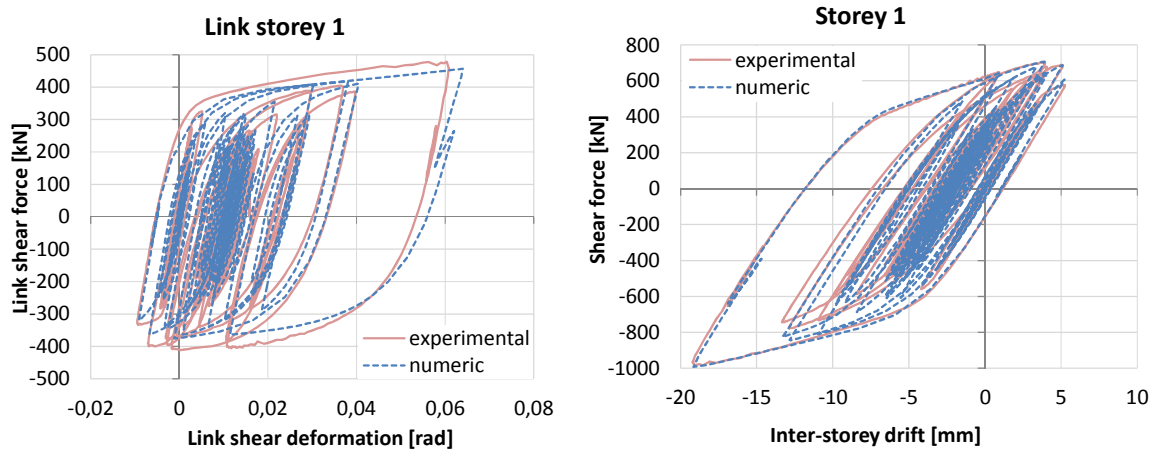


Figure 36. First storey - link and global hysteresis.

For a structure with re-centring capability, the design objective consists in preventing yielding in members other than removable dissipative ones, up to a desired deformation. Ideally the latter should be the ultimate deformation capacity of the removable dissipative member. From a preliminary pushover analysis, it was observed that following code-based capacity design rules was not enough to accomplish the objective stated above for the investigated structures. But, using S690 higher-strength steel in moment resisting frames was shown to be efficient in avoiding yielding in their members, increasing their strength, but not the stiffness, this being the material used in further analyses.

The calibrated 2D numerical models of the designed structures were subjected to pushover analyses on transversal direction, with a modal (inverted triangular) distribution of lateral forces, in order to assess their structural performance. The pushover curves presented in Figure 37 illustrate the seismic performance of the two structures.

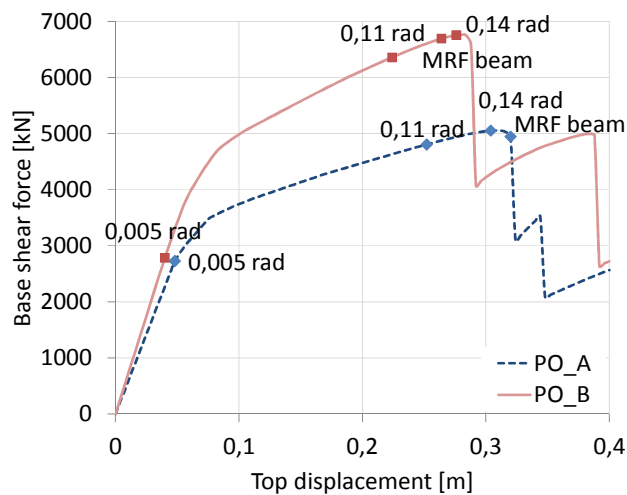


Figure 37. Pushover curves.

The objective of having no yielding in the MRFs before the attainment of the ULS deformation in the removable links (0.11 rad plastic rotation according to FEMA356) of the EBFs is accomplished, representing the basic design requirement for dual frames with removable dissipative members. MRFs provide the re-centring of the structure even until after the links ultimate deformation (0.14 rad plastic rotation according to FEMA356) in case of configuration A.

Seven natural seismic records of European earthquakes were used for seismic performance assessment of the test structure using nonlinear time-history analysis. Individual records were scaled to the target spectrum (EN 1998 type 1, soil type C, $a_g = 0.35g$) using EN 1998 criteria.

Structural performance was evaluated for the limit states shown in Table 5, where a_{gr} is the reference peak ground acceleration (corresponding to 10% / 50 years earthquake) and a_g represents the peak ground acceleration for a specific earthquake level.

At the Damage Limitation (DL) limit state all structural components except links are in the elastic range. Shear deformations in links exceed the FEMA 356 limits of 0.005 radians (0.039 rad for structure A and 0.026 rad for structure B), but this is normal, since the design carried out according to EN 1998 did not impose any limitation on yielding of structural members at DL limit state. Even so, peak inter-storey drifts are within the limits imposed (<0.75%). In these conditions, the advantage of the proposed system is obvious, since the damaged dissipative members (links) can be replaced easily due to negligible permanent drifts. Even if some structural damage is present, it can be repaired easily by replacing the bolted links.

At the Significant Damage (SD) limit state damage is still constrained to links only, which exhibit plastic deformation demands below 0.11 rad (0.092 rad for structure A and 0.078 rad for structure B). Permanent drifts are only slightly larger than at the DL limit state. Due to low permanent drifts, the structures are easily repairable at this limit state as well.

At the Near Collapse (NC) limit state the structural damage is widespread. Shear deformations in links are well over acceptable values of 0.14 rad (0.282 rad for structure A and 0.266 rad for structure B). However, due to moment resisting frames, the overall performance of the structures can be considered acceptable for this limit state. Plastic deformation demands are present in moment resisting frames (beams and columns) and braces. Even so, permanent inter-storey drifts are not very large. However, repairing of the structures is considered not to be feasible and desirable at these large levels of seismic input.

In order to numerically simulate the link removal order, the structures were subjected to a uniform distribution of lateral forces up to the attainment of 0.11 rad plastic rotation in links on the transversal direction, simulating the seismic action. Then the structures were unloaded, simulating the state of the structure after an earthquake and links are removed level by level.

Three possibilities of links removing order within a storey were studied: firstly removing the links on the longitudinal direction and secondly the ones on the transversal direction (see Figure 37a.d), vice versa (see Figure 37b.e), and in a circular pattern (see Figure 37c.f).

It was observed that for the first version (see Figure 37a-d) the residual shear force drop is about 21% (configuration A) and 16% (configuration B) smaller than for the second version (see Figure 37b-e) and the redistribution of forces between the links of the same storey is also smaller. The situation for the third version (see Figure 37c-f) is in between the other two.

On the first version of link removal order within a storey (see Figure 37a-d), was analysed also the removal of links starting from the most loaded to the least loaded storey (from the lower storey toward the upper one). In this case, was observed a larger interaction between stories, but values of the shear force drop with 43% (configuration A) and 39% (configuration B) smaller than in the case of eliminating links from the upper one toward the lower one and smaller redistribution of forces between the links of the same storey.

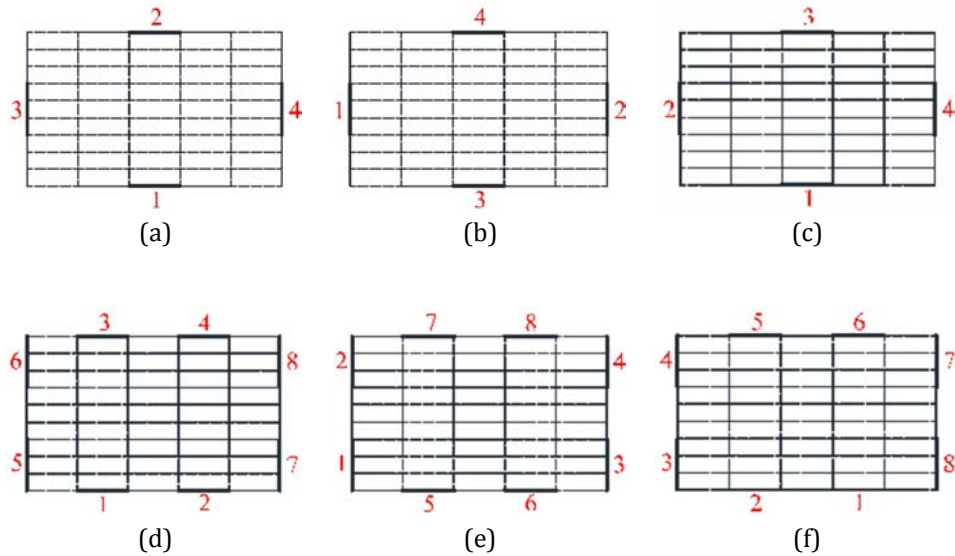


Figure 38. Link removal solution for configuration A (a to c) and for configuration B (d to f).

Numerical simulations were performed in order to investigate solutions for removing links. Three possibilities of links removing order within a storey were studied: (a) firstly removing the links on the longitudinal direction (the least loaded ones) and secondly the ones on the transversal direction (the most loaded ones), (b) vice versa, and (c) in a circular pattern. It was observed that for the first version the link's residual shear force drop is smaller than for the other two studied solutions and the redistribution of forces between the links of the same storey is also smaller. This is because, when removing links in version (a), the structure becomes more flexible (the least loaded links on the longitudinal direction are first removed and when removing the first link on the transversal direction, only the MRFs in the other direction are still working) and the links develop smaller residual forces.

On the first version (a) of link removal order within a storey, was analysed also the removal of links starting from the most loaded to the least loaded storey (from the lower storey toward the upper one). In this case, was observed a larger interaction between stories, but values of the shear force drop with about 30-40% smaller than in the case of eliminating links from the upper storey toward the lower one and smaller redistribution of forces between the links of the same storey.

2.1.6 OUTCOMES

Dual frames with removable dissipative members can be used to provide a structure with a re-centring capability, and can greatly reduce the costs and manpower required for post-earthquake repair. This work describes a large-scale experimental programme carried out at the European Laboratory for Structural Assessment (ELSA) on a three-storey dual eccentrically braced frame with replaceable links. The testing sequence on the mock-up in the reaction wall facility of ELSA consisted of modal evaluations, snap-back, and pseudo-dynamic tests.

The dual eccentrically braced structure exhibited excellent performance when subjected to seismic input with intensities corresponding to 95 and 475 years return period, corresponding to Damage Limitation and Significant Damage limit states, respectively. Small residual deformations were recorded for both seismic intensity levels, which were comfortably within the erection tolerance limits. Such small permanent deformations effectively mean that the structure is self-centring to a degree, which allows for an easy repair of the structure by the replacement of damaged links. Residual drifts are further reduced by removing and replacing the bolted links. Re-centring was

better for the frame with links disconnected from the slab. Moreover, damage to the concrete was avoided in this case. Nevertheless, good re-centring was observed even for the frame with the slab cast over the links, while damage to the reinforced concrete slab was insignificant at the Damage Limitation and Significant Damage tests. Provided the residual deformations after an earthquake are small, the links can be removed simply by untightening, as was demonstrated after the Damage Limitation test. If larger residual drifts occur, flame cutting of links is recommended to allow for smooth release of forces, as was done after the Significant Damage series of tests. The experimental investigation validated the re-centring capability of dual eccentrically braced frames with removable links, which was accomplished without major technological difficulties.

For a structure with re-centring capability, the design objective consists in preventing yielding in members other than removable dissipative ones, up to a desired deformation. Ideally the latter should be the ultimate deformation capacity of the removable dissipative member. Following code-based capacity design rules was not enough to accomplish this objective for the investigated structures. But, using higher-strength steel in moment resisting frames was shown to be efficient in avoiding yielding in their members.

2.1.7 PUBLICATIONS

- [1] Dubina, D., Stratan, A., Dinu, F. (2008). "Dual high-strength steel eccentrically braced frames with removable links". *Earthquake Engineering & Structural Dynamics*, Vol. 37, issue 15, pp. 1703-1720, (Online ISSN: 1096-9845, Print ISSN: 0098-8847).
- [2] Ioan, A., A. Stratan, and D. Dubina. (2013). "Numerical Simulation of Bolted Links Removal in Eccentrically Braced Frames." *Pollack Periodica* 8 (1): 15-26, DOI: 10.1556/Pollack.8.2013.1.2. Paper ISSN: 1788-1994, Online ISSN: 1788-3911.
- [3] Dubina, D., Stratan, A., Dinu, F. (2011). "Re-centring capacity of dual-steel frames", *Steel Construction: Design and Research*, Vol. 4, No. 2, pp. 73-84.
- [4] Ioan, A., Stratan, A., Dubina, D., Taucer, F. (2013), "Dual-Steel Eccentrically Braced Frames with Bolted Links – Simulation of Safe Removal Process", *Acta Technica Napocensis: Civil Engineering & Architecture*, vol. 56, No. 2, UTPRESS, ISSN 1221-5848, pp. 111-118.
- [5] Dubina, D., Stratan, A., Florea, D., Ioan, A. (2013). "Sisteme structurale cu componente disipative de siguranta seismica". *AICPS Review*, nr. 1-2/2013, ISSN: 2067-4546, pp. 41-50.
- [6] Dubina, D., Stratan, A., Dinu, F., Bordea, S., Neagu, C., Ioan, A. (2010). "Sisteme structurale cu elemente metalice disipative demontabile pentru clădiri multietajate în zone seismice". *AICPS Review*, nr. 2-3/2010, p. 106-112. ISSN: 2067-4546
- [7] Stratan, A., Ioan, A., Dubina, D. (2012). "Re-centring capability of dual eccentrically braced frames with removable bolted links". *Proceedings of the 7th International Conference on Behavior of Steel Structures in Seismic Areas (STESSA)*, 9-11 January 2012, Santiago, Chile, ISBN 978-0-415-62105-2, pp. 723-728.
- [8] Dinu, F., Dubina, D., Stratan, A. (2010). "Evaluation of re-centring capability of dual frames with removable dissipative members: case study for eccentrically braced frames with bolted links". *COST Action C26 "Urban Habitat Constructions under Catastrophic Events" Proceedings*, Naples, 16-18 September 2010, Mazzolani (Ed.), Taylor & Francis Group, London, p. 821-828. ISBN: 978-0-415-60685-1.
- [9] Dubina, D., Stratan, A. and Dinu, F. (2007). "High Strength Steel EB Frames with Low Strength Bolted Links". *Proc. of the 5th International Conference on Advances in Steel Structures*, Singapore, 5 – 7 December 2007, Research Publishing Services, JY Richard Liew & YS Choo (Eds.), ISBN 978-981-05-9365-0, Vol. III., pp. 249-254.

- [10] Stratan, A., Dogariu, A. and Dubina, D. (2007). "Bolted links for eccentrically braced frames: influence of link stiffness". Proc. of the 3rd Intl. Conf. on Steel and Composite Structures (ICSCS07), Manchester, UK, 30 July - 1 August 2007, Eds. Wang and Choi. Taylor&Francis, ISBN: 978-0-415-45141-3, pp. 847-853.
- [11] Stratan, A. and Dubina, D. (2004). "Bolted links for eccentrically braced steel frames". Proc. of the Fifth AISC / ECCS International Workshop "Connections in Steel Structures V. Behaviour, Strength & Design", June 3-5, 2004. Ed. F.S.K. Bijlaard, A.M. Gresnigt, G.J. van der Vegte. Delft University of Technology, The Netherlands. ISBN: 978-90-9019809-5, pp. 223-232
- [12] Stratan, A., Ioan, A., Dubina, D., Taucer, F., Poljanšek, M., Molina, J., Pegon, P., D'Aniello, M., Landolfo, L.(2014). "Experimental program for large-scale tests on a re-centring dual eccentrically braced frame", 7th European Conference on Steel and Composite Structures EUROSTEEL 2014, 10-12 September 2014, Napoli, Italy, Landolfo R, Mazzolani FM, editors, European Convention for Constructional Steelwork, ECCS, paper no. 37-300, 8 p. ISBN: 978-92-9147-121-8.
- [13] Ioan, A., Stratan, A., Dubina, D. (2014). "Link replacement order in high-rise re-centring dual eccentrically braced frames", 7th European Conference on Steel and Composite Structures EUROSTEEL 2014, 10-12 September 2014, Napoli, Italy, Landolfo R, Mazzolani FM, editors, European Convention for Constructional Steelwork, ECCS, paper no. 49-302, 6 p. ISBN: 978-92-9147-121-8.
- [14] Stratan, A., Ioan, A., Dubina, D., Poljanšek, M., Molina, J., Pegon, P., Taucer, F. (2014). "Dual eccentrically braced frames with removable links: Experimental validation of technical solution through large-scale pseudo-dynamic testing". Proceedings of the Fifth National Conference on Earthquake Engineering and First National Conference on Earthquake Engineering and Seismology – 5CNIS & 1CNIS, Bucharest, Romania, June 19-20, 2014. Radu Văcăreanu, Constantin Ionescu (Eds.), Bucharest: Conspress, 2014, ISBN (print) 978-973-100-342-9, ISBN (CD) 978-973-100-341-2, pp. 323-330, Paper No. 31 (on CD-ROM)
- [15] Stratan, A., Ioan, A., Dubina, D., D'Aniello, M., La Manna Ambrosino, G., Landolfo, R., Taucer, F., Poljansek, M. (2013). "Pre-test numerical simulation and experimental program on a dual eccentrically braced frame with replaceable links". XXIV Giornate italiane della Costruzione in Acciaio, Torino, 30 September – 2 October 2013, ISBN 978-88-905870-0-9, pp. 867-876.
- [16] Stratan, A., Ioan, A., Dubina, A., Taucer, F., Poljansek, M. (2014). "Pre-test numerical simulations and experimental program on dual eccentrically braced frame with removable links". Proceedings of the International Workshop "Application of High Strength Steels in Seismic Resistant Structures". Orizonturi Universitare, Timisoara, Romania, ISBN: 978-973-638-552-0, pp. 137-148.
- [17] Stratan, A., Dinu, F., Dubina, D. (2010). "Replacement of bolted links in dual eccentrically braced frames". Proc. of the 14th European Conference on Earthquake Engineering, August 30 – September 03, 2010, Ohrid, Republic of Macedonia. MAEE, Paper No. 1581. ISBN: 978-608-65185-0-9.
- [18] Dubina, D., Dinu, F., Stratan, A. (2009). "Post-earthquake intervention procedure on dual eccentrically braced frames with removable links". A 4-a Conferință Națională de Inginerie Seismică, București, 18 decembrie 2009. Editura Conspress. Vol. II. pp. 273-282. ISBN 978-973-100-096-1
- [19] Stratan, A., Dubina, D. (2008). "Removable bolted links for eccentrically braced frames", Proceedings of the International Symposium "Urban Habitat Constructions under Catastrophic Events", Malta, 22-23 October 2008, COST Action C26, Editors: Mazzolani,

Mistakidis, Borg, Byfield, De Matteis, Dubina, Indirli, Mandara, Muzeau, Wald, Wang, p. 181-186. ISBN 978-99909-44-42-6

- [20] Dinu, F., Dubina, D., Stratan, A. (2005). "Performance Criteria for Seismic Design of Steel Frames with Eccentric Bracings". Proceedings of the 4th European Conference on Steel and Composite Structures - Eurosteel 2005. Maastricht, The Netherlands, June 8-10, 2005, Volume C, Part. 5.2, 65-73.
- [21] Stratan, A. and Dubina, D. (2004). "Eccentrically braced dual steel frames with removable link". Improvement of Building's Structural Quality by New technologies, Outcome of the Cooperative Action, Final scientific report, September 2004. A.A. Balkema Publishers, ISBN 04-1536-610-0. p. 111-116.
- [22] Sabau G.A., Poljansek, M., Taucer, F., Pegon, P., Molina Ruiz, F.J., Tirelli, D., Viaccoz, B., Stratan, A., Dubina, D., and Ioan Chesoa, A. (2014). "Seismic engineering research infrastructures for european synergies. Full-Scale Experimental Validation of a Dual Eccentrically Braced Frame with Removable Links (DUAREM)". EUR - Scientific and Technical Research Reports. Publications Office of the European Union. JRC93136. <http://publications.jrc.ec.europa.eu/repository/handle/111111111/34024>. 147 p.
- [23] Stratan, A., Ciutina, A. and Dogariu, A. (2006). "Seismic-resistant steel structures with removable dissipative elements". Proc. of the 10th Nat. and 4th Int. conf. "Planning, design, construction and the construction industry". Editors R. Folic, V. Radonjanin, M. Trivunic. Novi Sad, November 22 - 24, 2006. pp: 559-566. ISBN 86-7892-016-5
- [24] Stratan, A., Ioan, A., Dubina, D., Poljanšek, M., Molina, J., Pegon, P., Taucer, F., Sabău, G. (in print). "Large-scale tests on a re-centring dual eccentrically braced frame", 8th International Conference on Behavior of Steel Structures in Seismic Areas STESSA 2015, Shanghai, China, July 1-3, 2015. Paper no. 111.
- [25] Ioan, A., Stratan, A., Dubina, D., D'Aniello, M., Landolfo, R. (in print). "Seismic performance and re-centring capability of dual eccentrically braced frames with replaceable links", 8th International Conference on Behavior of Steel Structures in Seismic Areas STESSA 2015, Shanghai, China, July 1-3, 2015. Paper no. 113.

2.2 COLD-FORMED STEEL PITCHED-ROOF PORTAL FRAMES WITH BOLTED JOINTS

The objective of the research carried out was to evaluate the performance of pitched roof cold-formed steel portal frames of back-to-back channel sections and bolted joints. Three different configurations of ridge and eaves joints were tested. The behaviour and failure mechanisms of joints were observed in order to evaluate their stiffness, strength and ductility. Joints between cold-formed members with bolts in the web only result in a reduction of joint moment capacity and premature web buckling. The component method was applied in order to characterise the joint stiffness and moment capacity for the purpose of frame analysis and design. The influence of joints characteristics on the global frame response under lateral (seismic) loads was analysed by considering three connection models. Full-scale tests were performed on cold-formed pitched-roof portal frames. Experimental observations and comparison to numerical predictions of frame response are presented.

Previous studies by Lim and Nethercot (2004) and Chung and Lau (1999) showed that bolted joints in cold formed steel portal frames have a semi-rigid behaviour. Also, these types of joints are partially resistant (Lim and Nethercot, 2003). When bolts are installed only on the web of cold-formed section, the local buckling is made more critical by stress concentrations, shear lag and bearing deformations around bolt holes (Dundu and Kemp, 2006), reducing the moment resistance well below the moment resistance of the effective cross-section. In case of usual cold-formed steel sections, both tests and numerical simulations show that elastic-plastic elongation of bolt-holes is by far the most important component controlling the stiffness and capacity of such type of connections (Lim and Nethercot, 2004, Yu et al., 2005). The contribution of other components, such as flanges in tension and compression due to bending action, and the web in shear due to transverse action is significantly lower.

The global behaviour of cold-formed steel portal frames of bolted joints was studied experimentally by Lim (2001), Dundu and Kemp (2006), and Kwon et al. (2006). All these studies provided evidence of the crucial importance of joint performance on the global response of frames.

In present research, the influence of joint characteristics on the global behaviour of cold-formed pitched-roof portal frames is investigated. An experimental program on ridge and eaves joints was carried out. Detailed results on joint behaviour are reported elsewhere (Dubina et al., 2004). Based on experimental results, a calculation procedure based on the component method (EN1993-1-8) was adapted to cold-formed joints. Joint stiffness and moment capacity obtained using the component method is used to develop a joint model for global structural analysis. Two full-scale tests on cold-formed pitched-roof portal frames with bolted joints were performed, with the primary objective to assess their performance under horizontal (seismic) loading. The results of the experimental investigation are presented and experimental response is compared to analytical predictions of frame response.

2.2.1 TESTS ON JOINT SPECIMENS

In order to be able to define realistic specimen configurations a simple pitched roof portal frame was first designed with the following configuration: span 12 m; bay 5 m; eaves height 4 m and roof angle 10°. This frame was subjected to loads common in the Romanian design practice: self weight 0.35 kN/m² (with a partial safety factor of $\gamma_{ULS}=1.1$ for the ultimate limit state), technological load 0.15 kN/m² ($\gamma_{ULS}=1.1$) and snow load 0.72 kN/m² ($\gamma_{ULS}=2.0$). These loads were totalling approximately 10 kN/m uniformly distributed load on the frame. The frame was analysed and designed according to EN 1993-1-3 (2001) rules. The size of knee and ridge specimens and testing setup were chosen to obtain in the connected members a distribution of bending moment similar to the one observed in the designed structure.

The elements of the portal frame were made from back-to-back built up sections made of Lindab C350/3.0 profiles (yield strength $f_y=350 \text{ N/mm}^2$). Using these cross section dimensions, three alternative joint configurations were designed (see Figure 39 and Figure 40), using welded bracket elements (S235: $f_y=235 \text{ N/mm}^2$)

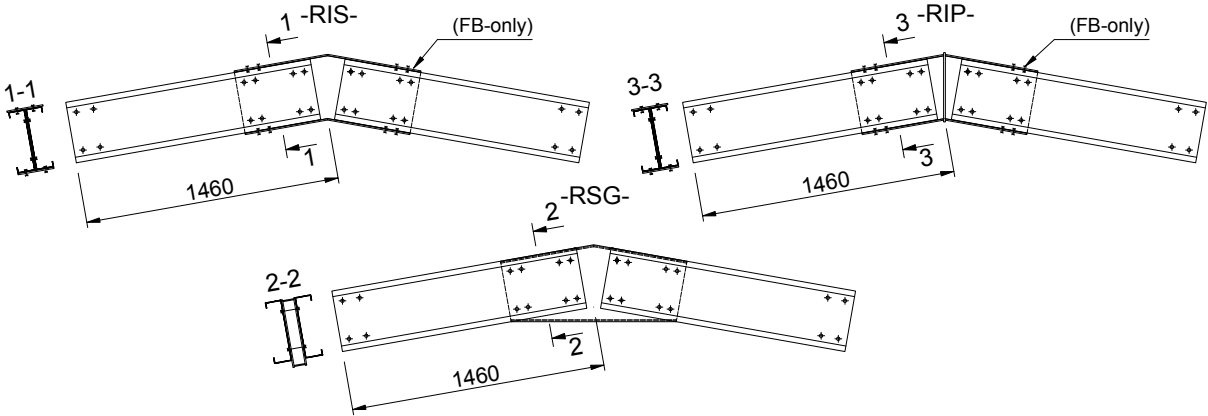


Figure 39. Configurations of Ridge Joints

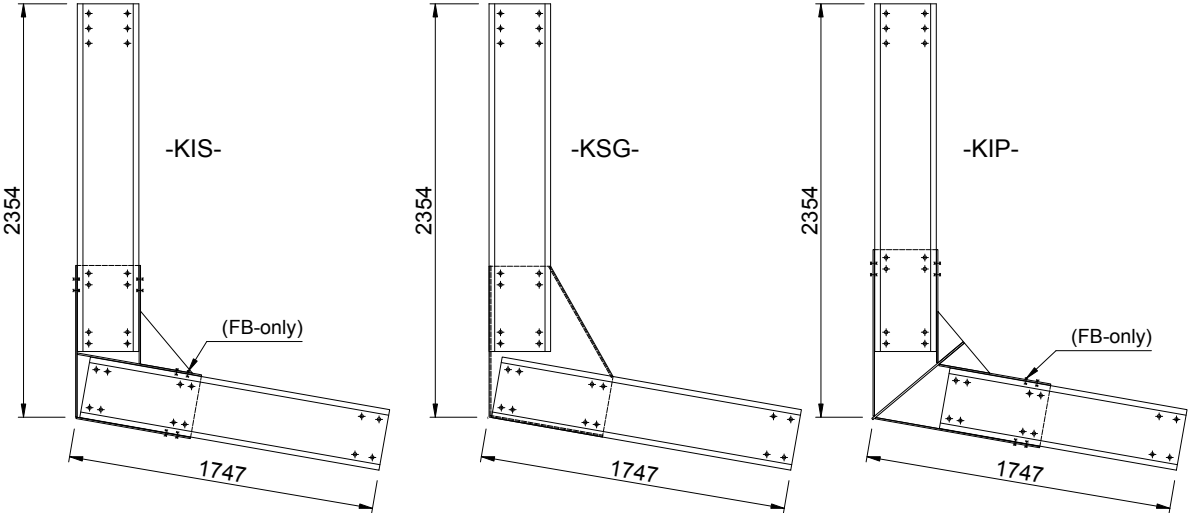


Figure 40. Configurations of Knee Joints.

The connecting bolts are subjected to shear and their design was carried out assuming the rotation of the joint around the centroid of the bolt group and a linear distribution of forces in each bolt, proportional to their distance from the centre of rotation. The joints were designed to resist the bending moment in the beam, at the location of the centroid of the bolt group.

One group of specimens (KSG and RSG) used spaced built-up gussets. In this case, bolts were provided only on the web of the C350 profile. In the other cases, where two different details were used for the connecting bracket - i.e. welded I sections only (KIS and RIS), and welded I section with plate bisector (KIP and RIP), respectively - bolts were provided on the web only, or both on the web and the flanges. Joints where bolts were provided on the web and on flanges were denoted by FB letters (see Table 9).

Table 9. Tests on Joint specimens.

Element type	Code	Loading type
RIS (Ridge connection with I Simple profile)	RIS-FB-M	Monotonic
	RIS-FB-C1*	Cyclic: modified ECCS
	RIS-FB-C2*	Cyclic: low cycle fatigue
RSG (Ridge connection with Spaced Gusset)	RSG-M	Monotonic
	RSG-C1	Cyclic: ECCS procedure
	RSG-C2	Cyclic: Modified ECCS
RIP (Ridge connection with I profile and end Plate)	RIP-M	Monotonic
	RIP-M	Monotonic
	RIP-C1	Cyclic - ECCS proc.
KSG (Knee connection with Spaced Gusset)	KSG-M	Monotonic
	KSG-C1	Cyclic - Modified ECCS
	KSG-C2	Cyclic - Low cycle fatigue
KIS (Knee connection with I Simple profile)	KIS-M	Monotonic
	KIS-FB-M*	Monotonic
	KIS-FB-C*	Cyclic - Modified ECCS
KIP (Knee connection with I profile and end Plate)	KIP-M	Monotonic
	KIP-FB-M*	Monotonic
	KIP-FB-C*	Cyclic - Modified ECCS

*FB Specimens (RIS, RIP, KIS, KIP) with supplementary bolts on the flange

Monotonic and cyclic experiments were performed for each specimen typology, all specimens being tested statically. Figure 41 shows the test setup and specimen instrumentation. In the knee connection tests, a short tie was used to prevent vertical displacements of the joint. For monotonically loaded specimens the loading velocity was approximately 3.33 mm/min, and the "yield" displacement (v_y) was determined according to the ECCS (1985) procedure, as the displacement corresponding to the intersection of the initial stiffness line and another line with a slope of 10% of the initial stiffness (see Figure 42a). For the cyclic tests several alternative loading procedures were used: (1) the standard ECCS cyclic procedure (see Figure 42b), (2) a modified cyclic procedure, suggested by the authors, which is based on the ECCS proposal (see Figure 42c) and (3) a cyclic procedure for low cycle fatigue. The ECCS loading procedure consists of four initial cycles in the elastic range, followed by groups of three inelastic cycles at $\pm 2v_y$, $\pm 4v_y$, $\pm 6v_y$, etc. The inelastic demand imposed on cold-formed specimens following this procedure is too severe, the specimen failing during the first inelastic cycle at $\pm 2v_y$. To overcome this problem, a modified procedure was used, that consisted of four initial cycles in the elastic range, followed by groups of three inelastic cycles at $\pm 1.2v_y$, $\pm 1.4v_y$, $\pm 1.6v_y$, etc.

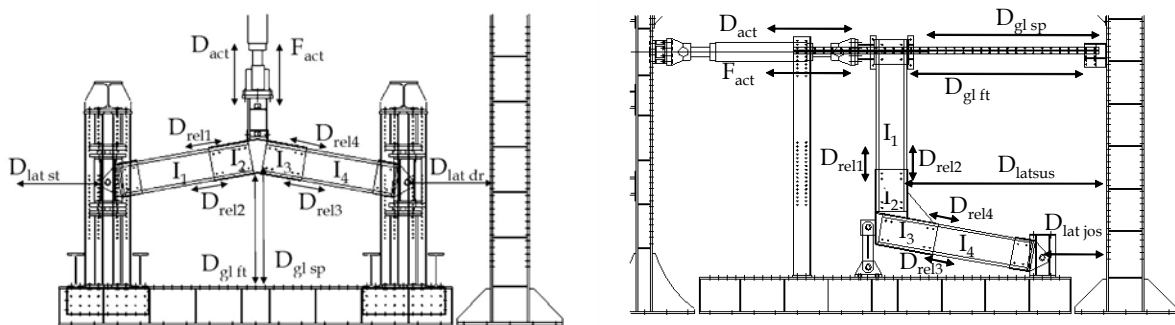


Figure 41. Loading scheme and instrumentation.

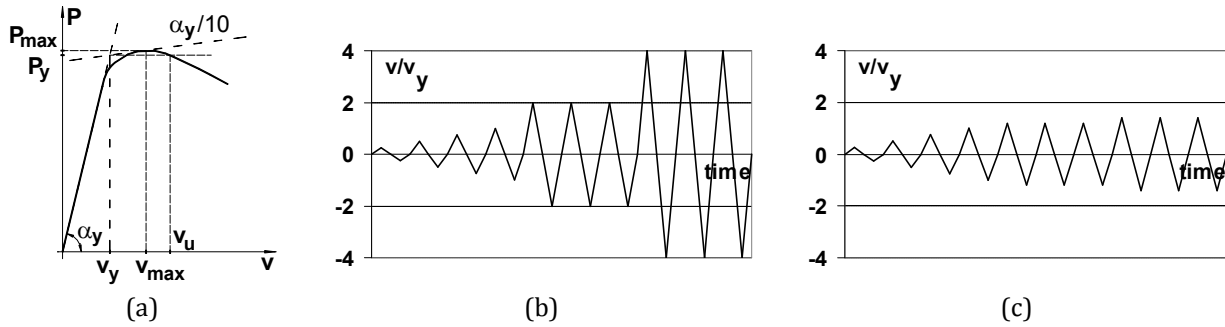


Figure 42. ECCS procedure for determining the yield displacement (a); ECCS loading procedure (b) and modified loading procedure (c)

The monotonic tests identified failure modes of the different joint typologies. All specimens had a failure due to local buckling of the cold formed profiles; however two distinctive modes were identified for specimens with flange bolts and those without (Figure 43; Figure 44).

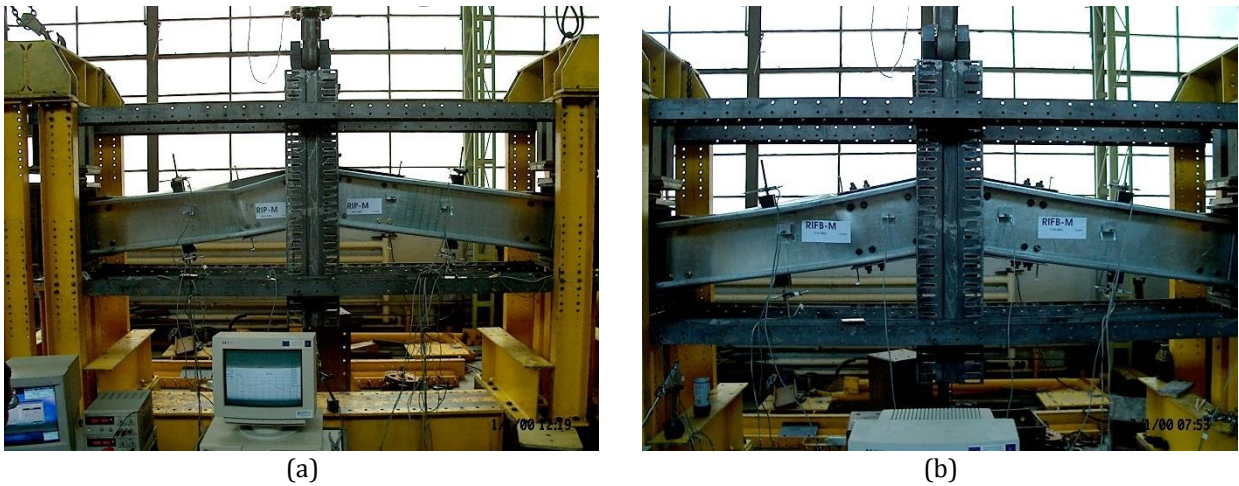


Figure 43. Failure of ridge specimens RIP-M (a) and RIS-FB-M (b).

If no bolts are provided on the flange of profiles, initially minor bearing elongation of the bolt holes were observed, the failure being due to stress concentration in the vicinity of outer bolt row. The resulting concentration of compressive stress in the web of the C profile causes in the ultimate stage local buckling followed suddenly by web-induced flange buckling. This phenomenon occurred in a similar way in the case of RSG and KSG specimens. No important differences were observed between specimens where no bolts were provided on the flanges. In the case of the specimens with flange bolts, the stresses concentrated in the vicinity of the outer bolt row on the flange. In this case no initial elongation of the bolt holes were observed; the buckling was firstly initiated in the flange, and only later was extended into the web.

To account for the flexibility of the bolted connection in structural analysis, two models are possible: one which considers both connections independently (see Figure 45a), and a simplified one, which considers the characteristics of the connection concentrated in one joint only (see Figure 45b). The former is believed to represent more exactly the real behaviour of the assembly, while the latter has the advantage of simplicity. Similar models can be used for knee joint configurations. Moment-rotation relationships characterising the connection response were derived for both the left and right ridge connections (beam and column connection in the case of knee joints). Moments were computed at the end of the bracket. The corresponding relative rotation between the bracket and the connected element θ_c^* was determined from acquired data, so as to

represent both the flexibility of the connection (due to bolt bearing) and post-buckling deformations in the element (Dubina et al., 2004). For the simplified joint representation (as in Figure 45b), both moment (M_j) and rotations were considered at the intersection of the element centrelines.

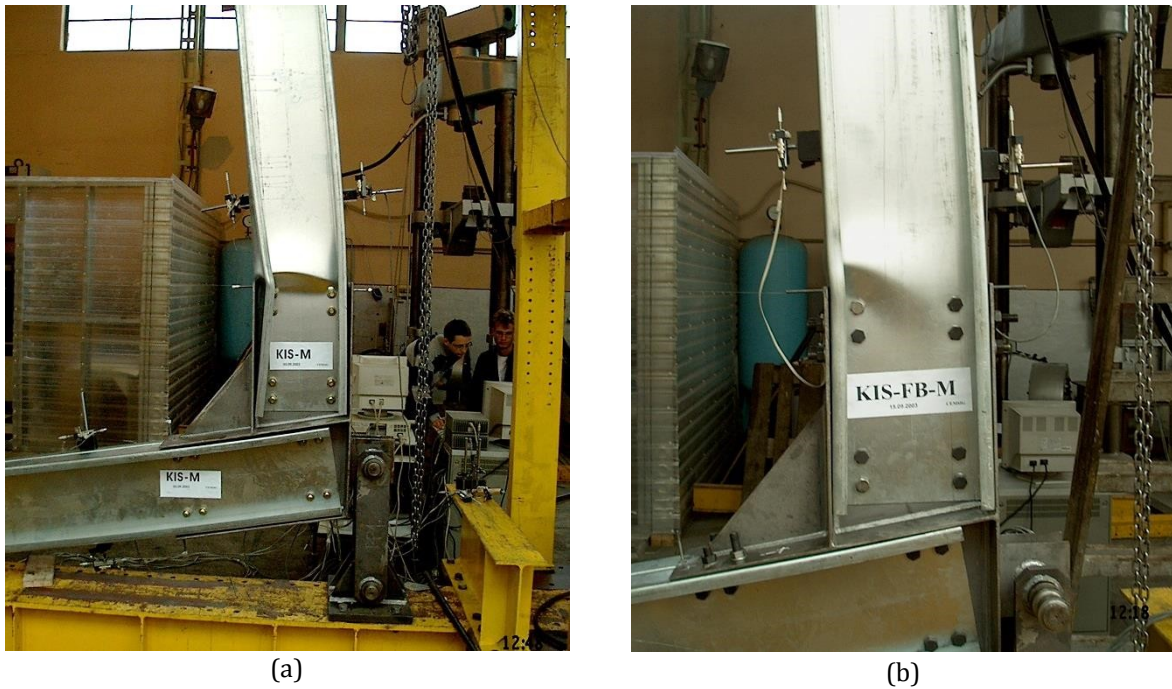


Figure 44. Failure of knee specimens KIS-M (a) and KIS-FB-M (b).



Figure 45. Two possible models for ridge joints: detailed (a) and simplified (b).

Comparative experimental curves for ridge and knee connections are presented in Figure 46a and Figure 47. There are no significant differences among the specimens without flange bolts (RSG-M, RIP-M, and KSG-M, KIS-M). This could be explained by the higher stiffness and capacity of the connecting bolts compared to the other components of the joint. On the other hand, there is an important gain in load bearing capacity and the initial joint stiffness when bolts are installed also on the flanges, although this joint type is more difficult to fabricate (RIS-FB-M and KIS-FB-M).

In Table 10 the yield and ultimate rotation ($\theta_{c,y}^*$; $\theta_{c,u}^*$), the initial stiffness (K_{mic}), and the maximum bending moment ($M_{c,max}$) are presented and compared for all monotonically tested specimens, for the failed connection. The initial stiffness was determined by a linear fit of moment-rotation values between 0.25 and 0.9 of the maximum moment. The lower-bound limit (0.25) was chosen different from zero in order to eliminate the effect of initial slip due to tolerance of bolt-holes. This initial slip is believed to be ineffective in the real structure, due to loading-unloading cycles under service loads. The upper-bound limit (0.9) was considered empirically as a limit of elastic response of the connection. Yield rotation was determined as the point on the initial stiffness line corresponding to maximum moment. Ultimate rotation was defined as the one corresponding to a 10% drop of

moment capacity relative to the maximum moment. Figure 46b presents graphical determination the initial stiffness, yield rotation and ultimate rotation for the RIS-FB-M specimen.

Obviously, the specimens with unbolted flanges that failed prematurely by web buckling due to stress concentration around the outer bolt rows, would be the weakest part of portal frames. Consequently, this joint typology is not recommended to be used in practice.

Table 10. Monotonic results: parameters of connection moment-rotation curves.

Specimen	K_{iniC} kNm/rad	$\theta_{C,y}^*$ Rad	$\theta_{C,u}^*$ rad	μ	M_{Cmax} kNm
RSG-M	4891.3	0.021	0.034	1.6	77.1
RIS-FB-M	6011.1	0.017	0.025	1.4	108.0
RIP-M	5806.8	0.018	0.028	1.6	74.3
RIP-M2	6541.2	0.012	0.013	1.1	72.9
KSG-M	6031.6	0.009	0.023	2.5	53.3
KIS-M	4115.0	0.020	0.033	1.6	78.4
KIS-FB-M	6432.3	0.016	0.029	1.8	102.9
KIP-M	7863.9	0.010	0.019	2.0	90.0
KIP-FB-M	6956.5	0.015	0.025	1.6	116.7

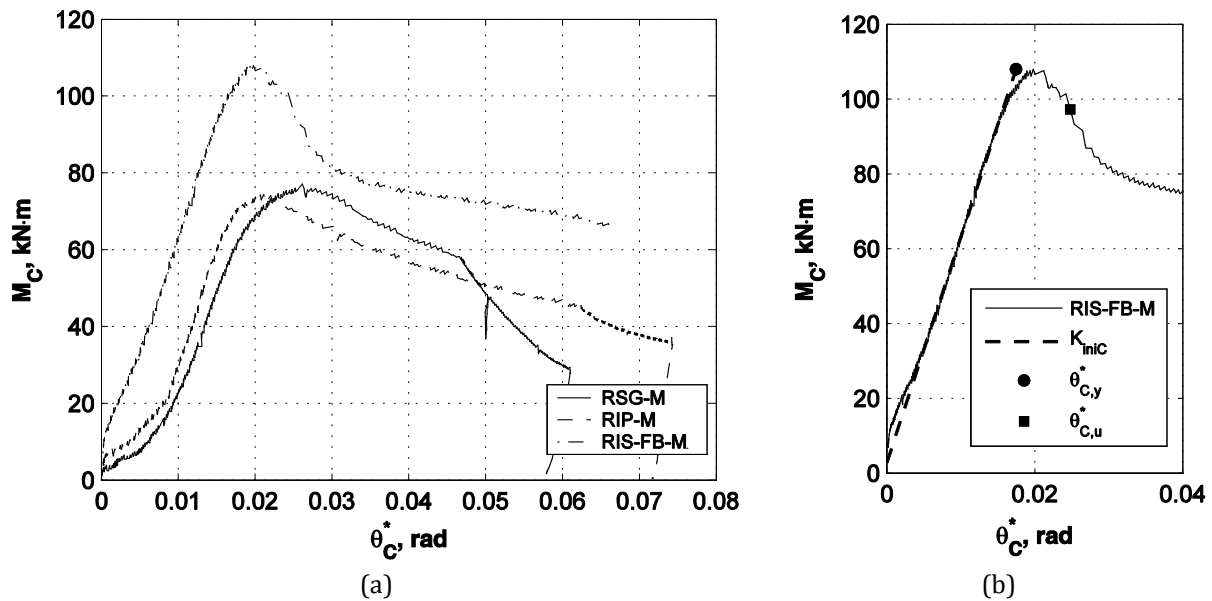


Figure 46. Comparative results from monotonic tests for ridge joints (a) and graphical representation of initial stiffness, yield and ultimate rotations for the RIS-FB-M specimen (b).

In the case of cyclic loading, failure of specimens started by elongation of bolt holes. Compared to monotonic loading, in the case of cyclic loading the phenomenon was amplified due to the repeated and reverse loading. However, the failure occurred also by local buckling, as in monotonic tests, but at the repeated reversals, the buckling occurred alternately on opposite sides of the profile. This repeated loading caused the initiation of a crack at the corner of the C profile, in 2-3 cycles following the buckling, closed to the point where the first buckling wave was observed in the flange.

The crack gradually propagated through the flange and web, causing an important decrease of the load bearing capacity in each consecutive cycle.

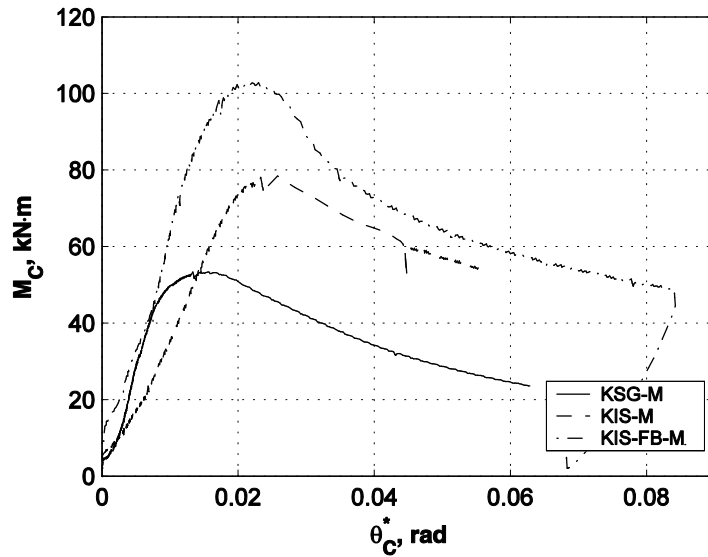


Figure 47. Comparative results from monotonic tests for knee joints.

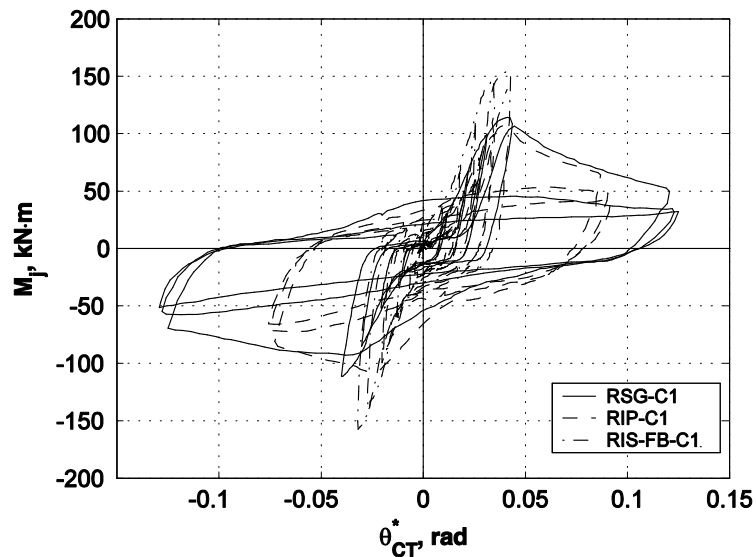


Figure 48. Comparative results from cyclic tests on ridge specimens.

The hysteretic $M-\theta$ curves show a stable behaviour up to the yield limit ($\theta_{c,y}^*$) with a sudden decrease of the load bearing capacity afterwards (Figure 48 and Figure 49). Therefore the low ductility of the specimens must be underlined again. Further, the cycles show the effect of slippage in the joint (i.e. pinching) and strength degradation in repeated cycles. Strength degradation is most significant in the first cycle, while in the consequent ones the behaviour is more stable.

In order to obtain connection characteristics under cyclic loading, an unstabilised envelope was first determined, by considering the points corresponding to maximum moment in each cycle. Based on envelope curves, connection strength, rotation capacity and ductility have been determined following a procedure identical to the one used in the case of monotonic specimens, and are reported in Table 11. Again, joints without flange bolts were weaker.

The component method is a general procedure for the design of the strength and stiffness of joints in building frames, and is implemented in EN1993-1-8. 2003. The procedure is primarily intended for heavy-gauged construction. Its application to joints connecting light-gauge members is investigated herein.

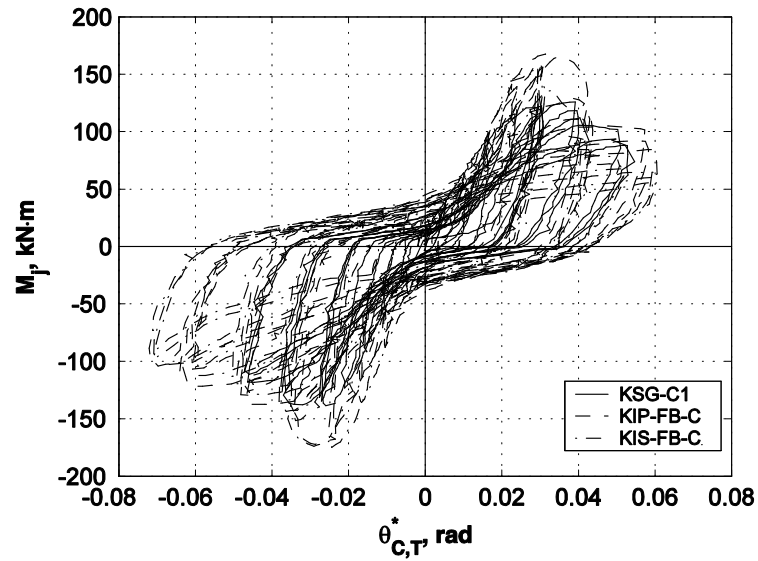


Figure 49. Comparative results from cyclic tests on knee specimens.

Table 11. Cyclic results: parameters of connection moment-rotation curves.

Specimen	K_{iniC} kNm/rad	θ_{cy}^* rad	$\theta_{c,u}^*$ rad	μ	M_{Cmax} kNm
RSG-C1	5060.0	0.017	0.028	1.7	78.8
	-5400.3	-0.019	*	*	-76.8
RSG-C2	4502.9	0.018	0.028	1.6	76.0
	-2792.5	-0.029	-0.036	1.2	-78.1
RIS-FB-C1	*	*	*	*	106.9
	*	*	*	*	-108.6
RIS-FB-C2	*	*	*	*	100.2
	*	*	*	*	-111.5
RIP-C1	6642.1	0.014	*	*	73.8
	-6585.1	-0.013	*	*	-74.7
KSG-C1	5395.5	0.013	0.022	1.7	82.5
	-6672.4	-0.015	-0.028	1.9	-90.9
KSG-C2	5067.6	0.014	0.022	1.5	84.5
	-4684.1	-0.014	-0.017	1.2	-76.8
KIS-FB-C	6914.7	0.014	0.021	1.5	102.3
	-9201.5	-0.012	-0.023	2.0	-114.4
KIP-FB-C	10051.8	0.012	0.026	2.1	102.2
	-8193.5	-0.011	-0.021	1.9	-105.1

* results not available due to faulty data acquisition

Application of the component method requires the following steps (Jaspart et al., 1998):

- identification of the active components within the joint
- evaluation of the stiffness and strength of individual components
- assembly of the components in order to evaluate stiffness and strength of the whole joint

Based on the conclusions of the experimental programme, the present study investigates only joints with both web and flange bolts (RIS-FB-M, KIS-FB-M, and KIP-FB-M). Qualitative FEM simulation (see Figure 50) showed that in the case of specimens with bolts on the web only there is a stress concentration in the web, which causes premature local buckling failure. The FEM simulation also demonstrated that load distribution in the bolts is not linear. In fact, due to member flexibility and

local buckling, the connected members do not behave as rigid bodies, and the centre of rotation of web bolts does not coincide with the centroid of web bolts. The centre of rotation of the connection is shifted towards the outer bolt rows (see Figure 51), whose corresponding force is an order of magnitude higher than the force in the inner bolts. Considering this observation, only the outer bolt group was considered for determination of connection characteristics using the component method. This assumption significantly differ in comparison with the behaviour models considered in the papers of the list of reference, which, all, consider the centroid of the bolt group as the rotation centre.

The centre of compression of the connection was considered at the exterior flange of the cold-formed member (see Figure 51), similarly with the model used for design of bolted connections with angle flange cleats in EN1993-1-8 (2003). There are a total of four bolt rows, of which three bolt rows are in the "tension" zone. The following components were identified and used to model the connection stiffness and strength:

- Cold-formed member flange and web in compression. Only the strength of this component was considered, while stiffness was considered infinite (similarly with Lim and Nethercot, 2004)
- Bolts in shear
- Bolts in bearing on the cold-formed member
- Bolts in bearing on the bracket

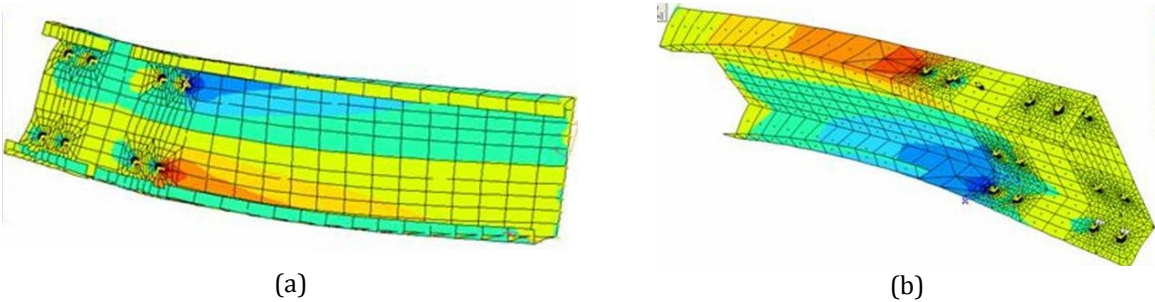


Figure 50. Stress concentration in the case of specimens with web bolts only (a), and both web and flange bolts (b).

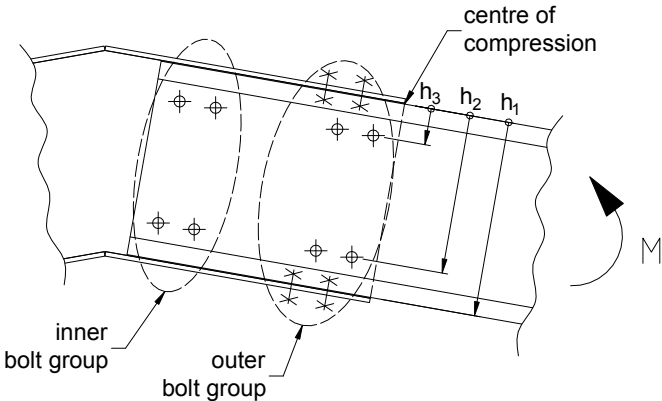


Figure 51. Bolt Groups considered in analysis.

The stiffness and strength of all these components are readily available in EN1993-1-8, only minor adjustments being required for the case of the particular case considered here. In order to facilitate comparison with the experimental results, the measured geometrical characteristics and strength (yield stress $f_y = 452 \text{ N/mm}^2$, and tensile strength $f_u = 520 \text{ N/mm}^2$) were considered in the case of the cold-formed member. Nominal characteristics were used for the bracket and bolt

characteristics, as experimental data was not available. Partial safety factors equal to unity were considered in all cases.

Only three components were considered to contribute to the stiffness of the connection: bolts in shear (denoted $k_{v,f}$ for flange bolts and $k_{v,w}$ for web bolts), bolts in bearing on cold-formed member (denoted $k_{b,eff}$ for flange bolts and $k_{b,cfw}$ for web bolts), and bolts in bearing on the bracket (denoted $k_{b,bf}$ for flange bolts and $k_{b,bw}$ for web bolts), see Figure 52a. Formulas for determination of stiffness coefficients are available in EN1993-1-8. For each of the bolt rows r , an effective stiffness coefficient $k_{eff,r}$ is determined, by combining the individual stiffness coefficients using the following relationship (EN1993-1-8, see Figure 52b):

$$k_{eff,r} = \frac{1}{\sum_i \frac{1}{k_{i,r}}} \quad (15)$$

The effective stiffness coefficients of the bolt rows in "tension" zone are replaced by an equivalent spring k_{eq} (EN1993-1-8, see Figure 52c):

$$k_{eq} = \frac{\sum_r k_{eff,r} h_r}{z_{eq}} \quad (16)$$

where h_r is the distance between bolt row r and the centre of compression; z_{eq} is determined using Eq. (17).

$$z_{eq} = \frac{\sum_r k_{eff,r} h_r^2}{\sum_r k_{eff,r} h_r} \quad (17)$$

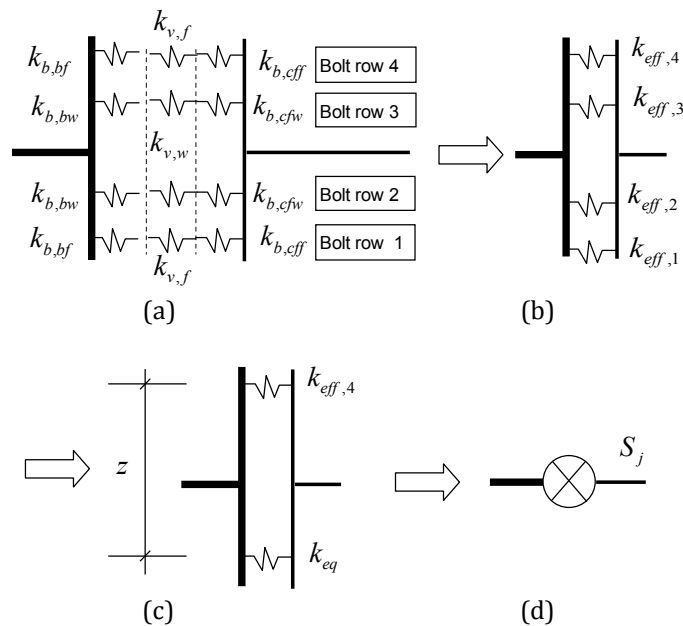


Figure 52. Main steps in the assembly of components for determination of connection stiffness.

Finally, the initial connection stiffness is determined as (see Figure 52d):

$$S_{j,ini} = \frac{E z_{eq}^2}{\sum_i 1/k_i} \quad (18)$$

The moment resistance of the bolted connection was determined using a two-step procedure. In the first step, only components related to bolt resistance were included in order to determine the moment resistance of the bolted connection $M_{bc,Rd}$. In a second step, the connection moment resistance was obtained as the minimum of the moment resistances of the bolted connection $M_{bc,Rd}$ and the connected cold-formed member $M_{beam,Rd}$:

$$M_{C,Rd} = \min(M_{C,Rd}^b, M_{beam,Rd}) \quad (19)$$

The adopted approach for determination of connection moment resistance allows to easily determine if the connection is full-strength or partial strength.

The moment resistance of the bolted connection was determined as (EN1993-1-8):

$$M_{C,Rd}^b = \sum_r F_{tr,Rd} h_r \quad (20)$$

where $F_{tr,Rd}$ is the effective tension resistance of bolt row r (minimum value of components related to bolt row r); h_r is the distance between bolt row r and the centre of compression.

The moment resistance of the cold-formed member $M_{beam,Rd}$ was determined using measured geometrical and mechanical characteristics, using effective cross-section modulus.

It was considered appropriate to use a linear distribution of forces on bolts in the case of a connection to light-gauge members. Therefore, the effective tension resistance of bolt rows was limited according to the following relationship:

$$F_{tr,Rd} \leq F_{t1,Rd} \frac{h_r}{h_1} \quad (21)$$

where $F_{t1,Rd}$ is the effective tension resistance of bolt row 1 (farthest from the centre of compression); h_1 is the distance between bolt row 1 and the centre of compression.

Table 4 and Table 5 present resistance and stiffness of bolt rows. The weakest component of flange bolts is bearing on cold formed member, while in the case of web bolts it is bearing on bracket (see Table 4). The difference is due to the fact that bolts are in simple shear on flanges and in double shear on web, as well as due to different number of bolts on flanges (4 bolts per row) and web (2 bolts per row). The main contribution to the flexibility of the connection is bearing on the cold-formed member, as well as bearing on bracket in the case of web bolts (see Table 5).

The configuration of the outer group of bolts being the same in the case of all three specimens with web and flange bolts (RIS-FB-M, KIS-FB-M, KIP-FB-M), a single set of analytical connection properties were determined. A comparison of experimental vs. analytical characteristics of connections (stiffness and moment resistance) is presented in Table 6. Generally a fair agreement between experimental and analytical stiffness of the connection can be observed. Larger experimental values of stiffness can be explained by the fact that the contribution of the inner bolt group was ignored in the analytical model. The stiffness of the connection is considerably lower than the EN1993-1-8 limits for classification of joints as rigid ($25EI_b/L_b$), which amounts to 25256 kN/m (considering the beam span L_b equal to frame span and using gross moment of inertia I_b).

Therefore, these types of connections are semi-rigid, and their characteristics need to be taken into account in the global design of frame.

Table 12. Resistance of connection components.

Bolt row	Component			Bolt-row resistance $F_{tr,Rd}$, kN
	Bolts in shear, kN	Bolts in bearing on the cold-formed member, kN	Bolts in bearing on the bracket, kN	
1	361.4	290.6	527.0	290.6
2	361.4	290.6	288.0	288.0
3	361.4	290.6	288.0	288.0
4	361.4	290.6	527.0	290.6

Table 13. Stiffness of connection components.

Bolt row	Component			Bolt-row effective stiffness $k_{eff,r}$, mm
	Bolts in shear, mm	Bolts in bearing on the cold-formed member, mm	Bolts in bearing on the bracket, mm	
1	2.286	0.7785	1.3886	0.4095
2	2.286	0.7785	0.7714	0.3313
3	2.286	0.7785	0.7714	0.3313
4	2.286	0.7785	1.3886	0.4095

Table 14. Experimental vs. analytical connection characteristics.

Specimen	Initial stiffness, K_{int} [kNm/rad]		Moment resistance, M_C , [kNm]	
	experimental	analytical	experimental	analytical
RIS-FB-M	6011	5224	108.0	117.8
KIS-FB-M	6432	5224	102.9	117.8
KIP-FB-M	6957	5224	116.7	117.8

The moment resistance of the bolted connection $M_{bc,Rd}$ determined by the component method amounted to 193.9 kNm, which was larger than the moment resistance of the cold-formed member Mbeam,Rd, amounting 117.8 kNm. Therefore, this type of connection is a full-strength one. This was demonstrated also by the experimental results, failure mode being local buckling of the cold-formed member.

2.2.2 TESTS ON FULL-SCALE PITCHED-ROOF PORTAL FRAMES

Following experimental tests on cold-formed joints, two full-scale tests on frames were performed. Frame dimensions were chosen identical to the ones in the initial design used to establish the dimensions of tested joints. Considering the poor performance of joints with web bolts only, RIS-FB and KIS-FB configurations (with both web and flange bolts) were used for frame construction. Pinned supports were used at the column bases. The objective of the full-scale tests was to assess the performance of pitched-roof cold-formed portal frames with moment-resisting joints under lateral loading, with particular emphasis on earthquake loading.

The test setup consisted of two frames in upward position, located 1.5 m apart. Tie bracing was provided between the two frames in order to provide out-of plane stability. The purlins were installed on the girders, but no side rails were provided on the columns. The schematic representation of test setup is shown in Figure 53. A reaction frame was used to apply lateral load.

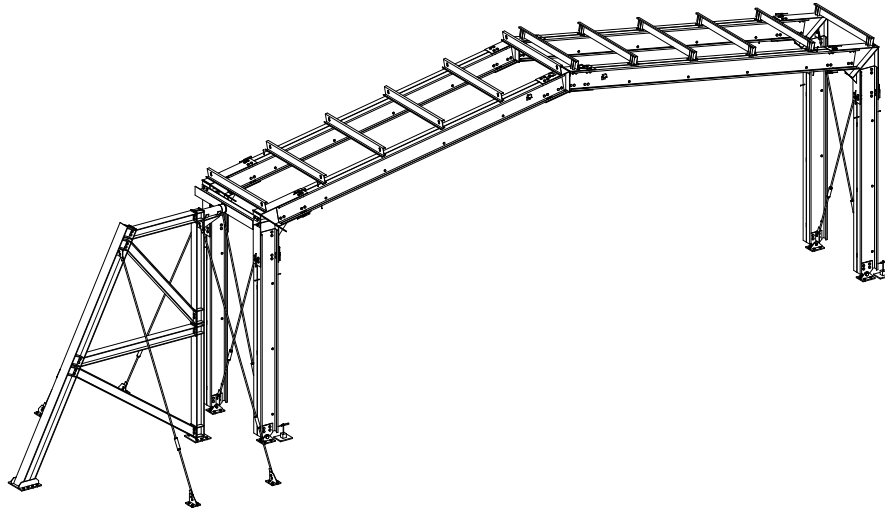


Figure 53. Experimental test setup for full-scale tests.

In the case of the first test (C1), only lateral loading was applied. For the second test (C2), gravity loading corresponding to seismic design situation (permanent and a 0.3 fraction of the snow load) was applied, followed by increasing lateral load up to failure. Total gravity loading amounted to 31.2 kN per frame, and was applied using 30 corrugated steel sheets laid on the purlins. A load cell was used in order to measure lateral load applied through a hydraulic jack. Frames were instrumented with displacement transducer to measure lateral in-plane and out-of plane displacements at the eaves, deflections at the ridge, as well as connection rotations.

Experimental tests on ridge and eaves joints showed that bolted connections of back-to-back channel cold-formed members are semi-rigid, even when bolts are provided not only on the web, but also on the flanges of the channel section. Therefore, deformations can be underestimated if connections are assumed rigid for global frame analysis. In order to assess the influence of connection stiffness and post-buckling resistance, three frame models were analysed (see Figure 54). A nonlinear static analysis under increasing lateral load was applied to the models, and the results were compared to experimental ones.

The first model was a conventional model, where connections were considered rigid. Nominal geometrical characteristics were used to model members. Finite dimensions of brackets were taken into account. Local buckling of members was modelled by rigid-plastic hinges located at the extremities of cold-formed members. an analytically determined moment capacity ($M_c=117.8$ kNm) was considered.

The second model (M_2 , see Figure 54b) was obtained from model M_1 by adopting an elastic perfectly-plastic model of the connection moment-rotation response. The initial stiffness ($K_{inc}=5224$ kNm/rad) and moment capacity ($M_c=117.8$ kNm) were the ones obtained using the analytical procedure described above (see Table 6).

In the case of the third model (M_3 , see Figure 54c), the elasto-plastic model was enhanced following two directions. The first one was related to connection behaviour under small loads, when experimental evidence showed a very stiff initial response. This response is attributed to wedging and friction between the cold-formed profiles and the bracket. Consequently, a rigid response was assumed before "slipping" up to moment M_s (see Figure 55a). The value of the "slipping" moment M_s was estimated based on experimental results, a value of 15% from the connection moment capacity being adopted. Following the initial rigid behaviour, the connection model consists of an elastic response at the initial stiffness K_{inc} (determined using the component method), up to the connection moment capacity M_c .

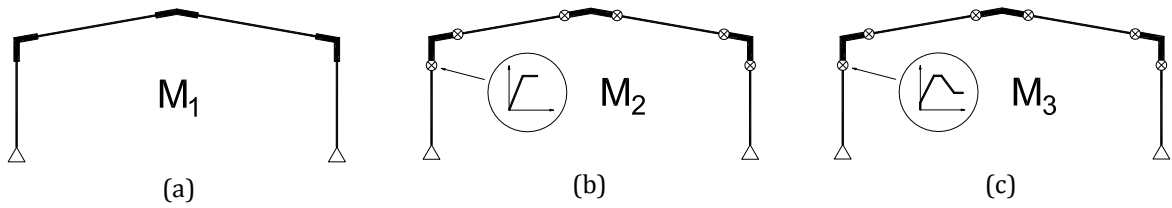


Figure 54. Considered structural models: rigid connections - M1 (a), elastic-perfectly plastic connections - M2 (b), and degrading connections – M3 (c).

The second enhancement of the model consisted in post-elastic response. The plastic rotation (plateau) was determined assuming an ultimate rotation θ_{cu} equal to 1.4 times the yield rotation θ_{cy} . The softening branch was determined by considering a drop of moment capacity to 50% from the maximum one, at a rotation θ_{cr} of 4.0 times the yield rotation (Figure 55a). The same moment-rotation characteristics were used for all connections (for both beams and columns). The influence of axial force on the stiffness and moment resistance of the connection were ignored. A comparison between the analytical and the experimental moment-rotation curves is shown in Figure 55b.

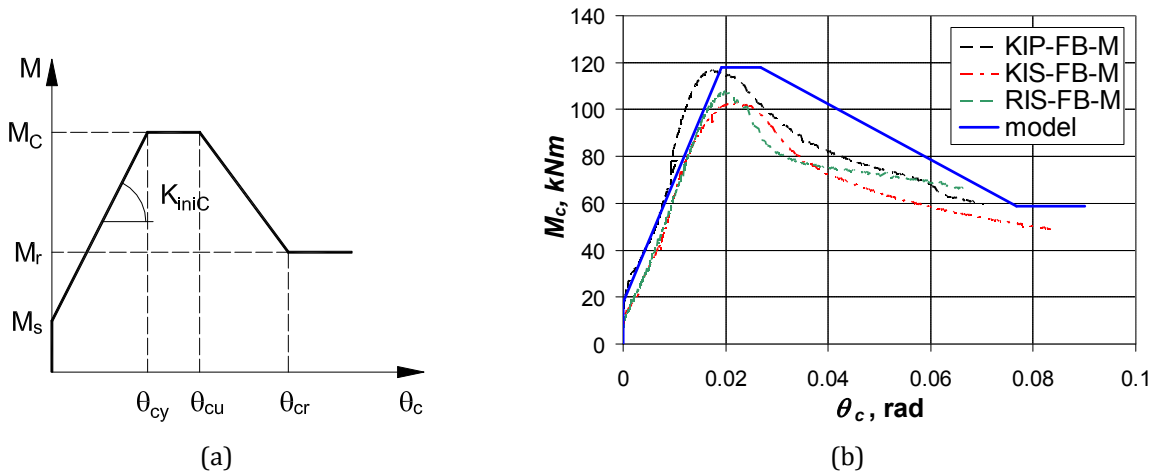


Figure 55. Parameters of the M3 connections model (a), and experimental and analytical M3 model of connection moment-rotation relationship (b).

Figure 56 a shows a global view of the C1 frame (tested under horizontal loading only) after the test. The frame response during the test was characterised by an almost linear response up to the first local buckle of the beam at the connection 2 (see Figure 56b, Figure 57, and Figure 58a), followed by a rapid loss of global frame resistance. The final collapse mechanism consisted of hinging of the beam at connections 2 and 5 (see Figure 58b) near the eaves.

A comparison of the experimental and numerical lateral force – deformation curves for the C1 frame is shown in Figure 57. The force corresponds to one of the two frames from the experimental setup, assuming the force equally distributed between the two frames. It can be observed that the rigid model (M1) provides a good approximation of the initial response of the frame up to lateral forces of about 10 kN. At larger forces, model M2, with semi-rigid connections, provide a better approximation of the experimental response. The M3 model, incorporating both the initial rigid response and subsequent semi-rigid behaviour shows the best agreement to the experimental results. The same pattern of member hinging as in the one observed in the experiment is obtained for the numerical model (see Figure 58b for the case of the M3 model). The M3 model captures well the initial and post-buckling response. M2 model overestimates lateral deformations. All three models slightly underestimate the global frame resistance.



(a)



(b)

Figure 56. C1 Frame: global view (a) and local buckling of the left beam connection (b).

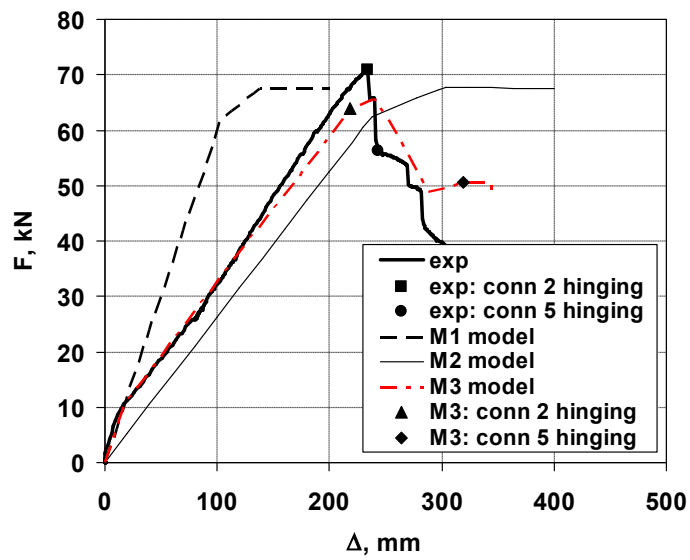


Figure 57. Frame C1: Experimental vs. numerical lateral force - deformation curves.

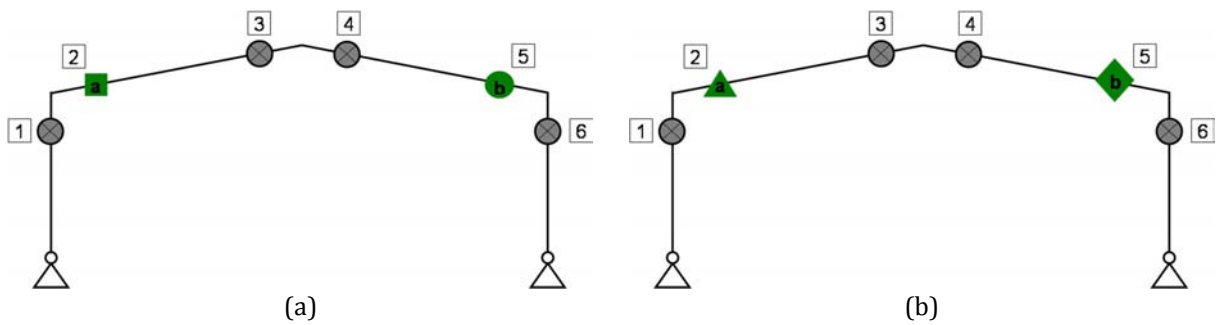


Figure 58. Frame C1: position of local buckling observed experimentally (b) and in the numerical model (c)

In the case of the C2 frame, gravity loading corresponding to seismic design situation was first applied, followed by increasing lateral loading up to complete failure of the frame. Figure 59a shows a view of the frame during loading. The global force-deformation response was very similar to the frame C1 up to 10-15 kN lateral loading. For larger lateral loading, the stiffness of the C2 frame was slightly larger than the one of the C1 frame. However, the global resistance under horizontal loading was smaller in the case of the C2 frame. The ultimate capacity was attained at the first local buckle in the beam near the right eaves (connection 5, see Figure 61a), when the lateral force resistance dropped suddenly. It was followed by a combined local buckling and lateral-torsional buckling of one of the columns at the mid-height (see Figure 59a and Figure 61a). Finally, local buckling of the beam at the left eaves was observed (at connection 2, see Figure 61a).

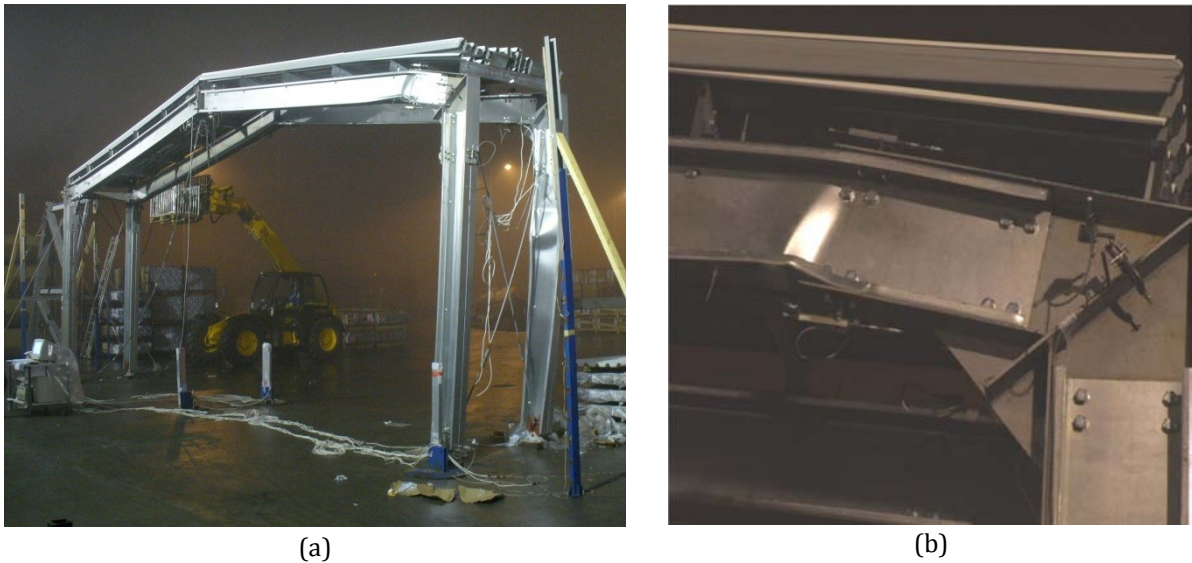


Figure 59. C2 Frame: global view (a) and local buckling of the right beam connection (b).

A comparison of the experimental and numerical lateral force – deformation response of the C2 frame is shown in Figure 60. As in the case of frame C1, The M_1 model (with rigid connections) provides a good approximation of the initial response of the frame, up to lateral forces of about 10 kN. For larger forces, the M_2 model, accounting for semi-rigid connection response, shows a better approximation of experimental response. The M_3 model shows the best agreement between the numerical and experimental results. All numerical models overestimate the global frame resistance under lateral loading. There are two factors that are believed to have contributed to this situation: (1) the numerical model did not consider buckling of the column and (2) the influence of axial forces was neglected when determining connection moment resistance. Higher axial forces are present in the right column under combined effect of gravity loading and lateral loading due to the effect of overturning. While the location of the first local buckle was correctly predicted by the numerical model (at connection 5, see Figure 61 and Figure 60b), column hinging (due to combined local and flexural-torsional buckling) observed in the experimental test was not confirmed by numerical models. Column hinging can be explained by neglected influence of axial force, combined with the effect of no lateral restraining at column flanges by side rails. Both of these effects were present in the experimental setup, but not in the numerical model.

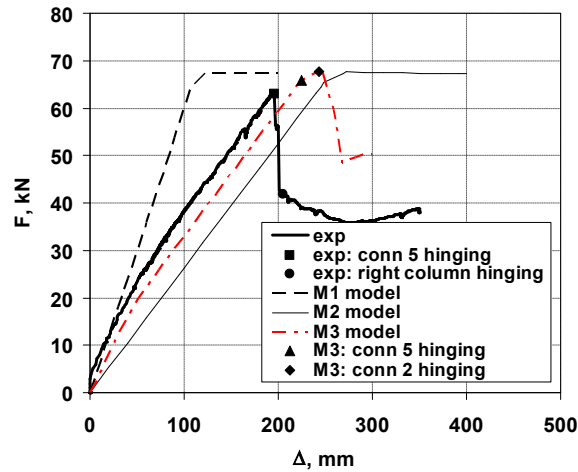


Figure 60. Frame C2: comparison of experimental and numerical lateral force – deformation curves.

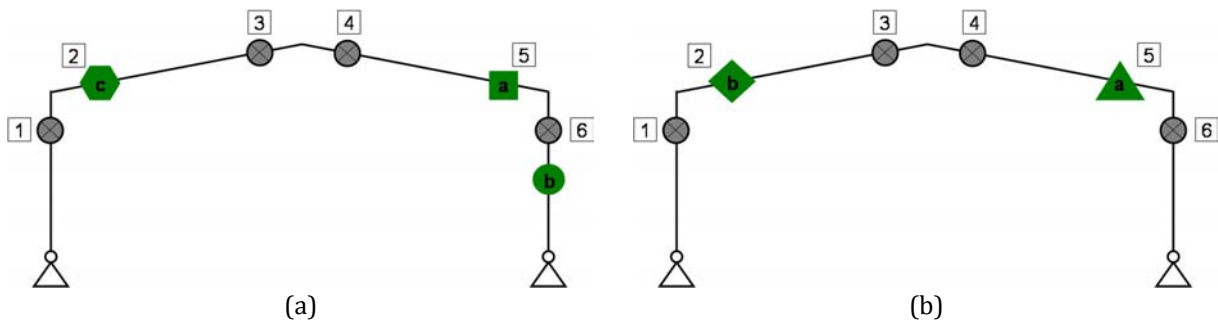


Figure 61. Frame C2: position of local buckling observed experimentally (b) and in the numerical model (c).

It can be concluded that the M3 model seems to provide the best agreement with the experimental results, if initial stiffness, lateral resistance, and post-buckling response are envisaged. The global frame resistance under lateral loads drops quickly after the first local buckling, when the maximum force is reached. This behaviour is attributed to the similar rapid drop in moment resistance of cold-formed cross-sections, as well as to the low redundancy of the frame. Therefore, for practical cases, the response to the first local buckle in members is important, which can be estimated using a simpler frame model, incorporating only the semi-rigid connection response, eventually an elastic perfectly plastic model. The Global frame stiffness determined using the bilinear moment-rotation characteristics obtained analytically by the component method is smaller than the experimental stiffness. The real initial stiffness of the connection may be higher at low moments, due to restraining provided by flanges of the bracket element and/or by the inner bolt group. The M3 connection model is capable of representing this higher stiffness and provides the closest match between experimental and numerical frame stiffness values.

2.2.3 OUTCOMES

This study suggests that the classical calculation model for connections, assuming the centre of rotation to be located at the centroid of the bolt group and a linear distribution of the forces on each bolt, is inappropriate for frames featuring cold-formed members. The force distribution is unequal due to the flexibility of the connected members. In fact, the force is an order of magnitude bigger in the outer bolt rows compared to most inner ones. A connection with bolts only on the web causes

concentrated forces in the web of the connected member and leads to premature web buckling, reducing the joint moment capacity. These type of connections are always partial strength. If the load bearing capacity of the connected beam is to be matched by the connection strength, bolts on the flanges become necessary. The ductility of the connection is reduced both under monotonic and cyclic loads and the design, including the design for earthquake loads, should take into account only the conventional elastic capacity. Because there is no significant post-elastic strength, there are no significant differences in ductility and capacity of cyclically tested specimens compared with the monotonic ones.

The application of the component method implemented in EN1993-1-8 for determination of connection characteristics in the case of cold-formed members is possible with a minimum number of adjustments. For the particular case of connection studied here (with both flange and web bolts), connection characteristics can be determined with a reasonable accuracy if only the outer bolt group of bolts is considered. The components contributing to the stiffness and strength of the connection are: cold-formed member flange and web in compression, bolts in shear, bolts in bearing on the cold-formed member, and bolts in bearing on the bracket. It is considered appropriate to use a linear distribution of forces on bolts in the case of a connection to light-gauge members.

The connection with both flange and web bolts is semi-rigid but full-strength. Therefore the design of light-gauge portal frames with the considered type of connection needs to account for connection flexibility. Connection characteristics obtained using the component method (EN1993-1-8) can be easily incorporated in the structural model, in order to obtain a realistic response under lateral forces. A connection model is developed that captures well both the behaviour in the elastic range and in the post-elastic range.

Though a detailed moment-rotation response representing the initial stiffness, moment resistance and post-buckling response provides the most realistic global response, a simple elastic structural analysis modelling connection stiffness alone can be sufficient for design purpose. Cold-formed steel pitched-roof portal frames of back-to-back channel sections and bolted joints are characterised by a rapid degradation of strength after the first local buckling in its members. This behaviour is attributed to the similar rapid drop in moment resistance of cold-formed cross-sections, as well as to the low redundancy of the frame analysed in this study. Therefore, for the considered frame configuration, global strength may be estimated at the attainment of the moment capacity in the most stressed cross-section using an elastic structural analysis. Axial forces can reduce moment resistance of cold-formed members and need be taken into account.

2.2.4 PUBLICATIONS

- [1] Dubina, D., Stratan, A., Nagy, Zs. (2009). "Full – scale tests on cold-formed steel pitched-roof portal frames with bolted joints". *Advanced Steel Construction* Vol. 5, No. 2, pp. 175-194. ISSN 1816-112X.
- [2] Dubina, D., Ungureanu, V., Stratan A., Nagy Zs. (2008). "Structural performance of pitched roof cold-formed steel frames of bolted joints". *Acta Technica Napocensis. Section: Civil Engineering – Architecture*. Nr. 51, vol. 1, 2008, ISSN 1221-5848, p. 385-396. *Proceedings of the International Conference – CONSTRUCTIONS 2008, 9-10 May 2008, Cluj-Napoca*.
- [3] Nagy, Zs., Stratan, A., Dubina, D. (2006). "Application of component method for bolted cold-formed steel joints". *Proc. of the international conference in metal structures, Poiana Brasov, Romania, September 20-22, 2006. Steel – a new and Traditional Material for Building*, Dubina and Ungureanu (eds.), Taylor and Francis Group, London, ISBN 0-415-40817-2, pp: 207-215

- [4] Dubina, D., Stratan, A., Ciutina, A., Fulop, L., Nagy, Zs. (2004). "Performance of ridge and eaves joints in cold-formed steel portal frames". Proc. of the 17th int. Specialty conf. "Recent advances and developments in cold-formed steel design and construction", Orlando, Florida, USA, 04-05 Nov. 2004. Univ. of Missouri-Rolla, Ed. R.A. LaBoube, W-W. Yu, p. 727-742.
- [5] Stratan, A., Nagy, Zs., and Dubina, D. (2006). "Cold-formed steel pitched-roof portal frames of back-to-back plain channel sections and bolted joints". Proc. of the 18th int. Specialty conf. "Recent research and developments in cold-formed steel design and construction", Orlando, Florida, USA, Oct. 26-27. Univ. of Missouri-Rolla, Ed. R.A. LaBoube, W-W. Yu, p. 351-365.
- [6] Dubina, D., Stratan, A., Ciutina, A., Fulop, L., Nagy, Zs. (2004). "Monotonic and cyclic performance of joints of cold formed steel portal frames", Thin-Walled Structures: Advances in Research, Design and Manufacturing Technology, Ed. J. Loughlan, IOP, ISBN 0 7503 1006 5, proceedings of the Fourth International Conference on Thin-Walled Structures, Loughborough, UK, 22-24 June 2004. pp: 381-388.
- [7] Dubina, D., Ungureanu, V. and Stratan, A. (2008). "Ultimate design capacity of pitch-roof portal frames made by thin-walled cold-formed members". Proceedings of the 5th International Conference on Thin-Walled Structures: Recent Innovations and Developments, Gold Coast, Australia, 18-20 June 2008, Vol. 1, p. 387-394, ISBN: 978-1-74107-239-6.
- [8] Dubina, D., Stratan, A., Nagy, Zs. (2007). "Full – scale testing of cold-formed steel pitched-roof portal frames of back-to-back channel sections and bolted joints". Proc. of the Sixth Intern. Conf. on Steel and Aluminium Structures, 24-27 July 2007, Oxford, UK. Beale, R.G. (Ed.), Oxford Brookes University, ISBN: 978-0-9556254-0-4, pp. 931-939.
- [9] Dubina, D., Nagy, Zs., Stratan, A., Fulop, L. and Ungureanu, V. (2006). "Design assisted by testing of cold-formed steel frame structures". Proc. of the 10th Nat. and 4th Int. conf. "Planning, design, construction and the construction industry". Editors R. Folic, V. Radonjanin, M. Trivunic. Novi Sad, November 22 - 24, 2006. pp: 203-212. ISBN 86-7892-016-5.
- [10] Dubina, D., Stratan, A., Ciutina, A., Fulop, L., and Nagy, Zs. (2004). "Monotonic and cyclic tests on cold-formed steel joints". COST C12 Improving Buildings Structural Quality by New Technologies, April 23-24, 2004, Rzeszow, Poland.
- [11] Dubina, D., Stratan, A., Ciutina, A., Nagy, Zs. (2004). "Experimental Research on Monotonic and Cyclic Performance of Joints of Cold-Formed Pitched Roof Portal Frames". Proc. "The Second International Conference on Steel & Composite Structures ICSCS'04", Ed. Chang-Koon Choi, Hwan-Woo Lee, Hyo-Gyong Kwak, ISBN 89-89693-13-6-98530. 2-4 September 2004, Seoul, Korea. pp: 176-190.
- [12] Dubina, D., Stratan, A., Ciutina, A., Fulop, L., Nagy, Zs. (2004). "Strength, stiffness and ductility of cold-formed steel bolted connections". Proc. of the Fifth AISC / ECCS International Workshop "Connections in Steel Structures V. Behaviour, Strength & Design", June 3-5, 2004. Ed. F.S.K. Bijlaard, A.M. Gresnigt, G.J. van der Vegte. Delft University of Technology, The Netherlands. ISBN: 978-90-9019809-5, pp. 263-272.

2.3 HIGH STRENGTH STEEL IN SEISMIC RESISTANT STRUCTURES

Seismic resistant building frames designed as dissipative structures, must allow for plastic deformations to develop in specific members, whose behaviour is expected to be predicted and controlled by proper calculation and detailing. Members designed to remain elastic during earthquake, such as columns, are characterized by high strength demands. Dual-steel structural systems, optimized according to Performance Based Design (PBD) philosophy, in which High Strength Steel (HSS) is used in predominantly "elastic" members, while Mild Carbon Steel (MCS) is used in dissipative members, can be very reliable and cost efficient. Current European seismic design codes do not cover this specific configuration. An extensive research project, HSS-SERF – High Strength Steel in Seismic Resistant Building Frames, was carried out with the aim to investigate and evaluate the seismic performance of dual-steel building frames. Main results investigated at the Politehnica University of Timisoara are presented in the following.

2.3.1 STEEL-CONCRETE CONNECTION IN CONCRETE-FILLED RECTANGULAR HOLLOW SECTION COLUMNS

Concrete filled tubes (CFT) have the advantage of improved rigidity and resistance to fire, as well as similar cross-sectional properties on principal loading directions. The combination the two materials (steel and concrete) may lead to a reduced steel section. However, a particular attention should be given in order to distribute the stresses between the steel tube and the concrete core. Within the current research, the goal was to count on both materials (steel and concrete) and to have a composite action ensured by the use of shot fired nails, also termed as powder-actuated fasteners.

The nailed shear connection was developed in a research project conducted at the Technical University of Innsbruck: Fink (1997) and Larcher (1997). As a result, the use of powder-actuated fasteners is a relatively new method for assuring shear connection in areas where loads are induced to composite tubular columns – Beck and Reuter (2005). The powder-actuated fasteners are driven through the tube walls from the outside and then protrude inside the tube. The connection between the surrounding tubular section and the concrete inside is then provided by direct pressure of the concrete against the shanks of the nails. The main advantage of this solution is that it is quick and easy to apply, especially for columns which are continuous over several storeys.

Extensive experimental investigations were performed by Beck (1999) covering a number of 30 push-out tests with pipe specimens. Influences of pipe geometry, concrete strength and type of fastener on the load-deflection characteristics were investigated. The load deflection behaviour exhibited excellent ductility combined with high load-bearing capacity per fastener. Based on these findings the nailed shear connection was introduced into practice with the Millennium Tower in Vienna, a fifty storey high rise building completed in 1999, where it has proven to be a reliable and cost effective connection method as no welding work was required: Huber (2001). Additional experimental investigations were performed, by Hanswille et al (2001) with the aim to investigate the behaviour of the shear connection subjected to a serviceability limit state loading sequence, and the long term behaviour and influence of concrete creep on the nailed shear connections.

The aim of the experimental program was to evaluate the load introduction within composite columns realized as concrete filled tubes of high strength steel (see Figure 62). For this purpose load introduction tests were performed on a number of 6 specimens varying parameters such as: loading procedure (monotonic, cyclic), connection type (steel-concrete bonding, steel-concrete bonding combined with connectors), and steel grade (S460, S700). The objective of research was to assess the efficiency of the shot fired nails in providing the shear connection between the steel tube

and the concrete core under monotonic and cyclic loading. As connectors, a number of 24 Hilti X-DSH32 P10 shot fired nails were used per column stub.

The particularities of the current experimental program, with regard to the previous studies, are related to: rectangular hollow section tubes, high strength steel (S460, S700), cyclic loading procedure, evaluation of the friction forces between the steel tube and the concrete core. The experimental program is summarised in Table 15. Consequently, a number of 6 tests on column stubs were performed under monotonic and cyclic loading taking into consideration the cases below:

- 1 monotonic and 1 cyclic test on the column stub taking into account only the adhesion between the steel tube and the encased concrete (S700-F-M / S700-F-C);
- 1 monotonic and 1 cyclic test on the column stub containing steel-concrete bonding combined with connectors (S700-F-H-M / S700-F-H-C);
- 1 monotonic and 1 cyclic test on the column stub containing steel-concrete bonding combined with connectors (S460-F-H-M / S460-F-H-C);



Figure 62. Specimen configuration for the load introduction tests.

Table 15. Experimental program - load introduction tests.

Nr.	Specimen	Tube	Bond	Load
1	S700-F-M	RHS 250x10 S700	Friction	Monotonic
2	S700-F-C	RHS 250x10 S700	Friction	Cyclic
3	S700-F-H-M	RHS 250x10 S700	Friction and Nails*	Monotonic
4	S700-F-H-C	RHS 250x10 S700	Friction and Nails*	Cyclic
5	S460-F-H-M	RHS 300x12.5 S460	Friction and Nails*	Monotonic
6	S460-F-H-C	RHS 300x12.5 S460	Friction and Nails*	Cyclic

* 24 Hilti X-DSH32 P10 shot fired nails

The column stub specimens were manufactured using cold formed steel hollow section tubes of 800 mm length. The concrete core was considered with a depth of 600 mm inside the steel tubes. For the application of the load, plates were welded in the shape of a double T beam on two opposite tube walls.

For the positioning of the connectors, installation instructions were prepared by Beck (2010) at Hilti AG based on the particularities of the current experimental program (steel grade and thickness of the tubes). Consequently, it was recommended to use the X-DSH32 P10 nails and to apply them before concreting in order to drive them consistently straight through the tube walls. Furthermore, due to the use of high-strength steel, pre-drilling of the steel with a small pilot hole would be necessary. The installation instructions contained also information related to the powder-actuated fastening tool equipment and the step-by-step nail application procedure.

With the aim to assess the behaviour and the characteristics of the connection between the steel tube and the encased concrete, an experimental test set-up was designed (see Figure 63a) in order to be used within a universal testing machine, and considering the following:

- monotonic as well as cyclic loading conditions of the specimens;
- top and bottom supports (see Figure 62) in contact with concrete core only;
- load to be applied on the steel tube;
- load path from the steel tube to the concrete core:
- friction / friction + connectors;

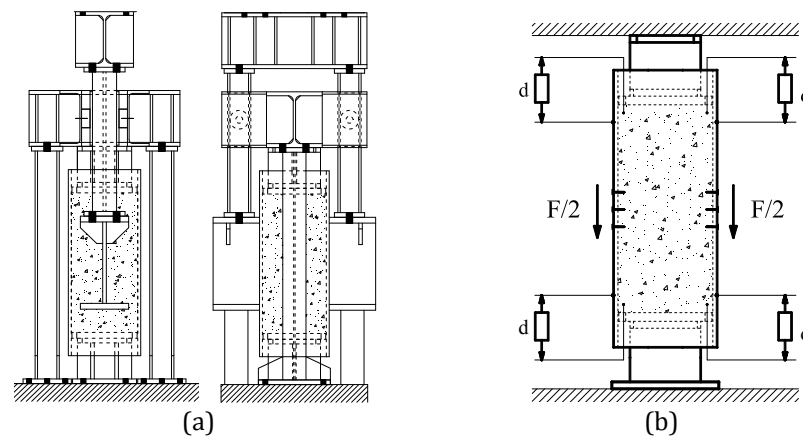


Figure 63. Conceptual scheme (front and lateral view), and illustration of the test set-up (a) and Conceptual scheme and illustration of instrumentation arrangement (b).

The instrumentation of the specimens (see Figure 63b) consisted in the measurement of the force applied by the testing machine and the relative displacement between steel tube and concrete core, using two displacement transducers at the top side and two at the bottom side.

The parameters used to control the load introduction tests, were the relative displacement "d" between the steel tube and the concrete core, and the force "F". Three alternating cycles with a peak load of up to 25% of the expected yield load were applied to the test assembly before the test itself in order to stabilize the system. During the test itself, the load was applied in force control within the elastic range and in displacement control for the plastic range. For the cyclic loading, the ECCS (1986) procedure was used.

At 28 days from concrete casting, compression tests were performed on concrete cube samples. Consequently, the average characteristic strength was obtained in amount of 35.88 N/mm², a value slightly lower than the minimum characteristic strength (37 N/mm²) corresponding to a C30/37 concrete class.

The X-DSH32 P10 nails of 4.5 mm diameter were tested to shear by Hilti AG (1998) obtaining an average shear force in amount of 21.85 kN (at 25°C). Consequently, the corresponding shear stress was in amount of 1374 N/mm² and the equivalent stress was obtained in amount of 2380 N/mm². In addition, according to Hanswille et al. (2001), the ultimate strength of the X-DSH32 P10 nails was corresponding to $f_u = 2200$ N/mm².

The test assemblies of the three column stub configurations are shown in Figure 64. The experimental investigations started with the three monotonic tests. The obtained force vs. relative displacement curves allowed assessing the yield displacements "d_y", necessary for the ECCS (1986) cyclic loading procedure. Accordingly, the yield displacements were as follows: 0.75 mm for the column stub with friction bond only, and 1 mm for the two column stubs with friction and connectors.



Figure 64. Test assembly of the three column stub configurations

The monotonic and cyclic response of the friction, developed between the steel tube and the concrete core, is shown in Figure 65 and Figure 66. It can be observed that above a relative displacement of 2 mm the monotonic force transmitted through friction was measured in amount of 200 kN. Under cyclic loading the force developed through friction was lower (approximately 160 kN corresponding to the maximum amplitude of a cycle and 20 kN corresponding to the initial position, i.e. 0 relative displacement).

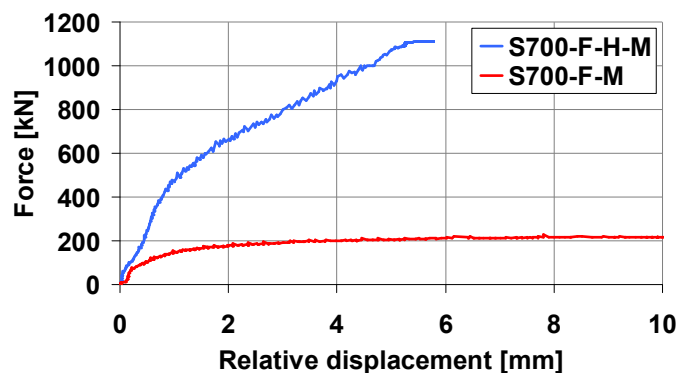


Figure 65. Contribution of the connectors under monotonic loading.

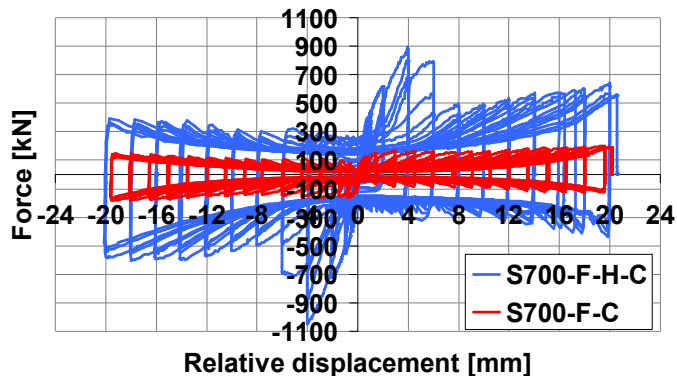


Figure 66. Contribution of the connectors under cyclic loading.

A graphical comparison in terms of monotonic response corresponding to the column stubs without nails (S700-F) and with nails (S700-F-H) can be seen in Figure 65. It can be observed that the contribution of the 24 connectors is significant. In addition, the response under cyclic loading of the column stubs without and with connectors can be seen in Figure 66. The connectors show a significant contribution also under cyclic loading conditions. It can be observed that exceeding a relative displacement of approximately 5 mm, the capacity of the steel-concrete connection decreased due to fracture of the connectors at the interface between steel tube and concrete core as will be further shown.

The response under cyclic loading of the two specimens with both connectors and steel-concrete bonding is compared in Figure 67. The difference between the two configurations is given by the steel tube. The S460 tube is a square RHS 300x12.5, while the S700 tube is a square RHS 250x10. In the first case the thickness of the tube is 12.5 mm and in the other case the thickness is 10 mm. The lateral surface of the concrete core is 660000 mm² within the S460 tube, and 552000 mm² within the S700 tube. It is to be noted that the concrete depth in both cases was 600 mm. A slightly higher friction force was therefore developed within the column stub with larger steel tube (S460).

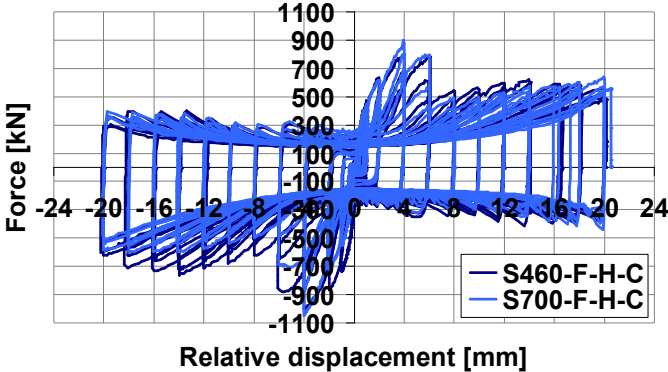


Figure 67. Cyclic response of the stubs with steel-concrete bonding and connectors.

In order to observe the deformations developed within connectors and the concrete around them, two side walls of the column stubs S460-F-H-M and S460-F-H-C, were cut out with flame. The response of concrete and connectors to monotonic loading can be observed in Figure 68. It can be observed that the concrete was crushed in a small amount at the contact with the shot fired nails which were bent. The response of concrete and connectors to the cyclic loading condition is shown in Figure 69. It can be observed that under alternating cycles the connectors were broken at the interface between concrete core and steel tube. The protruding part of the steel tube, rubbed on the concrete surface.



Figure 68. Detail of concrete and connector after monotonic loading.



Figure 69. Detail of concrete and connector after cyclic loading.

2.3.2 EXPERIMENTAL TESTS ON WELDED BEAM TO CONCRETE-FILLED RHS COLUMN JOINTS

An experimental program was developed and carried out with the aim to characterize the behaviour of two types of moment resisting joints in multi-storey frames of concrete filled high strength steel rectangular hollow section (RHS) columns and steel beams. Reduced beam section and cover plate beams are welded to columns in order to obtain ductile and over-strength joints, according to EN 1998-1 request.

The study of the beam-to-column joints is related to the seismic performance evaluation of the dual-steel building frames within HSS-SERF research project, i.e. moment resisting frames, dual concentrically braced frames (D-CBF) and dual eccentrically braced frames (D-EBF) in which mild carbon steel (MCS) is used in dissipative members while high strength steel (HSS) is used in non-dissipative "elastic" members. Accordingly, the beams in MRF are realized of S355 steel grade, while the columns are concrete filled rectangular hollow section tubes (CF-RHS) of high strength steel (S460 and S700). As basis for definition of the experimental program on beam-column joints, cross-sections from the D-CBF frame designed by GIPAC (2011) were used (Figure 70), considering two combinations of HSS/MCS:

- CF-RHS 300x12,5 S460 column and IPE 400 S355 beam;
- CF-RHS 250x10 S700 column and IPE 400 S355 beam.

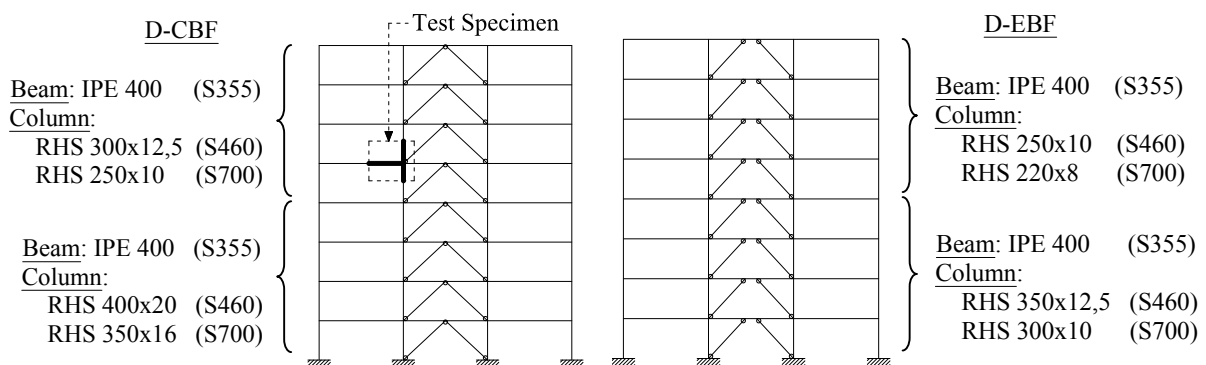


Figure 70. Designed frames with CFT columns.

The beams are welded to the columns considering the two types of connections: with reduced beam section (RBS), and with cover plates (CP). Due to the flexibility of the tube walls under transverse forces, the connection solution of the beams and columns within the current research was based on the use of external diaphragms. The design was performed considering the development of the

plastic hinge in the beams. Further with the bending moment and shear force from the plastic hinge, the welded connections and the components of the joint (cover plates, external diaphragm and column web panel) were designed or checked so as to comprise an equal or higher capacity in comparison to the fully yielded and strain hardened plastic hinge. Figure 71 illustrates the two beam-to-column joint configurations, i.e. with reduced beam section (a) and with cover plates (b).

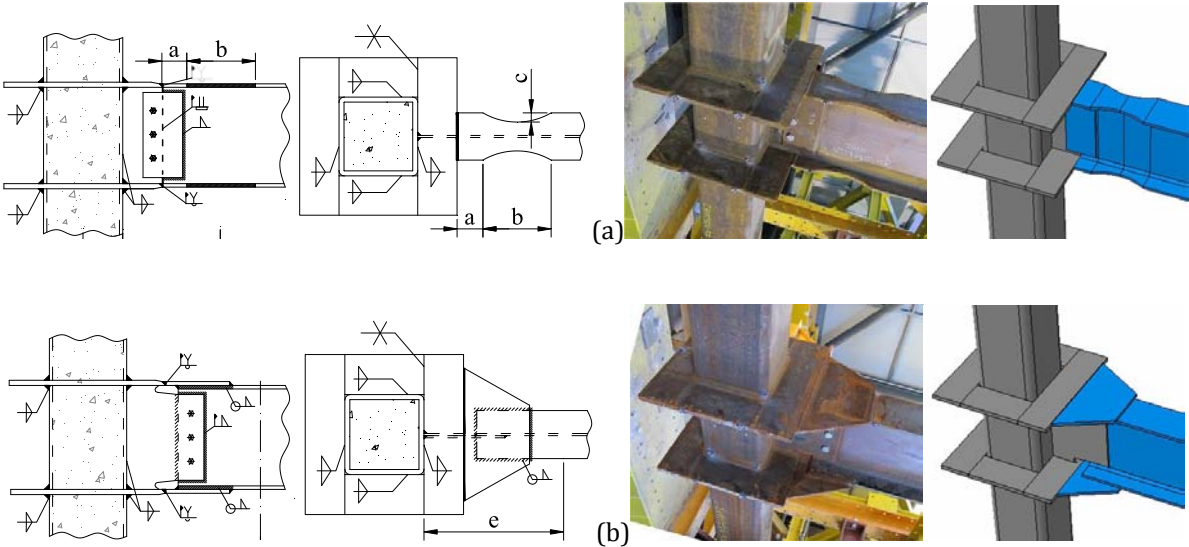


Figure 71. Configuration of the designed beam-to-column joints: with reduced beam section (a), and with cover plates (b).

The main objective of the experimental tests was to pre-qualify by tests welded connections in moment resisting frames and dual braced frames designed using the dual-steel concept. The experimental program on beam-to-column joints with CF-RHS columns is summarized in Table 16. The variations in the configuration of the joints are given by two joint typologies (reduced beam section – RBS, and cover-plate – CP), two steel grades for the rectangular hollow section tubes (S460 and S700) and two intended failure modes (beam and connection zone). In addition two loading conditions were considered for each beam-to-column joint configuration, i.e. monotonic and cyclic loading procedure.

Table 16. Experimental program on beam-to-column joints with CF-RHS columns.

Parameter	Variable	No. of variations	No. of specimens
Loading	Monotonic and Cyclic	2	16
Joint type	Reduced Beam Section and Cover-Plate	2	
HSS grade	S460 and S690	2	
Failure mode	Weak beam / Weak connection	2	

Considering the two joint typologies (RBS and CP) and two steel grades for the tubes (S460 and S700), a number of four beam-to-column joint configurations were designed. Additionally, in order to assess the over-strength of the connection zone and to observe the base components of the joint configurations, tests were considered on the corresponding joints for which the beam was strengthened with the aim to avoid the formation of the plastic hinge in the beam and to force the plastic deformations in the connection zone.

The intended plastic mechanism corresponding to the four designed beam-to-column joints is related to the formation of the plastic hinge in the beam and an elastic response of the connection and joint components. In contrast, for the beam-to-column joints with strengthened beam the

intended failure mode is related to the connection and joint components. Table 17 describes for each of the 16 beam-to-column joints, the labelling, column and beam, joint typology, loading procedure and intended failure mode.

Table 17. Beam-to-column joint configurations.

Nr.	Specimen name	Column	Beam	Joint type	Loading	Intended failure mode
1	S460-RBS-M	RHS 300x12.5 S460	IPE400 S355	RBS	Monotonic	Beam
2	S460-RBS-C				Cyclic	
3	S700-RBS-M	RHS 250x10 S700	IPE400 S355	RBS	Monotonic	Beam
4	S700-RBS-C				Cyclic	
5	S460-CP-M	RHS 300x12.5 S460	IPE400 S355	CP	Monotonic	Beam
6	S460-CP-C				Cyclic	
7	S700-CP-M	RHS 250x10 S700	IPE400 S355	CP	Monotonic	Beam
8	S700-CP-C				Cyclic	
9	S460-RBS-R-M	RHS 300x12.5 S460	IPE400 S355	RBS	Monotonic	Connection
10	S460-RBS-R-C				Cyclic	
11	S700-RBS-R-M	RHS 250x10 S700	IPE400 S355	RBS	Monotonic	Connection
12	S700-RBS-R-C				Cyclic	
13	S460-CP-R-M	RHS 300x12.5 S460	IPE400 S355	CP	Monotonic	Connection
14	S460-CP-R-C				Cyclic	
15	S700-CP-R-M	RHS 250x10 S700	IPE400 S355	CP	Monotonic	Connection
16	S700-CP-R-C				Cyclic	

The conceptual scheme and an illustration of the experimental test set-up is shown in Figure 72. A hydraulic actuator connected at the tip of the beam served as loading device. The column was supported at both ends considering a pinned connection. The horizontal and vertical displacements were blocked by the right support, and only the vertical displacements were restrained by the left support. A lateral support system was used to block the out of plane deformations of the beam.

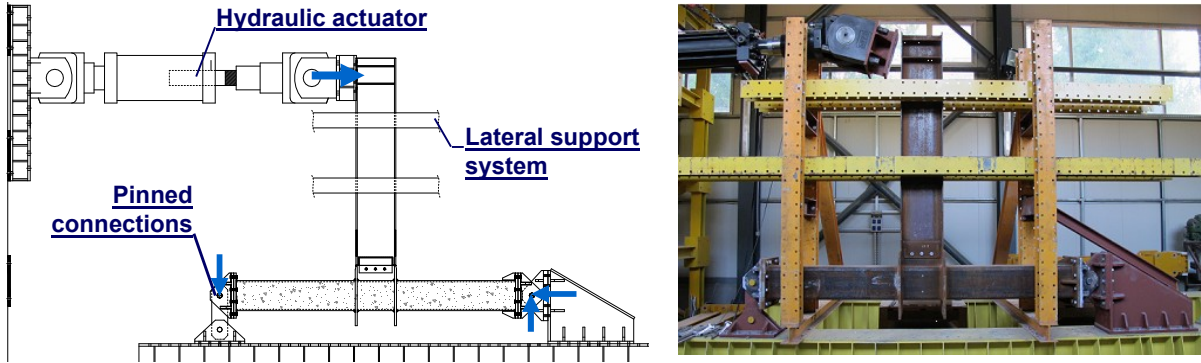


Figure 72. Conceptual scheme and illustration of the test assembly.

Global as well as local instrumentation of the specimens was considered using the measuring instruments of the loading device, displacement transducers, and an optical measuring system (Vic 3D). From the global instrumentation, information was obtained related to the force in the actuator, the displacement at the tip of the beam, the horizontal and vertical displacement at supports (see Figure 73a). The measurements at the supports were performed at the front side as well as at the back side of the joint assembly. Local instrumentation was aimed to measure the deformations within the dissipative zone and the connection zone (see Figure 74), as well as in the column web panel (see Figure 73b). In order to identify the sequence of yielding, the connection zone was prepared by whitewashing (see Figure 74). The optical measuring system Vic 3D was used in order

to observe the initiation of yielding. Depending on each joint configuration and on the intended failure mode, different components were investigated using the optical measuring system, i.e. the beam web from the dissipative zone, the external diaphragm, or the column web panel.

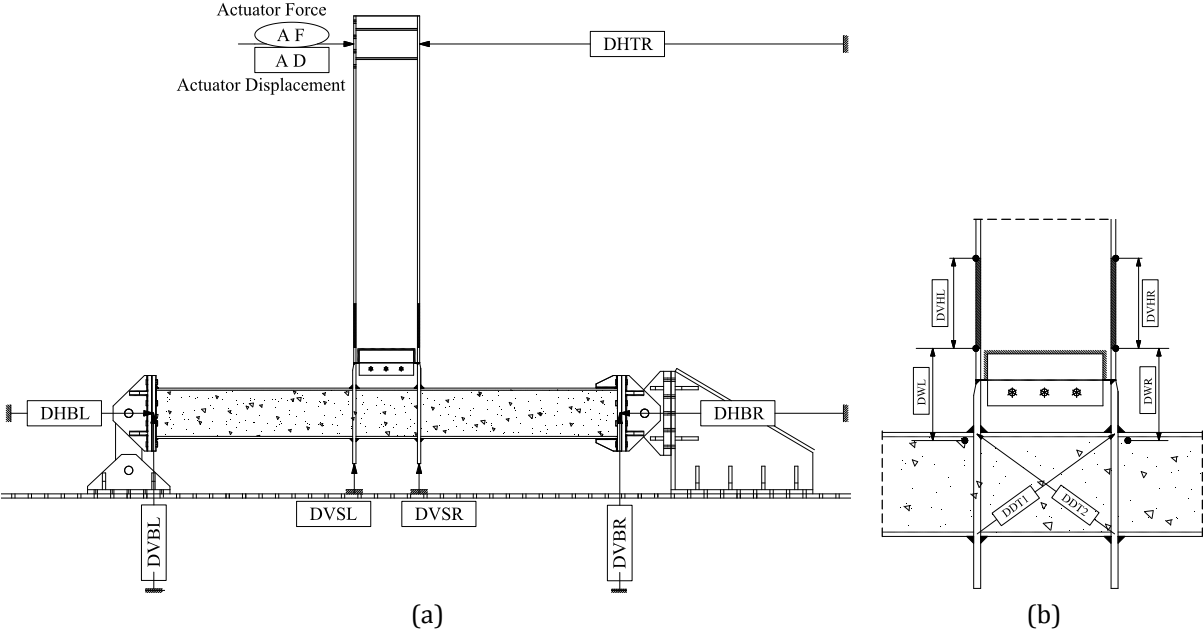


Figure 73. Global instrumentation (a) and local joint instrumentation (b).

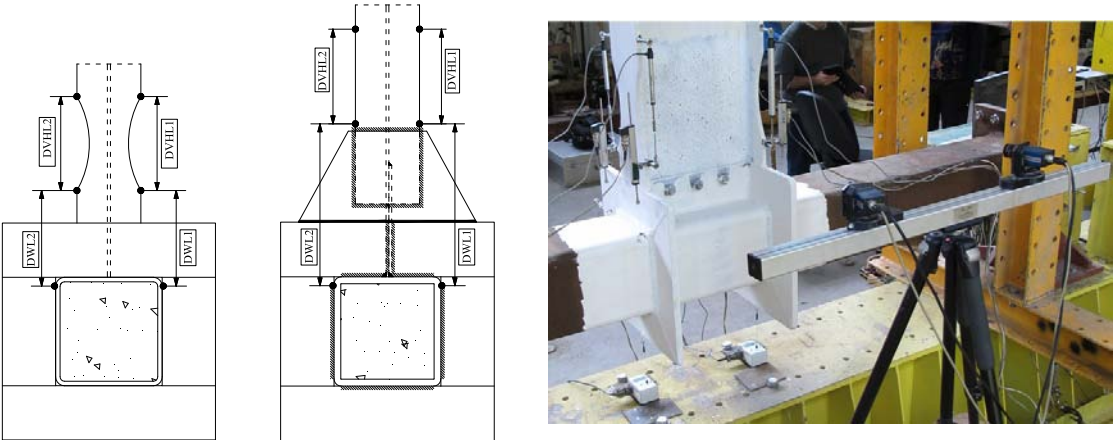


Figure 74. Instrumentation of joint, and connection zone prepared by whitewashing.

The parameters used to control the tests were the inter-storey drift " θ " of test assembly and the bending moment " M " computed at column centerline. Monotonic loading was applied by progressively increasing the displacement at the tip of the beam. One unloading-reloading phase was considered for a better estimation of the initial stiffness. The ANSI/AISC 341 loading protocol was used for the cyclic loading.

Experimental investigations were performed also on material samples with the aim to assess the characteristics of all parts of the joint assemblies. Compression tests on concrete cube samples were performed at 28 days from concrete casting, obtaining an average characteristic strength in amount of 35.88 N/mm². In addition, tensile and Charpy V-notch impact tests were performed on the steel samples prepared from additional material (profiles and plates as summarized in Table 18) associated to each component of the beam-to-column joints.

For each component of the joint assemblies (i.e. beam, cover plates, external diaphragms, RHS tubes, stiffeners, etc.), a number of three samples were prepared and tested considering both tensile and Charpy V-notch test. The results obtained are summarized in Table 18. Consequently, for each component the average values are shown regarding the yield strength (R_{eH}), ultimate strength (R_m), elongation at fracture (A) and elongation at maximum force (A_g). The table shows also the results obtained from the Charpy V-notch tests, i.e. the average value of the absorbed energy, the temperature of the samples during the test and the minimum required energy. It is to be noted that the samples marked with "*" were prepared with 7.5 mm thickness. The results obtained on steel samples allowed assessing the properties of all joint parts and confirmed that the steel grades were in accordance with the code requirements.

Table 18. Tensile and Charpy V-notch test results for steel samples

Steel component / grade			Tensile tests				Charpy V-notch tests		
			R_{eH}	R_m	A	A_g	T	KV _{min}	KV
			N/mm ²	N/mm ²	%	%	°C	J	J
1	IPE 400 flange	S355 JR	393.9	491.9	30.9	16.3	20	27	57.6
2	IPE 400 web *	S355 JR	439.5	507.5	29.1	15.8	20	27	99.6
3	Cover plates	S355 J0	432.7	489.1	30.8	16.2	0	27	266.6
4	Splice plate	S355 J2	415.3	503.0	26.9	15.2	-20	27	221.3
5	RHS 300x12.5	S460 M	497.7	554.1	22.4	7.7	-20	40	247.3
6	RHS 250x10 *	S700 QL	725.4	830.	11.8	-	-20	40	102.3
7	External diaphragm	S460 NL	463.4	618.9	24.2	13.6	-30	40	58.6
8	External diaphragm	S690 QL	725.8	807.1	16.3	5.5	-20	40	233.3
9	Vertical stiffener	S460 NL	495.1	622.4	25.9	13.6	-30	40	152.3
10	Vertical stiffener *	S690 QL	806.9	854.7	14.2	5.7	-20	40	150.6

Due to the innovative joint configurations, it was needed to have an accurate prediction for the behaviour of the joints in order to avoid unacceptable failure during the experimental tests. Therefore, a set of numerical simulations have been performed. In a first step the material model was calibrated based on results from compression tests on concrete samples and tensile tests on steel samples. Using the calibrated material model, the behaviour of each joint configuration was obtained. The pre-test numerical simulations allowed assessing for each joint configuration, the stress distribution and plastic strain, as well as the moment-rotation curve, confirming a good design of the joints and the intended failure mechanism.

Figure 75 and Figure 76 show the response and failure mechanism of RBS joints subjected to monotonic and cyclic loading. The yielding was initiated in the beam flanges within the RBS zone and was followed by large plastic deformations – local buckling of flanges and web under compression.

Figure 77 and Figure 78 show the response and failure mechanism of CP joints subjected to monotonic and cyclic loading. The yielding was initiated in the beam flanges near the cover plates and was followed by large plastic deformations – local buckling of flange and web under compression. No damage was observed in cover plates, external diaphragm and column web panel.

Figure 79 and Figure 80 show the response and failure mechanism of the joints with strengthened beam flanges (RBS-R), subjected to monotonic and cyclic loading. The yielding was initiated in beam flanges (between the reinforcing plate and external diaphragm) under compression/tension and was followed by yielding of web and external diaphragm. Finally, the beam flanges fractured in the heat affected zone (HAZ) due to tension forces.

Figure 81 and Figure 82 show the response and failure mechanism of joints with extended cover plate (CP-R) subjected to monotonic and cyclic loading. For the S460-CP-R joints, the yielding was initiated in the external diaphragm and was followed by local deformations of cover plates under compression/tension and yielding of the column web panel. For the S700-CP-R joints, the yielding was initiated in the compressed cover plate and was followed by failure of the welded connection between plates that composed the external diaphragm, however at forces higher than the design capacity.

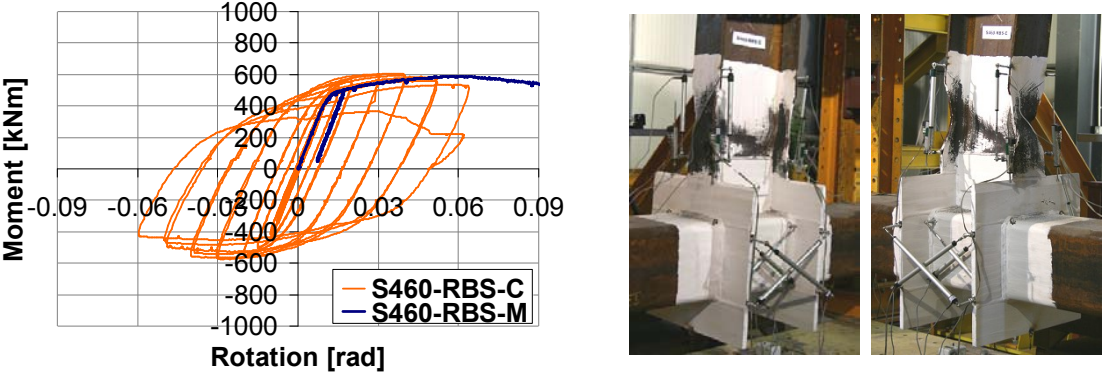


Figure 75. S460-RBS-C joint: cyclic response and illustration of failure mode.

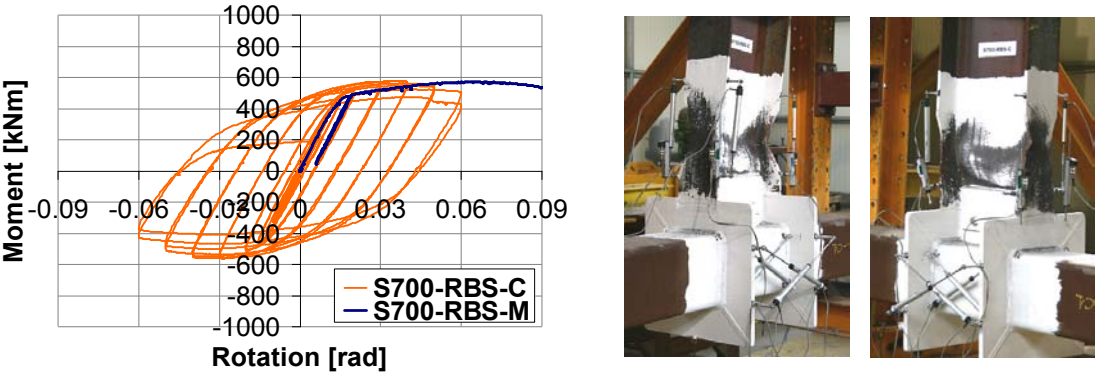


Figure 76. S700-RBS-C joint: cyclic response and illustration of failure mode.

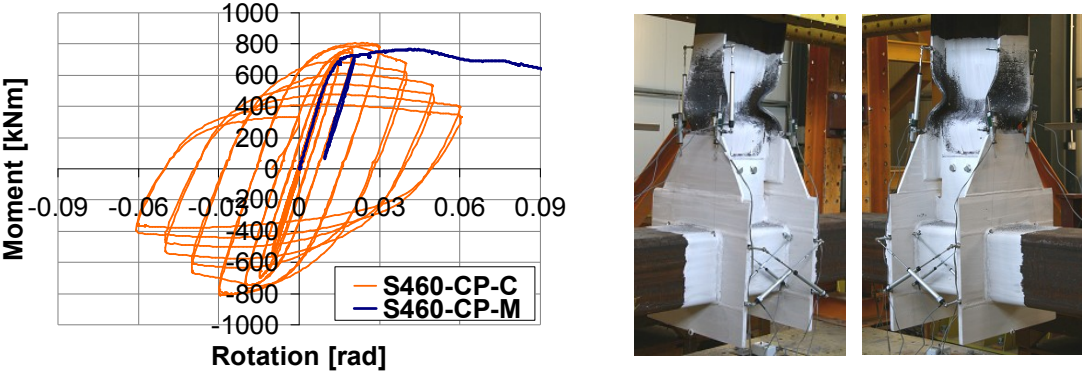


Figure 77. S460-CP-C joint: cyclic response and illustration of failure mode.

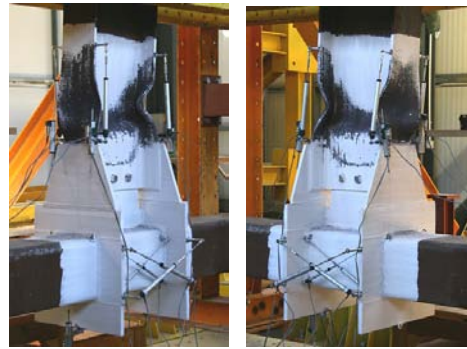
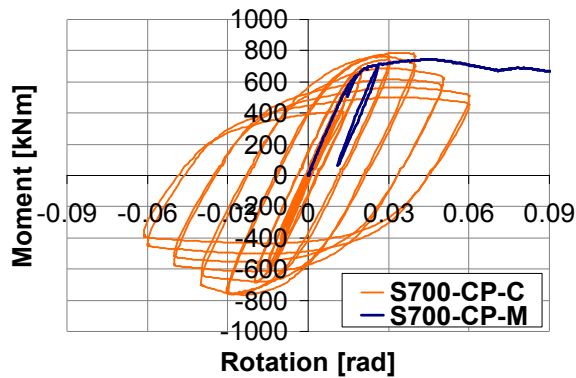


Figure 78. S700-CP-C joint: cyclic response and illustration of failure mode.

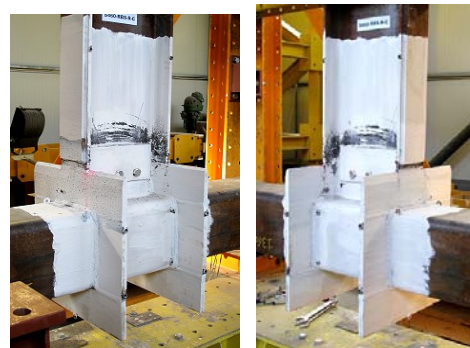
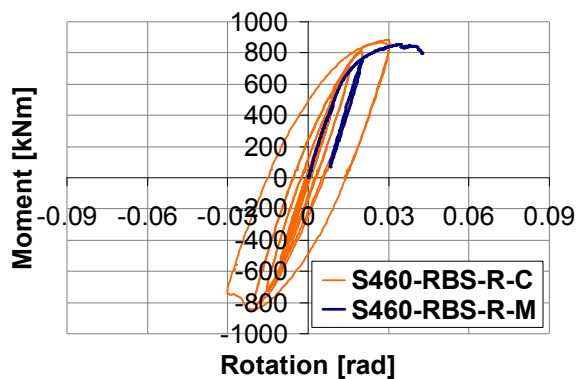


Figure 79. S460-RBS-R-C joint: cyclic response and illustration of failure mode.

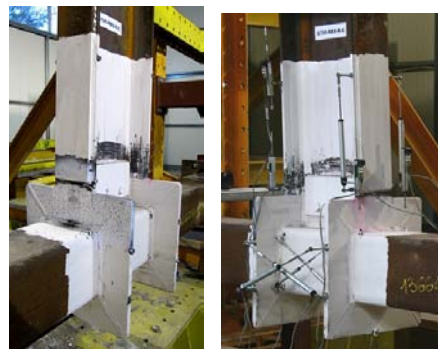
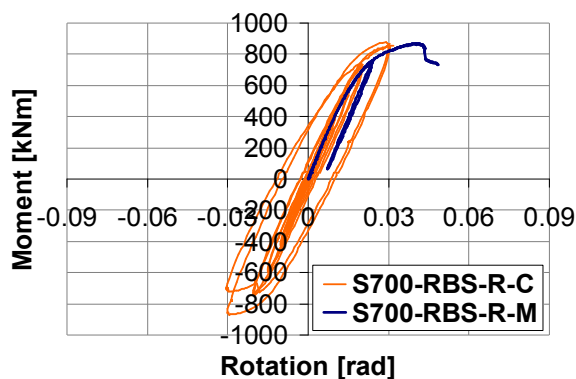


Figure 80. S700-RBS-R-C joint: cyclic response and illustration of failure mode.

The interpretation of results is made in relation to the following aspects:

- Overstrength of connection zone;
- Contribution of components to the joint rotation;
- Evaluation of the rotation capacity.

With the aim to assess the overstrength of the joint and connection zone, a comparison was made between the four designed joints and the corresponding joints with reinforced beam. Figure 83 illustrates the overstrength of the RBS joints and Figure 84 illustrates the overstrength of CP joints.

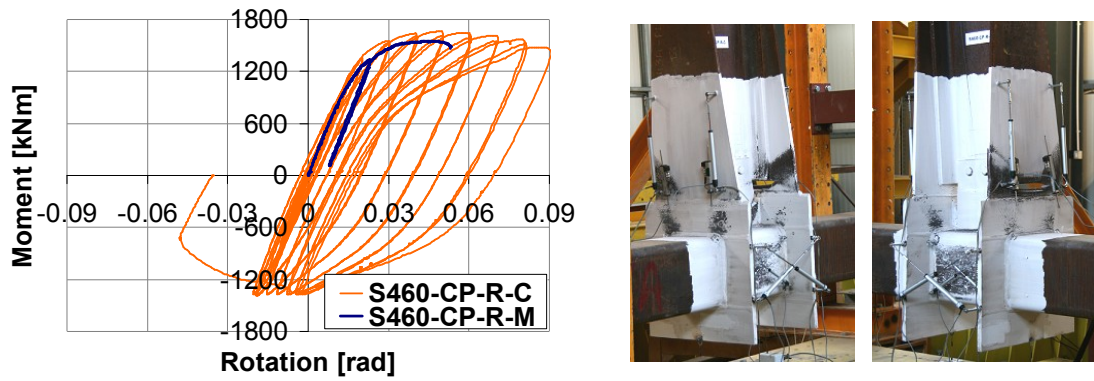


Figure 81. S460-CP-R-C joint: cyclic response and illustration of failure mode.

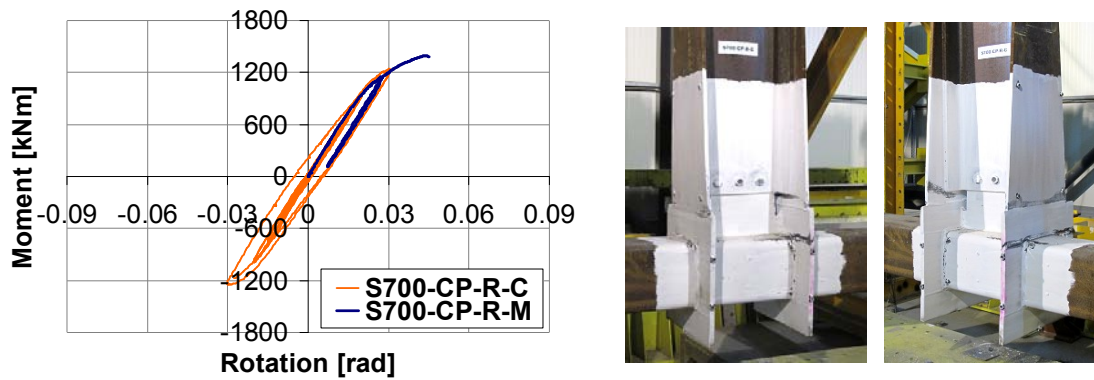


Figure 82. S700-CP-R-C joint: cyclic response and illustration of failure mode.

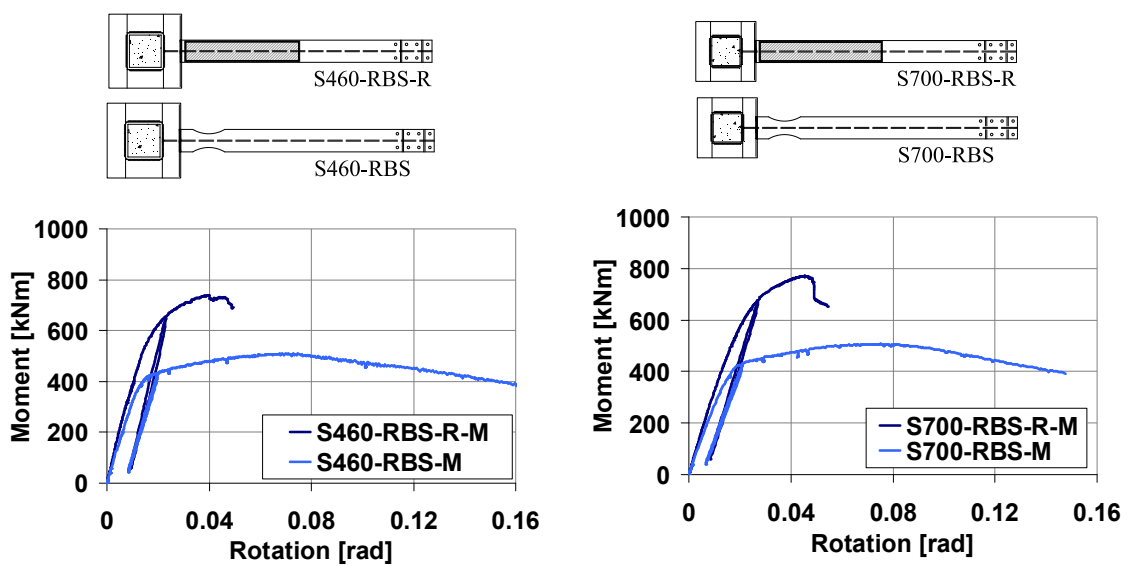


Figure 83. Overstrength of connection zone for RBS joints

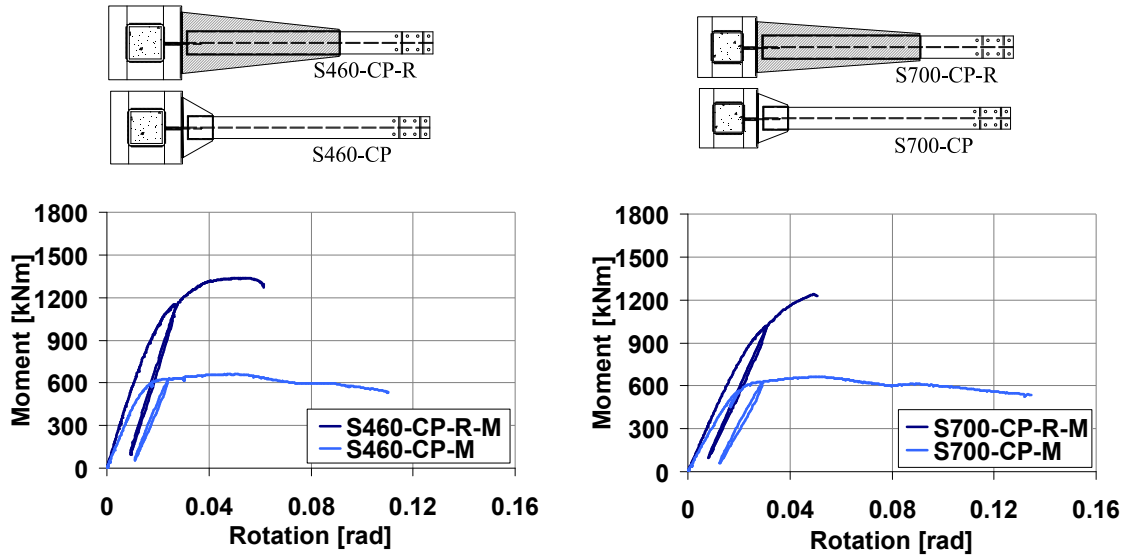


Figure 84. Overstrength of connection zone for CP joints

Table 19. Contribution of components to the rotation capacity of the joints [mrad].

	S460-RBS	S700-RBS	S460-CP	S700-CP
Total assembly rotation (EN1998-1 criterion)	50	50	40	40
Column web panel	1.1	3.8	1.6	2.1
Connection	6.7	7.6	1.9	3.7
Plastic hinge	43.1	38.2	34.1	29.1
Elastic rotation	3.7	4.5	5.7	6.7

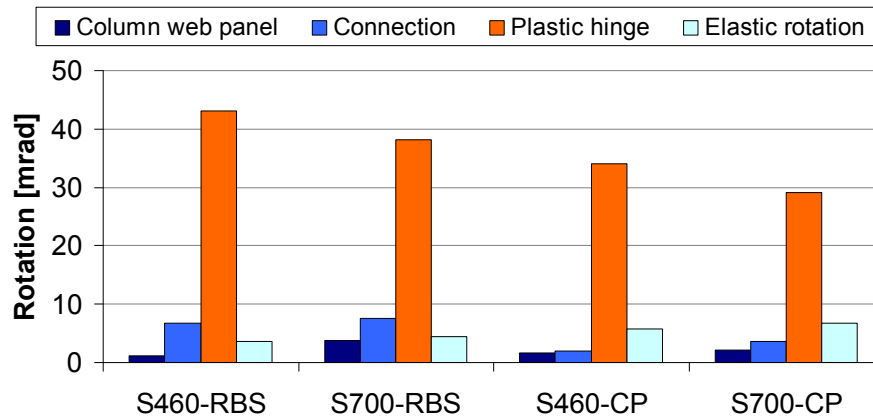


Figure 85. Contribution of components to the rotation capacity of the joints.

The moment-rotation curves were computed at the connection to the external diaphragm, and the overstrength was evaluated corresponding to the yield point and to the maximum capacity. Consequently, the overstrength of the connection zone for the RBS joints (S460 and S700) was evaluated in the amount of 34% and 35% at yield, and respectively 53% and 60% at maximum capacity. The overstrength of the connection zone for the CP joints (S460 and S700) was computed in amount of 55% and 43% at yield, and respectively 101% and 86% at maximum capacity.

The main plastic deformations occurred in the dissipative zone of the beam (plastic hinge). The contribution of the connection and column web panel to the overall joint rotation was observed to

be low. The rotation capacity of the RBS and CP designed joints was evaluated considering the EN 1998-1 (2004) criterion for which the reduction of stiffness and capacity is not greater than 20%. The total assembly rotation for which the reduction of stiffness and capacity was not greater than 20% was corresponding to the 50 mrad cycle for RBS joints and to the 40 mrad cycle for the CP joints. The contribution of the components, including the elastic rotation, to the total joint rotation is summarized in Table 19 and illustrated in Figure 85.

2.3.3 NUMERICAL INVESTIGATION OF WELDED BEAM TO CONCRETE-FILLED RHS COLUMN JOINTS

The objectives of the numerical investigation program conducted on the welded beam-to-CF-RHS column joints are represented by the following aspects:

- Calibration of the material model based on material sample tests;
- Pre-test numerical simulations aimed to offer an accurate prediction of the behaviour of the joints in order to avoid unacceptable failure during the experimental tests;
- Calibration of the numerical model of the joints based on the monotonic and cyclic test results, allowing for a better understanding of the behaviour and response of each beam-to-column joint configuration;
- Extension of the experimental program with additional cases, i.e. parametric study for the investigation of: influence of the concrete core, influence of the axial force acting on the column, influence of the external diaphragm, response of joints with two and respectively four beams;
- Validation of the design relations for the joint components and design procedure;
- In a first step the material model was calibrated based on material sample tests. The pre-test numerical simulations, containing the calibrated material model, allowed assessing for each joint configuration, the stress distribution and plastic strain, as well as the moment-rotation curve, confirming a good design of the joints and the intended failure mechanism.

The calibration of the numerical models of the joints started with the calibration of the material model for each part of the beam-to-column joint assemblies. The stress-strain relationship used for concrete, was computed using the results from the compression tests, and the analytical stress-strain model as reported by Ali et al. (1990). The concrete damaged plasticity model was used and in addition the plasticity parameters, compression damage and tensile behaviour from Korotkov et al. (2004). The calibration of the material model for the steel grades was performed based on the tensile test results. Consequently, Figure 86 illustrates for the IPE400 beam flange, the comparison between test and simulation, in terms of force-displacement curve, for which a good correlation can be observed. The young modulus was considered equal to $E=210000 \text{ N/mm}^2$, and the Poisson ratio was considered as $\nu=0.3$.

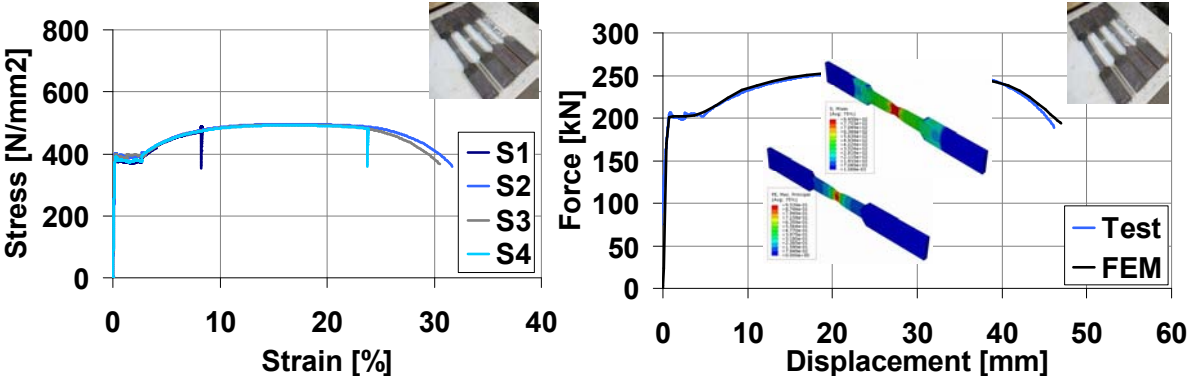


Figure 86. Calibration of the material model for steel (IPE400 beam flange).

The numerical investigations were performed with the finite element modelling software Abaqus (2007). All the components of the beam-to-column joints were modelled using solid elements. Due to the large amount of contact surfaces between the concrete core and surrounding steel tube, the Dynamic Explicit type of analysis was considered. For the interaction between the steel tube and the concrete core, a contact law, characterised by normal as well as tangential properties, was defined that allowed the two parts to separate. The load was applied through a displacement control at the tip of the beam and the boundary conditions considered at the ends of the column were consistent with the experimental test set-up, i.e. pinned and simple support. The discretisation of the elements was performed using linear hexahedral elements of type C3D8R.

The comparison between test results and pre-test simulations was observed to be relative close. Consequently, the calibration and refinement of the numerical models was performed using the measured geometry of the specimens. In addition, because the beam was not completely restrained by the out of plane lateral system, a lateral contact was defined (see Figure 87) considering a small gap between flanges and the contact elements. It is to be noted that within the numerical simulations it was not accounted for material fracture or crack propagation, phenomena that were observed at some of the joint specimens. Because in the numerical models of these joints, no fracture developed, the capacity did not suffer as in the experimental tests.

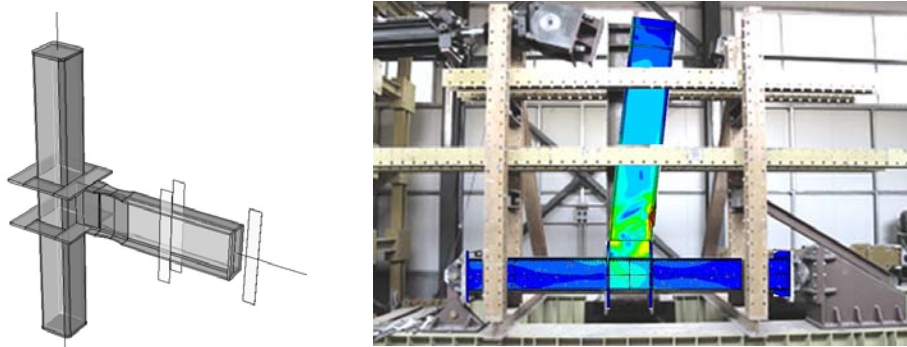


Figure 87. Illustration of the joint model accounting for the out of plane lateral system.

From the calibration, a set of numerical models were obtained which were capable to reproduce with a good accuracy the response of the joints in both moment-rotation curve and failure mechanism, i.e. formation of the plastic hinge in the beam (RBS and CP designed joints) and yielding of components (joints with strengthened beam). Consequently, for each joint configuration, a comparison is shown between test and simulation in terms of moment-rotation curve computed at column centreline. The plastic strain is shown in comparison to the failure mode observed during the test. The results from the calibration of the monotonic tests on beam-to-column joints are shown in Figure 88 for the joints with reduced beam section.

The numerical models calibrated based on the joints subjected to monotonic loading were further used for the numerical calibration of the cyclic tests. A combined isotropic/kinematic cyclic hardening model was therefore adopted. The input for the material model was represented by the yield strength of the steel part, and in addition the cyclic hardening parameters as given by Dutta et al. (2010), i.e. $C_1=42096$, $\gamma_1=594.45$, $Q_\infty=60$, $b=9.71$.

The results from the cyclic analysis are shown for each beam-to-column joint configuration in terms moment-rotation curve (computed at column centreline), von Mises stress distribution and equivalent plastic strain. An illustration of the failure mode, as obtained from the experimental investigations, is shown as well. The comparison between test and numerical simulation is shown in Figure 89a for the RBS joints, in Figure 89b for the CP joints.

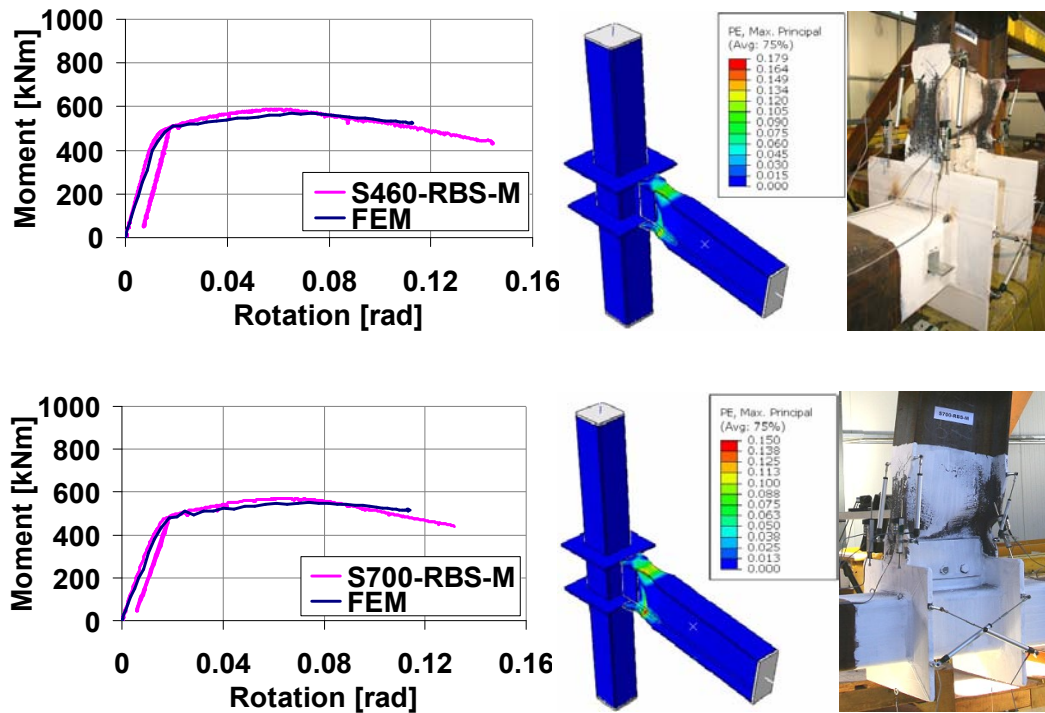


Figure 88. Comparison between test and simulation for RBS joints.

The results from the numerical investigations of the cyclic tests show a good correlation with the experimental results considering the moment-rotation hysteretic loops as well as the failure mechanism (plastic hinge - buckling of flanges and web of beam in the dissipative zone, yielding of components - failure in the heat affected zone of the reinforced RBS joints, plastic deformations in the external diaphragm and column panel zone). In case of S460-CP-R-C joint, the capacity corresponding to the negative amplitudes was obtained higher in the numerical simulations compared to the test where a crack was developed in the cover plate (between external diaphragm and beam flange) and which did not develop in the FE model.

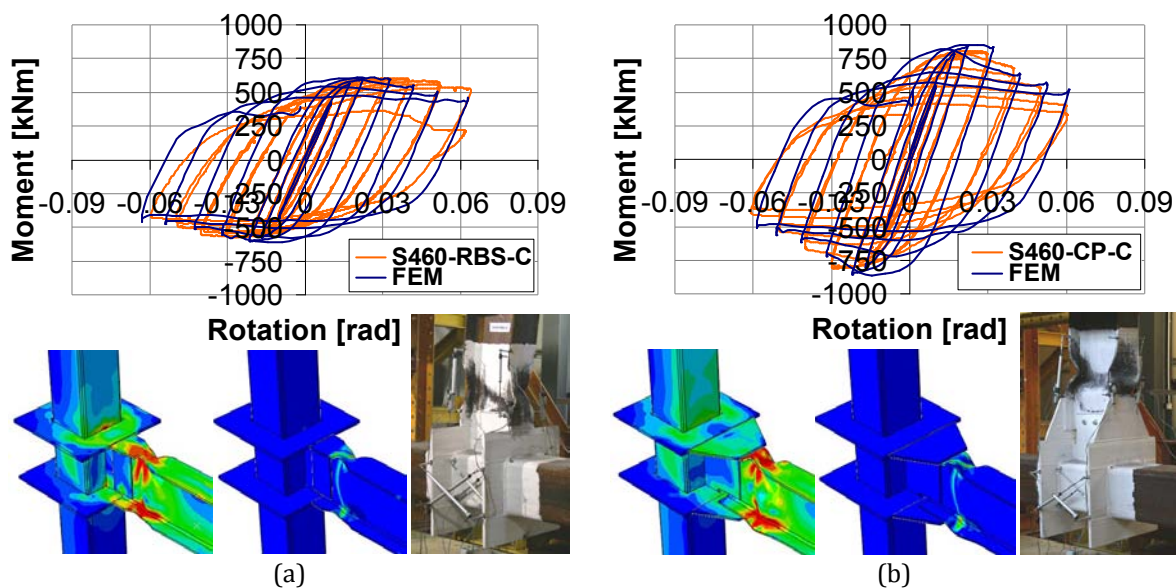


Figure 89. Comparison between test and simulation for RBS and CP designed joints subjected to cyclic loading.

A set of complementary testing cases were considered for the investigation through numerical simulations with the aim to assess the influence of different parameters on the joint behaviour, such as:

- Influence of the concrete core – i.e. the response of the joint without concrete core in comparison to the reference joint with CFT column.
- Influence of the axial force – i.e. the response of the joint with axial force in the column ($N=0.5 \cdot N_{pl}$) in comparison to the reference model.
- Response of the joints with two and four beams welded around the concrete filled tube.
- Influence of the external diaphragm.

With the aim to evaluate the influence of the concrete core – i.e. the response of the joint without concrete core in comparison to the reference joints with composite column (CF-RHS) – a set of additional numerical simulations were performed on the calibrated numerical models from which the concrete part was eliminated (NC → no concrete). The results are shown in terms of moment-rotation curve computed at column centreline. It can be observed in Figure 90 for RBS joints, and in Figure 91 for CP joints, that the absence of concrete core did not affect significantly the response (only a minor reduction of the capacity was observed).

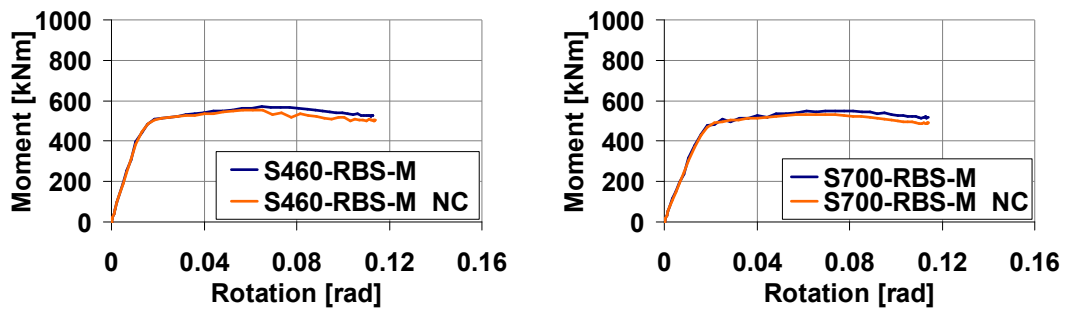


Figure 90. Influence of concrete core – RBS joints

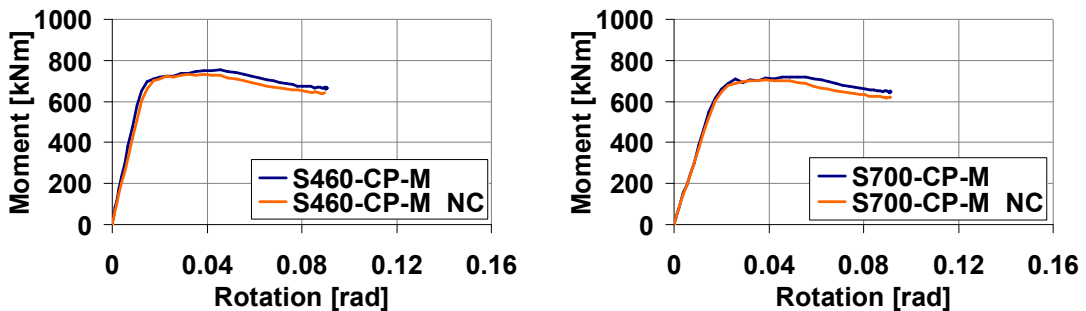


Figure 91. Influence of concrete core – CP joints.

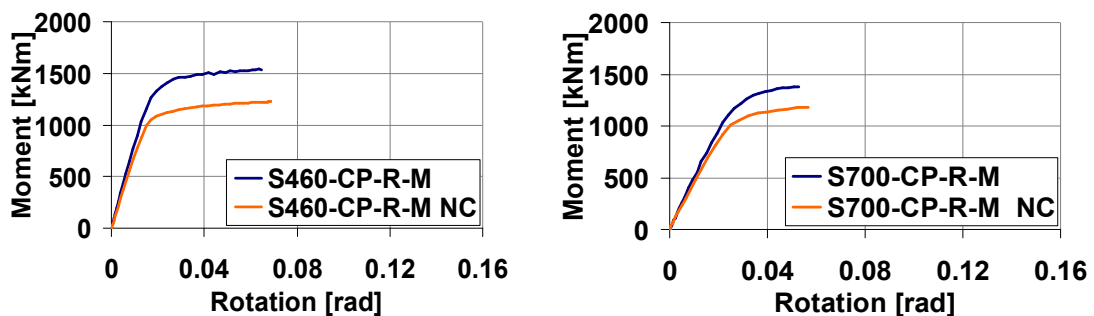


Figure 92. Influence of concrete core – reinforced CP joint

In contrast, for the reinforced joints (extended CP) a significant reduction of capacity can be observed in Figure 92. In these cases, the bending moment and implicitly the shear force in the column web panel were much higher than in the cases shown above. In other words, the shear force in the column web panel exceeded the capacity of the steel tube in shear, and therefore a higher capacity was corresponding to the joints with concrete core.

With the aim to assess the influence of the axial force in the column with respect to the behaviour of the beam-to-column joint, numerical simulations were performed on one of the joints (S460-CP) considering the following cases:

- Joint with concrete core and an axial force level in the column corresponding to 50% of $N_{pl,Rd,composite}$.
- Joint without concrete core and with an axial force level in the column corresponding to 50% of $N_{pl,Rd,steel}$.

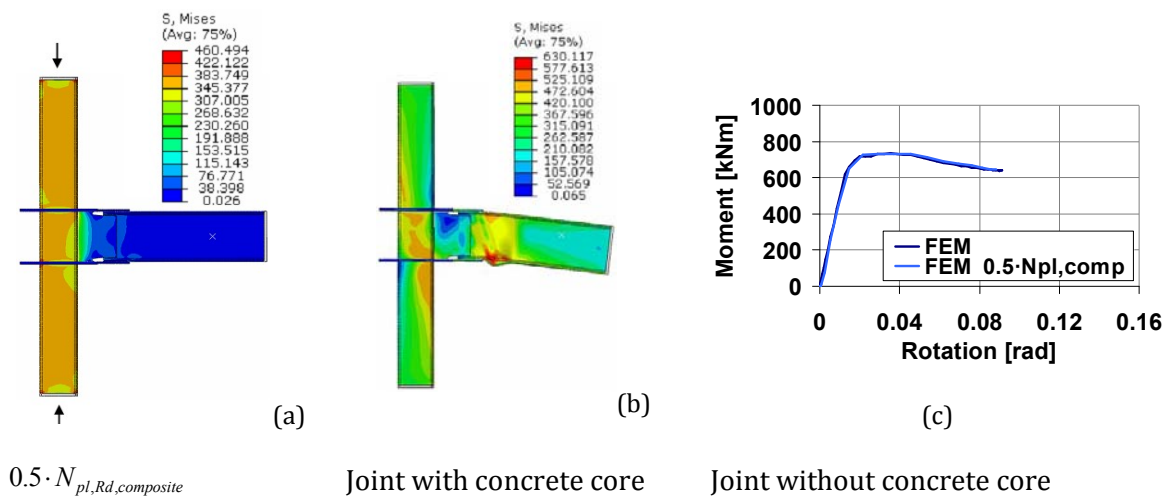


Figure 93. Influence of $0.5 \cdot N_{pl,Rd,composite}$ axial force: S460-CP joint

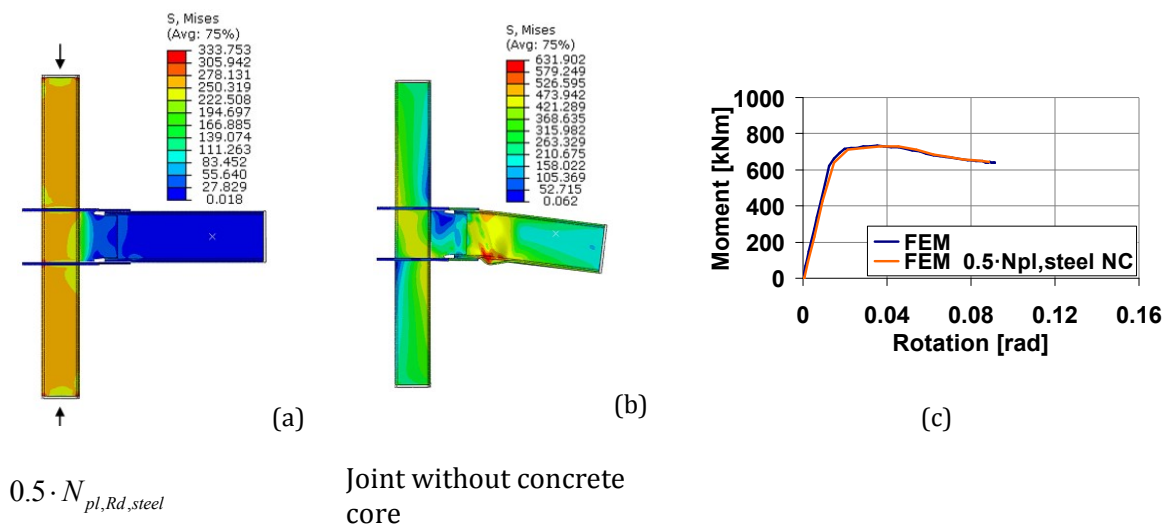


Figure 94. Influence of $0.5 \cdot N_{pl,Rd,steel}$ axial force: S460-CP joint without concrete core.

For each of the two cases, in a first step, the column was axially loaded up to the considered level (see Figure 93a and Figure 94a), and in a second step the beam was loaded. The stress distribution and implicitly the failure mechanism of the joint with concrete core are shown in Figure 93b. The corresponding moment rotation curve is compared in Figure 93c with the reference model. It can be observed that the axial force in the column did not affect the response of the joint compared to

the reference model, and that the plastic hinge formed in the beam. In addition, the stress distribution and implicitly the failure mechanism of the joint without concrete core are shown in Figure 94b. The moment-rotation curve is compared in Figure 94c with the reference model. Also in this case it can be observed that the axial force in the column did not affect the response of the joint without concrete core compared to the reference model and that the plastic hinge formed in the beam.

The experimental tests were performed on single sided beam-to-column joints. It was therefore necessary to assess the behaviour of the joints (including column web panel) in the situation of loading from two sides which corresponds to a more demanding scenario. Figure 95 a and b show the plastic strain corresponding to the S700-CP joints with- and respectively without concrete core. Consequently, for the case with composite column and two beams (FEM 2G), a reduction of the stiffness can be observed in Figure 96a compared to the test curve, but the failure mode was not affected (see in Figure 95 plastic hinges in the beams). The absence of the concrete core (NC → no concrete) lead to reduction of the capacity (Figure 96b) and to the yielding of the column panel – plastic hinges did not form in the beam as for the joint with concrete core.

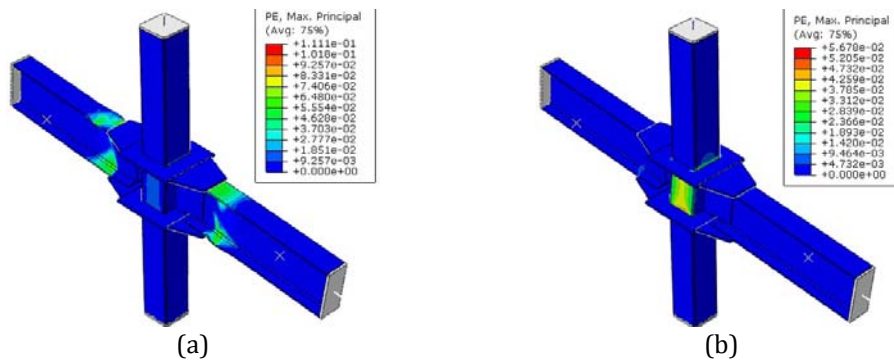


Figure 95. Behaviour of S700-CP joint with beams welded on two sides: CFT (a) and without concrete (b).

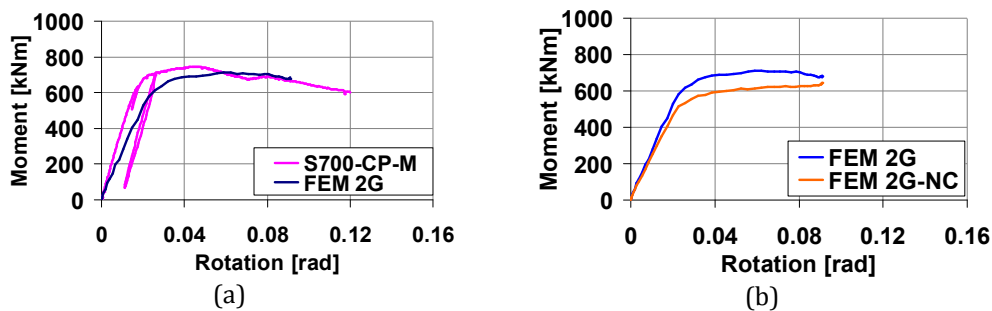


Figure 96. Response of S700-P joints with beams welded on two sides.

A similar investigation was performed also for the joint configuration with reduced beam section. Therefore, Figure 97 a and b show the stress distribution and plastic strain corresponding to the joints with- and respectively without concrete core. A reduction of the stiffness can be observed also in this case (see Figure 98a) compared to the test curve. The absence of the concrete core did not affect the capacity or the failure mode (see Figure 98b). Consequently, the plastic hinges developed in the beams.

The weak-beam/strong-column concept was therefore confirmed for the CP and RBS joints, considering the case with beams welded on two sides, and in addition the study showed the contribution of the concrete core to joint behaviour.

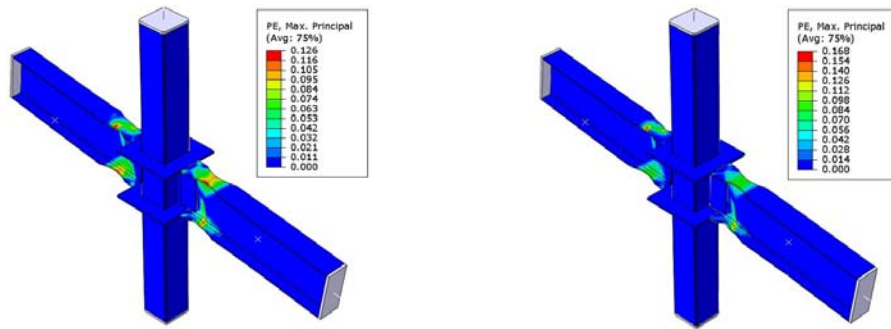


Figure 97. Behaviour of S700-RBS joint with beams welded on two sides: CFT (a) and without concrete (b).

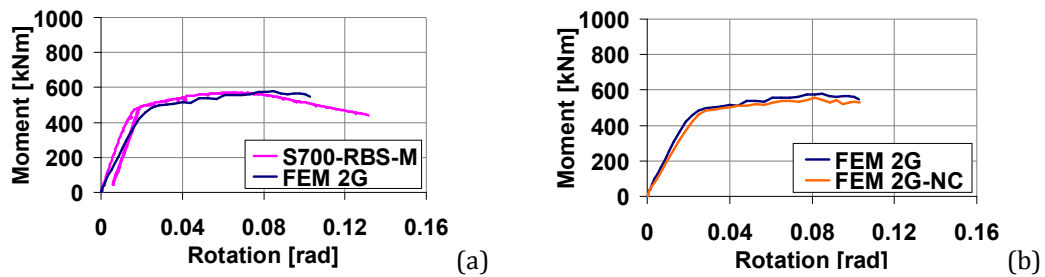


Figure 98. Response of RBS joints with beams welded on two sides.

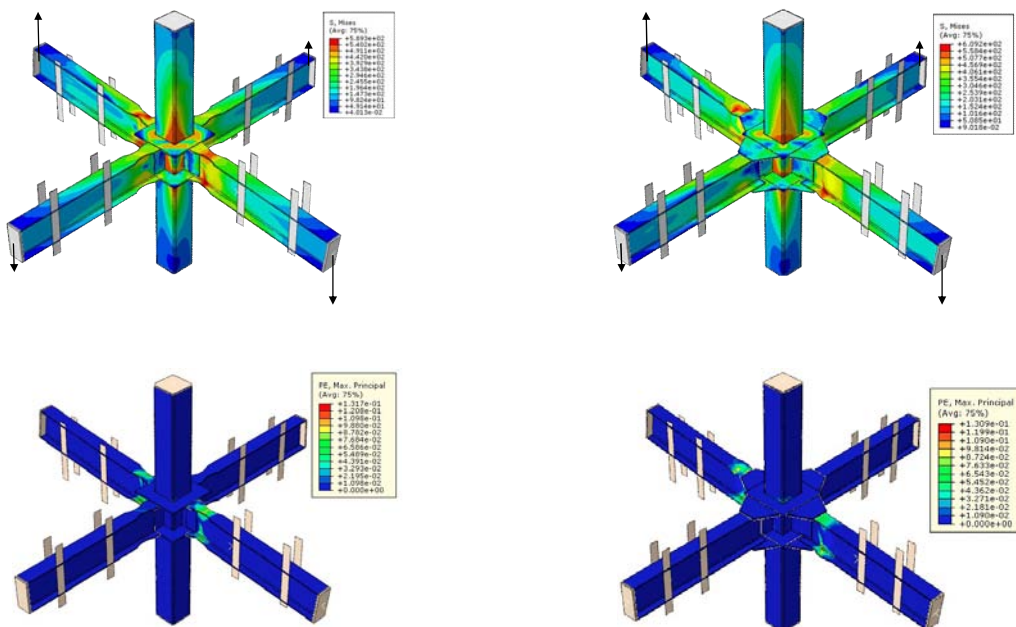


Figure 99. Joints with four beams – von Mises stress distribution and plastic strain.

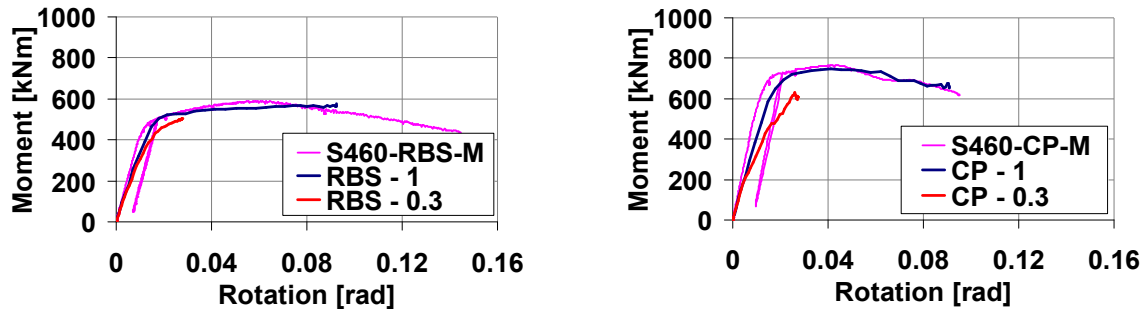


Figure 100. Joints with four beams – moment-rotation curves.

The response of the joints was also investigated considering the case with four beams welded around the concrete filled tube. As reference, the S460-RBS and S460-CP joint models were used. The loading was applied in displacement control at the tip of the beams. The load ratio was considered in amount of 100 % on one direction and respectively 30 % on the other direction. As a result the moment rotation curves are shown in Figure 100 compared to the test results. As it can be observed, on the main loading direction the moment-rotation curve suffered a small reduction of the stiffness but the capacity or the failure mode was not affected. Figure 99 shows the von Mises stress distribution and the plastic strain in the two joint configurations. Therefore, considering the loading of the joints from two directions it can be observed that the joint components (external diaphragm, column web panel) did not suffer plastic deformations.

2.3.4 OUTCOMES

The parameters investigated within the steel-concrete connection tests consisted of loading procedure (monotonic, cyclic), connection (friction, friction+ connectors) and steel grade (S460, S700). The aim was to assess the efficiency of shot fired nails in providing the connection between steel tube and concrete core. The shear strength that developed at the interface between steel tube and concrete core (column stub with friction only) was obtained in amount of 0.4 N/mm², which is equal to the value recommended by EN 1994-1 (2004) for rectangular hollow sections. In relation to the specific loading (push-out tests), it was observed that the connectors have a significant contribution to the load transfer from steel tube to the concrete core, in both monotonic and cyclic loading. From the investigation of the behaviour and failure mode, it was observed that under monotonic loading the concrete was crushed in a small amount at the contact with the shot fired nails which bent. Under alternating cycles the nails eventually broke at the interface between concrete core and steel tube. In addition it was observed that from the cyclic loading the capacity of the connectors decreased slightly compared to the monotonic loading. In conclusion, as observed by Beck (1999), the X-DSH 32 P10 shot fired nails proved a significant contribution to the steel-concrete connection considering the monotonic and cyclic loading, as well as HSS tubes (S460 and S700).

The experimental investigations performed on beam-to-column joints under both monotonic and cyclic loading evidenced a good conception and design of the joints (RBS and CP) justified by the following observations:

- elastic response of the connection zone;
- formation of the plastic hinge in the beam;
- corresponding to cyclic tests performed according to the ANSI/AISC 341 (2005) loading protocol, the RBS and CP designed joints evidenced rotation capacities of 50 mrad (RBS joints) and respectively 40 mrad (CP joints) for which the degradation of strength and stiffness were not greater than the 20% limit defined in EN 1998-1 (2004);

- good response of joint detailing and welded connections with one exception (S700-CP-R-M / C) which evidenced weld failure, however corresponding to a force level higher than the design capacity computed using the real material properties.

From the comparison between the four designed joints and the corresponding joints with reinforced beam, a significant overstrength of the welded connections, respectively of the external diaphragm and column web panel was observed. Therefore the overstrength requirements from EN 1998-1 (2004) were satisfied.

The contribution to the joint rotation was evaluated for the following regions: dissipative zone (plastic hinge), connection (welded connection and external diaphragm), and column web panel. For the joints with reduced beam section and with cover plates, the main plastic deformations occurred in the beam (plastic hinge). The contribution of the connection and column panel to the overall joint rotation was observed to be low. For the joints with reinforced beam, the main contribution to the overall joint rotation was given by the connection zone including external diaphragm (for strengthened RBS joints), and respectively external diaphragm and column panel (for strengthened CP joint).

A set of numerical models were obtained that were capable to accurately reproduce the behaviour of the tested joint configurations in both monotonic and cyclic loading conditions. This allowed a better understanding of the joint behaviour and validation of the analytical model based on the results of the calibrated joint models. In addition the experimental program was extended in order to evaluate the influence of the concrete core, axial force in the column, response of the joints with multiple beams and influence of the external diaphragm.

2.3.5 PUBLICATIONS

- [1] Dubina, D., Vulcu, C., Stratan, A., Ciutina, A., Grecea, D., Ioan, A., Tremeeea, A., Braconi, A., Fülöp, L., Jaspert, J.-P., Demonceau, J.-F., Hoang, L., Comeliau, L., Kuhlmann, U., Kleiner, A., Rasche, C., Landolfo, R., D’Aniello, M., Portioli, F., Beg, D., Cermelj, B., Može, P., da Silva, L. S., Rebelo, R., Tenchini, A., Kesti, J., Salvatore, W., Caprili, S., and Ferrini, M. (2015). High strength steel in seismic resistant building frames (HSS-SERF). Research Fund for Coal and Steel, Final report, European Commission, B-1049 Brussels, 181 p.
- [2] Vulcu, C., Stratan, A., Dubina, D. (2012). "Numerical simulation of the cyclic loading for welded beam-to-CFT column joints of dual-steel frames", *Pollack Periodica*, vol. 7, no. 2, pp. 35–46. DOI: 10.1556/Pollack.7.2012.2.3. Paper ISSN: 1788-1994, Online ISSN: 1788-3911.
- [3] Vulcu C., Stratan A., Ciutina A., Dubina D. (2011). "Beam-to-column joints for seismic resistant dual-steel structures", *Pollack Periodica* 6 (2), pp. 49-60. Paper ISSN: 1788-1994, Online ISSN: 1788-3911.
- [4] Dubina, D., Stratan, A., Vulcu, C., and Ciutina, A. (2014). "High strength steel in seismic resistant building frames." *Steel Construction: Design and Research*, 7(3), 173–177.
- [5] Cristian Vulcu, Aurel Stratan, Adrian Ciutina, Dan Dubina (2014). "Studiul comportării stâlpilor tubulari umpluți cu beton cu conectori din bolțuri împușcate, solicitați monoton și ciclic". *AICPS Review*, nr. 1-2/2014, ISSN: 2067-4546, pp. 80-85.
- [6] Cosmin Maris, Cristian Vulcu, Aurel Stratan, Dan Dubina (2014). "Evaluarea eficienței tehnico-economice a structurilor realizate în soluție «dual-steel»". *AICPS Review*, nr. 1-2/2014, ISSN: 2067-4546, pp. 191-198.
- [7] Dubina, D., Grecea, D., Stratan, A. and Muntean, N. (2009). "Performance of dual-steel connections of high strength components under monotonic and cyclic loading". *Proc. of the 6th Int. Conf. on Behaviour of Steel Structures in Seismic Areas, STESSA 2009*, August 16 - 20.

- F.M. Mazzolani, J.M. Ricles & R. Sause (eds). Taylor & Francis Group, London, ISBN 13 978-0-415-56326-0. p. 437-442.
- [8] Dubina, D., Dinu, F., Stratan A. (2008). "Performance based analysis of high strength steel building frames under seismic actions". Acta Technica Napocensis. Section: Civil Engineering – Architecture. Nr. 51, vol. 1, 2008, ISSN 1221-5848, p. 361-372. Proceedings of the International Conference – CONSTRUCTIONS 2008, 9-10 May 2008, Cluj-Napoca.
- [9] Dubina, D., Muntean, N., Stratan A., Grecea, D., Zaharia, R. (2008). "Performance of moment-resisting joints of high-strength steel components". Acta Technica Napocensis. Section: Civil Engineering – Architecture. Nr. 51, vol. 1, 2008, ISSN 1221-5848, p. 373-384. Proceedings of the International Conference – CONSTRUCTIONS 2008, 9-10 May 2008, Cluj-Napoca.
- [10] Dubina, D., Stratan, A., Dinu, F., Grecea, D., Muntean, N., Zaharia, R. (2008). "Structuri în cadre multietajate realizate în sistem dual-steel: cerințe de performanță și program experimental". AICPS Review, nr. 1-2/2008, p. 39-52. ISSN: 1454-928X
- [11] Muntean, N., Stratan, A., Dubina, D. (2008). "Experimental evaluation of strength and ductility performance of weld details and T-stub bolted connections between high-strength and mild carbon steel", Scientific Bulletin of the "Politehnica" University of Timisoara, Transactions on Civil Engineering and Architecture, Vol. 53 (67) No. 1, 2008, ISSN 1224-6026, p. 45-55.
- [12] Dubina, D., Stratan, A., Dinu, F., Grecea, D., Muntean, N., Vulcu, C. (2010). "Application of high strength steel to seismic resistant multi-storey buildings". COST Action C26 "Urban Habitat Constructions under Catastrophic Events" Proceedings, Naples, 16-18 September 2010, Mazzolani (Ed.), Taylor & Francis Group, London, p. 355-363. ISBN: 978-0-415-60685-1.
- [13] Dubina, D., Dinu, F., Stratan, A., Muntean, N., Zaharia, R., Ungureanu, V., Grecea, D. (2008) "Utilizarea oțelurilor de înaltă performanță în structura de rezistență a clădirilor multietajate amplasate în zone cu risc seismic ridicat: studii de eficiență și program experimental". Structuri metalice amplasate în zone seismice - preocupări actuale. Ed. D. Dubina, V. Ungureanu. Editura Orizonturi Universitare, Timișoara. ISBN 978-973-638-377-9, p. 89-106.
- [14] Dubina, D., Muntean, N., Stratan A., Grecea, D. and Zaharia R. (2008). "Testing program to evaluate behaviour of dual steel connections under monotonic and cyclic loading". Proc. of the 5th European Conference on Steel and Composite Structures EUROSTEEL 2008, 3-5 September, Graz, Austria. R. Ofner, D. Beg, J. Fink, R. Greiner, H. Unterweger (Eds). ISBN 92-0147-000-90, p.609-614.
- [15] Dubina, D., Stratan, A., Muntean, N., Grecea, D. (2008). "Dual-steel T-Stub behaviour under monotonic and cyclic loading". Proceedings of the Sixth International Workshop "Connections in Steel Structures VI", June 22–25, Chicago, USA. Ed. R. Bjorhovde, F.S.K. Bijlaard, L.F. Geschwindner, American Institute of Steel Construction, p. 185-196.
- [16] Dubina, D., Stratan, A., Muntean, N., Dinu, F. (2008). "Experimental program for evaluation of moment beam-to-column joints of high strength steel components". Proceedings of the Sixth International Workshop "Connections in Steel Structures VI", June 22–25, Chicago, USA. Ed. R. Bjorhovde, F.S.K. Bijlaard, L.F. Geschwindner; American Institute of Steel Construction, p. 355-366.
- [17] Vulcu, C., Stratan, A., Dubina, D., Bordea, S. (2012). "Seismic performance of dual frames with composite CF-RHS high strength steel columns", Proceedings of the 15th World Conference on Earthquake Engineering, September 24 - 28, 2012, Lisbon, Portugal, paper 4937.
- [18] Dubina, D., Stratan, A., Vulcu, C., Ciutina, A. (2014). "High strength steel in seismic resistant building frames", 7th European Conference on Steel and Composite Structures EUROSTEEL 2014, 10-12 September 2014, Napoli, Italy, Landolfo R, Mazzolani FM, editors, European

- Convention for Constructional Steelwork, ECCS, paper no. 10-202, 6 p. ISBN: 978-92-9147-121-8.
- [19] Vulcu, C., Stratan, A., Ciutina, A., Dubina, D. (2014). "Steel-concrete connection in case of concrete filled rectangular hollow section columns", 7th European Conference on Steel and Composite Structures EUROSTEEL 2014, 10-12 September 2014, Napoli, Italy, Landolfo R, Mazzolani FM, editors, European Convention for Constructional Steelwork, ECCS, paper no. 08-409, 6 p. ISBN: 978-92-9147-121-8.
- [20] Dubină, D., Stratan, A., Vulcu, C., Ciutina, A. (2013). "Structuri în cadre multietajate cu componente din oțel de înaltă rezistență pentru clădiri amplasate în zone seismice". A XIII-a Conferință Națională de Construcții Metalice, București, 21-22 noiembrie 2013, Editori: Daniel Bîtcă și Paul Ioan, pp. 165-172, ISBN 978-973-100-306-1.
- [21] Vulcu, C., Stratan, A., Ciutina, A., Dubina, D. (2014). "Experimental Evaluation of the Steel-Concrete Connection in Case of Concrete Filled Rectangular Hollow Section (CF-RHS) Columns". Proceedings of the International Workshop "Application of High Strength Steels in Seismic Resistant Structures". Orizonturi Universitare, Timisoara, Romania, ISBN: 978-973-638-552-0, pp. 95-104.
- [22] Vulcu, C., Stratan, A., Ciutina, A., Dubina, D. (2014). "Experimental Evaluation of Welded Reduced Beam Section (RBS) and Cover Plate (CP) Beam-to-CF-RHS Column Joints". Proceedings of the International Workshop "Application of High Strength Steels in Seismic Resistant Structures". Orizonturi Universitare, Timisoara, Romania, ISBN: 978-973-638-552-0, pp. 105-120.
- [23] Vulcu, C., Stratan, A., Ciutina, A., Dubina, D. (2014). "Numerical Investigation of Welded RBS and CP Beam-to-CF-RHS Column Joints". Proceedings of the International Workshop "Application of High Strength Steels in Seismic Resistant Structures". Orizonturi Universitare, Timisoara, Romania, ISBN: 978-973-638-552-0, pp. 121-136.
- [24] Vulcu, C., Stratan, A., Dubina, D. (2012). "Seismic Performance of EB Frames of Composite CFHS High Strength Steel Columns". Proceedings of the 10th International Conference on Advances in Steel Concrete Composite and Hybrid Structures, ASCCS 2012, Singapore, 2-4 July 2012. ISBN-13: 978981-07-2615-7, pp. 953-960.
- [25] Vulcu, C., Stratan, A. and Dubina, D. (2012). "Seismic resistant welded connections for MRF of CFT columns and I beams", Proceedings of the 7th International Workshop on Connections in Steel Structures, May 30 - June 2, 2012, Timisoara, Romania, ECCS, Dan Dubina and Daniel Grecea (Eds), ISBN 978-92-9147-114-0, pp. 275-290.
- [26] Vulcu, C., Stratan, A., and Dubina, D. (2011). "Evaluation of Welded Beam-to-CFT Column Joints", EUROSTEEL 2011, August 31 - September 2, 2011, Budapest, Hungary, p. 489-494. ISBN: 978-92-9147-103-4.
- [27] Vulcu, C., Stratan, A., Ciutina, A., Dubina, D. (2010). "Simularea comportării unui model experimental pentru noduri de cadre etajate cu stâlpi din țevi umplute cu beton și grinzi dublu T". Lucrările celei de-a 12-a Conferințe Naționale de Construcții Metalice "Realizări și preocupări actuale în ingineria construcțiilor metalice", Timișoara, 26-27 noiembrie 2010, Dubina, Ungureanu, Ciutina (Ed.), Editura Orizonturi Universitare, p. 233-244. ISBN: 978-973-638-464-6.
- [28] Dubina, D., Vulcu, C., Stratan, A., Ciutina, A. (in print). "Dual frames of high strength steel RHSCF columns for seismic zones", 8th International Conference on Behavior of Steel Structures in Seismic Areas STESSA 2015, Shanghai, China, July 1-3, 2015. Paper no. 123.